EVALUATION OF CEMENT-TREATED SOILS SUBJECTED TO CYCLES OF FREEZING AND THAWING

by

Reza Jolous Jamshidi

Submitted in partial fulfilment of the requirements
for the degree of Doctor of Philosophy

at

Dalhousie University
Halifax, Nova Scotia
August 2014

Contents

List of Tables

List of Figures

Abstract

An extensive experimental study was performed to provide an insight on design and evaluation of cement-treated materials subjected to freeze/thaw (f/t) cycles. Poorly designed stabilized materials showed increases of up to three orders of magnitude in hydraulic conductivity and decreases of up to 95 percent in unconfined compressive strength values. Decrease in water to cement ratio was shown to partially improve f/t resistance for some of the scenarios investigated.

A factorial experiment was designed to investigate the influence of curing time (immature vs. mature), freezing temperature (-2°C vs -10°C), and number of f/t cycles (4 vs. 12) during laboratory evaluation of a cement-treated silty sand. Results showed all the factors were significant in the observed changes in mechanical and hydraulic performance of the specimens. Observations emphasized the need for developing site-specific exposure scenarios in assessment of soil-cement under f/t exposure. An investigation on the influence of freezing dimensionality also showed a more practical three-dimensional f/t exposure can adequately represent a realistic one-dimensional f/t exposure scenario in terms of mechanical and hydraulic performance degradation.

Monitoring percent mass loss (an indicator commonly used in industry) and compressive strength after f/t exposure under various scenarios showed they are not reliable indicators for predicting changes in hydraulic conductivity values under exposure to cycles of f/t. Resonant frequency measurements performed using the impact resonance method was suggested as a non-destructive technique in evaluation of hydraulic performance of cement-treated materials after f/t exposure.

Microstructural evaluation of specimens using transmitted light microscopy showed matrix disruption and aggregate-paste interface cracking to be the main damage mechanisms for highly affected specimens. However, this technique was found unsuitable in detecting early stages of damage.

List of Abbreviations and Symbols Used

ANOVA: Analysis of variance

C-S-H: Calcium-Silicate-Hydrate

f/t: Freeze/thaw

IR: Impact resonance

ITZ: Interfacial transition zone

$\widehat{R}$: Logarithm of the hydraulic conductivity ratios, [-]

K_0: Initial hydraulic conductivity, [LT^{-1}]

K_{12}: Hydraulic conductivity after 12 freeze/thaw cycles, [LT^{-1}]

$K_{exposed}$: Exposed hydraulic conductivity, [LT^{-1}]

K_{healed}: Hydraulic conductivity after the healing period, [LT^{-1}]

LOI: Loss on ignition, [-]

m_0: Initial mass, [M]

m_m: Mass measured after the m^{th} freeze/thaw cycle, [M]

NDT: Non-destructive test

OWC: Optimum water content, [-]

RF: Resonant frequency, [T^{-1}]

RF_0: Initial resonant frequency, [T^{-1}]

RF_{12}: Resonant frequency after 12 freeze/thaw cycles, [T^{-1}]

RF_m: Resonant frequency after the m^{th} freeze/thaw cycle, [T^{-1}]

RSD: Relative standard deviation, [-]

s/s: Solidification/stabilization

SD: Standard deviation

UCS: Unconfined compressive strength, [MLT^{-2}]

w/c: water to cement ratio, [-]

w/s: water to solids ratio, [-]

β_0: Initial resonant frequency ratio, [-]

β_{12}: Resonant frequency ratio at the end of the 12^{th} freeze/thaw cycle, [-]

β_{healed}: Resonant frequency ratio after the healing period, [-]

β_m: Resonant frequency ratio at the end of the m^{th} freeze/thaw cycle, [-]

Δ_m: Percent mass loss at the m^{th} freeze/thaw cycle, [-]

Acknowledgements

First and foremost, I would like to thank my advisor, Dr. Craig Lake, for the guidance, patience, and all the support he provided during the course of my study at Dalhousie University. I have been extremely fortunate to work with him and have him as an example, both academically and personally, in my life. Without his understanding and positive attitude this journey wouldn't have been as enjoyable as it was.

I am grateful to the members of my advisory committee Dr. Chris Holt and Dr. Nouman Ali for their comments and involvement during different stages of this work. I am thankful to Dr. Chris Barnes for introducing the Impact Resonance method to me, teaching me to use and troubleshoot the related equipment, and reviewing our results. I really appreciate the help from Dr. Colin Hills and Dr. Peter Gunning in processing the petrographic thin sections and interpreting the observations.

I would like to acknowledge the financial support from the NSERC CREATE's STEWARD program, Canada Foundation for Innovation, and the Faculty of Graduate Studies at Dalhousie University. Without their support this research wouldn't have been possible.

I am sincerely grateful to the staff of the Civil and Resource Engineering department of Dalhousie University for their kindness and support. Blair Nickerson, Brian Kennedy, Brian Liekens, Jesse Keane, Shelly Parker, June Ferguson, and Allyson Bremner helped me in different ways through this work.

I have been fortunate to be surrounded by many great friends at the Civil Engineering Department of Dalhousie University, and I am grateful for their encouragement and support. Vincent Goreham, Pejman Razi, Hun Choi, Mohammed Al-Mala Yousif, Sarah Jane Payne, Wenwen Pei, Megan MacLellan, Mohammed Shamsuzzaman, Vahid Farajkhah, Pouria Behnam, and Ehsan Nasiri, thank you all for the great times that we have

shared. I would also like to thank Mitch Woodworth for assisting me in performing parts of the experimental works in the study.

I am deeply thankful to my parents, Hosein and Mansooreh, and my brother, Ehsan, for their love, support, and encouragement during all these years that I have been away from home. I hope that I have made them proud. Finally, I have saved these last words to thank the love of my life, Farzaneh, for providing an unlimited source of support, patience, and understanding during all these years. Moving forward to the next stage of my life, I am excited for the future that we will build together.

CHAPTER 1: INTRODUCTION

1.1. Overview

With an increasing demand for construction materials and a limited supply of quality natural resources, there is often a requirement to modify accessible materials to meet engineering properties required for a specific project. Chemical stabilization of soils using Portland cement is a ground improvement technique which was developed about 100 years ago to facilitate the utilization of the existing low quality materials in the pavement industry (ACI (1990)). Currently, this technique is widely used by geotechnical engineers to enhance mechanical and hydraulic properties of "problematic" soils in numerous applications including base layer for roads and foundations, slope protection, water retaining systems (e.g. dams, lagoons, canals, etc.), and contaminant containment and immobilization systems (e.g. vertical cut-off walls, cement-based solidification/stabilization (s/s)) (ACI (1990); Conner & Hoeffner (1998); ACI (1999)).

Design of cement-stabilized systems relies on two basic principles. Firstly, the final product is expected to meet the performance objectives of the intended application, which may include a target strength, allowable settlement or heaving, leaching properties, or hydraulic conductivity value. Secondly, the treated material should maintain the expected performance over the service life of the project. Previous studies (e.g. Klich et al. (1999); Fitch & Cheeseman (2003)) have shown that processes such as leaching, chemical attack, wet/dry (w/d) cycling, and freeze/thaw (f/t) cycling can influence the structure of cement-treated materials.

Historically cement stabilization of soils has predominantly been applied to projects requiring improvement in the mechanical properties of the initial materials. This focus on mechanical properties has largely influenced the direction of past research studies in this field. A quick review of the available literature would show that previous studies were mostly performed on specific designs of soil-cement, usually compacted near optimum water content (OWC) conditions from the standard proctor test (ASTM-D558 (2011)), customary in the pavement industry. In addition, numerous studies have been performed

to evaluate compressive strength, modulus of elasticity, and mechanical frost heave of compacted soil-cement. Similarly, with the exception of less than a handful of publications in the literature, durability studies to examine changes in the performance of stabilized soils have been exclusively conducted on compacted soil-cement and were focused on establishing proper correlations between the mix and strength related parameters.

Application of soil-cement in hydraulic and contaminant barrier systems, as well as remediation of contaminated soils (i.e. cement-based s/s) didn't start until the 1950s, about 40 years after the first engineered cement stabilization project (ACI (1990); Conner & Hoeffner (1998)). Often times in these applications, the soil-cement mixture is in a plastic form (i.e. plastic soil-cement prepared at wet of OWC conditions) and is designed to maintain a low hydraulic conductivity after curing. The different consistency of soil-cement in these applications may be a result of construction requirements (e.g. self-consolidation, as opposed to compaction in vertical cut-off walls), or may be imposed by the initial high water content of the native materials (e.g. remediation of contaminated sludge in cement-based s/s projects). Despite the widespread use of these technologies in North America, few studies exist that have demonstrated the performance of cement-stabilized soils at higher water contents relative to OWC conditions. Moreover, changes in the hydraulic performance of these materials during environmental exposure such as f/t cycles have not been addressed.

Exposure to cycles of f/t can negatively influence the structure of a soil-cement due to the expansive forces that develop during the freezing of water in near saturated conditions. In Canada and parts of the United States the weather conditions provide the ideal settings (i.e. both sub-zero temperatures and precipitation required for the saturation of the materials) for the degradation of cement-stabilized soils under f/t exposure. Studying the influence of f/t cycles on the hydraulic performance of cement-stabilized materials is needed and is critical in the acceptance of cement-based s/s in cold regions of the world, since deviation of the performance from design objectives in these applications can result in release of contaminants to the environment. Cement-based s/s is an established remediation technique in the United States (USEPA (2013)), and its application in Canada is expected

to grow after the implementation of some recent projects, most notably the Sydney Tar Ponds and Coke Ovens remediation project (AECOM (2013)) which used this technique for remediation of over one million tons of contaminated soils and sediments.

Research needs to be performed to assess the influence of f/t exposure, at various freezing temperatures and exposure scenarios, on the hydraulic performance of cement-treated materials. Furthermore, current f/t evaluation techniques for soil-cement specimens are long and labor intensive processes, as they require the specimens to be exposed to 12 f/t cycles for 24 days (ASTM-D560 (2003)) in addition to the curing time required for the hydration of cement. Monitoring the hydraulic conductivity values during f/t exposure tests can potentially add a significant amount of time to the already long testing time for these materials. Therefore, finding alternative test methods to reduce the length of these experiments will be desirable from economic perspective, and hence, acceptance of the developed technique(s) by industry.

1.2. Research Objectives

The research in this thesis is intended to expand the available knowledge on the hydraulic and mechanical performance of cement-treated soils in cold regions and to provide a guideline for the design of laboratory procedures to evaluate these materials under exposure to f/t cycles. The overall objectives of this study were to:

- Analyze the influence of various laboratory testing conditions for the evaluation of f/t effects on the performance of soil-cement materials.
- Investigate the hydraulic and mechanical performance of a wide range of mix designs and curing ages for cement-treated soils prior to, and after exposure to f/t cycles.
- Assess the usefulness of percent mass loss measured using the brushing test (ASTM-D560 (2003)), a technique routinely used in the industry, in predicting changes in the hydraulic performance of soil-cement after f/t exposure.

- Investigate application of the impact resonance (IR) method as a non-destructive technique (NDT), in predicting hydraulic conductivity changes of f/t exposed specimens.
- Investigate the healing potential of f/t exposed soil-cement in recovery of the hydraulic performance after a post exposure curing period.
- Study the mechanisms of damage propagation in cement-treated soils exposed to f/t cycles under various testing and curing age conditions.

1.3. Organization of Chapters

This thesis contains seven chapters. Chapters three to six are organized as independent journal paper publications based on the experimental studies performed in the thesis. A summary of the content of each chapter is presented below:

Chapter one provides an introduction on the research subject and outlines the objectives of the study.

Chapter two provides background information and definitions on soil-cement as well as available literature related to the issue of f/t durability of soil-cement. Also, presented is the IR method and its application as a non-destructive technique in health monitoring of cement-based materials.

Chapter three reports the results of a factorial experimental program designed to study the influence of three testing conditions; number of f/t cycles, freezing temperature, and curing age; on the observed changes in the performance (i.e. hydraulic conductivity and unconfined compressive strength (UCS)) of cement-treated silty sand specimens. The influence of modifications in the mix design at enhancing the f/t resistance of soil-cement specimens is discussed. Results of the resonant frequency (RF) measurements performed using the IR technique are presented and compared to the changes in the performance of the specimens.

Chapter four provides the results of an experimental program designed to evaluate the influence of the soil's fines content and water/cement (w/c) ratio in the mix design on the hydraulic conductivity and UCS of cement-treated soils at different curing ages. Changes in the performance after twelve cycles of freezing (-10±1°C) and thawing (22±1°C) are reported. Changes in the hydraulic performance are compared to the mass loss data obtained from the brushing test performed on the specimens from each mix design. Also, the healing potential of damaged specimens in recovery of hydraulic conductivity values is discussed.

Chapter five provides the results of the IR tests performed on specimens studied in chapter four. The application of the IR method in predicting the curing progression, specimen degradation due to f/t exposure, and healing potential of soil-cement is discussed. A pre-screening scheme is proposed based on the results of the IR tests that can significantly reduce the time required for hydraulic conductivity evaluation in f/t studies of cement-stabilized soils.

Chapter six provides the results of an experimental program designed to evaluate the possible variations of the performance and structural degradation in one-dimensional f/t tests compared to a three-dimensional exposure scenario used in the experimental works in chapters three to five. Mechanisms of damage propagation are also discussed for a range of damaged specimens by studying thin section samples from unexposed and exposed specimens using optical transmitted light microscopy.

Chapter seven provides the summary and conclusions of the thesis. Recommendations for future work is also presented in this chapter.

1.4. References

ACI, 1999. *Controlled low-strength materials*, Farmington Hills, MI: Americal Concrete Institute (ACI) Committee 229, ACI229R-99.

ACI, 1990. *Report on soil cement*, Farmington Hills, MI: American Concrete Institute (ACI) Committee 230, ACI230.1R-90.

AECOM, 2013. Sydney Tar Ponds and Coke Ovens site remediation. *Accessed on April 8, 2014 at: http://www.aecom.com/vgn-ext-templating/v/index.jsp?vgnextoid=b5d743dfa94c5310VgnVCM100000089e1bacRCRD&cpsextcurrchannel=1*.

ASTM-D558, 2011. Standard test methods for moisture-density (unit weight) relations of soil-cement. In *Annual Book of ASTM Standards*. West Conshohocken, PA: ASTM International.

ASTM-D560, 2003. Standard test methods for freezing and thawing compacted soil-cement mixtures. In *Annual Book of ASTM Standards*. West Conshohocken, PA: ASTM International.

Conner, J.R. & Hoeffner, S.L., 1998. The history of stabilization/solidification technology. *Critical Reviews in Environmental Science and Technology*, **28**(4):pp.325–396.

Fitch, J. & Cheeseman, C.R., 2003. Characterisation of environmentally exposed cement-based stabilised/solidified industrial waste. *Journal of Hazardous Materials*, **101**(3):pp.239–255.

Klich, I., Batchelor, B., Wilding, L.P. & Drees, L.R., 1999. Mineralogical alterations that affect the durability and metals containment of aged solidified and stabilized wastes. *Cement and Concrete Research*, **29**:pp.1433–1440.

USEPA, 2013. *Superfund remedy report, Forteenth Edition*, USEPA Solid Waste and Emergrncy Respose, EPA 542-R-13-016.

CHAPTER 2: BACKGROUND

2.1. Introduction

This chapter is intended to provide an overview of the terminology and relevant literature on cement-stabilized materials, particularly the influence of freeze/thaw (f/t) exposure on the structure and performance of these materials. Five main subjects are covered in this review:

1. Common definitions and applications for cement-treated soils.
2. Issues of f/t durability in cement-treated materials and relevant literature in this regard; this includes mechanisms of damage development due to f/t exposure, available testing methodologies to assess f/t damage, and previous studies related to the assessment of structural and performance degradation of f/t exposed materials.
3. Influence of f/t exposure on the hydraulic conductivity of compacted clay, given the potential similarity to soil-cement materials.
4. Application of the impact resonance (IR) method, as a non-destructive technique (NDT), in health monitoring of cement-based materials.
5. Healing potential of f/t exposed cementitious materials after post exposure curing.

This literature review will assist the reader in understanding the current state of research related to f/t exposure of soil-cement materials.

2.2. Cement Treatment of Soils

Cement has been extensively used for improving the engineering properties of soils. A successful soil stabilization project usually consists of treatability and pilot studies prior to a full-scale implementation in the field (Fleri and Whetstone (2007)). The mixing process for soil-cement constituents in the field can be performed using a wide range of in-situ (e.g. shallow and deep mixing, hydraulic shearing, and backhoe mixing) and ex-situ (e.g. in-drum mixing and plant processing) techniques. Selection of a mixing technique depends

on several factors including treatment depth, availability of space for the required equipment, type of soil, and economic considerations. Quality control testing is performed during the mixing and placement process of soil-cement to ensure the final product meets the design specifications confirmed under controlled laboratory conditions.

Cement treatment of soil can result in increases in strength (i.e. bearing capacity), modulus of elasticity, as well as reductions in plasticity and hydraulic conductivity of the original soil (Felt & Abrams (1957); BRAB (1969); ACI (1990)). Depending on the consistency of the soil-cement mixture and the final product, cement treated soils may fall within one of the following categories (BRAB (1969)):

- Cement-modified soils are created by adding relatively low amounts of cement (less than three percent) to the soil. The final product has a soil-like texture and is designed for a slight increase in the strength or reduction in the plasticity and hydraulic conductivity of the original soil.

- Compacted soil-cement is created through careful control of water in the mix design (usually close to optimum water content (OWC) conditions using the standard proctor test, performed according to ASTM-D558 (2011)). The soil-cement mixture is compacted in place and results in a "hardened" product due to the hydration of cement. Compacted soil-cement is usually required to withstand durability tests including exposure to wet/dry (w/d) and f/t cycles performed in accordance to ASTM-D559 (1996) (withdrawn in 2012) and ASTM-D560 (2003), respectively.

- Plastic soil-cement, sometimes referred to as flowable fill, flowable mortar, or controlled low strength material (CLSM) (ACI (1999)), is a self-compacting soil-cement that contains relatively higher amounts of water in its mixture compared to compacted soil-cement resulting in consistencies similar to plastering mortar. Due to its increased water content, more cement may have to be incorporated in the mix design of plastic soil-cement to ensure the desired integrity of the final product.

Experiments performed in the current research study are designed to assess performance of compacted and plastic soil-cement under unexposed and f/t exposed conditions. Throughout this thesis, unless specifically mentioned, both of these materials are, interchangeably, referred to as soil-cement, cement-treated soils, and cement-stabilized soils, as is routinely done in industry practice.

2.3. Structure of Soil-Cement Materials

Soil-cement is produced by mixing soil, water (either existing or added to the soil) and cement as basic constituents at specific proportions. Some other additives such as fly ash, lime, and slag may be used as well. Through a series of chemical reactions between water and cement (i.e. hydration process) a hardened cement paste binds the soil particles together. Unlike concrete, soil particles in soil-cement (specifically in compacted soil-cement) are not completely coated by the paste (ACI (1990)). In the study of cement-based materials, the assumption that their structure is a two-phase composite material may be an oversimplification of the problem (Mindess et al. (2003)). The transition zone between paste and aggregates, referred as the interfacial transition zone (ITZ) in the literature, has a unique structure and influences the final performance of the material (Mindess et al. (2003)).

A brief description of the hydration process, pore size distribution in cement paste, and the interfacial transition zone (ITZ) between the paste and aggregates is presented in this section.

2.3.1. Hydration of Cement

According to Mindess et al. (2003), there are five major mineral phases in ordinary Portland cement as summarized in Table 2.1. However, the cementing action of Portland cement is mainly a result of the hydration reactions of tricalcium silicate (i.e. alite) and dicalcium silicate (belite) as shown below:

$2(3CaO\text{-}SiO_2) + 11H_2O \rightarrow 3CaO\text{-}2SiO_2\text{-}8H_2O + 3Ca(OH)_2$ Equation 2.1

alite + water → calcium-silicate-hydrates (C-S-H) + calcium hydroxide

$2(2CaO\text{-}SiO_2) + 9H_2O \rightarrow 3CaO\text{-}2SiO_2\text{-}8H_2O + Ca(OH)_2$ Equation 2.2

belite + water → calcium-silicate-hydrates (C-S-H) + calcium hydroxide

In the above equations the formula presented for calcium-silicate-hydrates (i.e. $C_3S_2H_8$) is an estimate of the products from hydration of alite and belite as the composition of the resulting hydrate may vary.

Table 2.1: Typical composition of ordinary Portland cement (Mindess et al. (2003)).

Chemical name	Chemical formula	Shorthand notation	Weight, percent
Tricalcium silicate	$3CaO\text{-}SiO_2$	C_3S	55
Dicalcium silicate	$2CaO\text{-}SiO_2$	C_2S	18
Tricalcium aluminate	$3CaO\text{-}Al_2O_3$	C_3A	10
Tetracalcium aluminoferrite	$4CaO\text{-}Al_2O_3\text{-}Fe_2O_3$	C_4AF	8
Calcium sulfate dehydrate (Gypsum)	$CaSo_4\text{-}2H_2O$	CSH_2	6

Calcium hydroxide and calcium-silicate-hydrates account for over 70 percent of the total products during the hydration of cement (examples of other products include monosulfoaluminate and ettringite) (Mindess et al. (2003)). While calcium hydroxide has a well-crystalized structure and develops in the solution, calcium-silicate-hydrates are poorly crystalline materials (therefore often referred to as C-S-H gel in the literature) and form around cement particles in the initial stages of the hydration process. As the hydration process continues, the thickness of this C-S-H layer on the cement particles increases resulting in a barrier which restricts the access of water to the unreacted alite and belite phases (i.e. the reaction becomes diffusion controlled). As a result, the hydration of cement is a very slow process and the structure of the cement paste continues to evolve over time. Figure 2.1 shows a schematic illustration of microstructural development of the paste over 90 days (Mindess et al. (2003)).

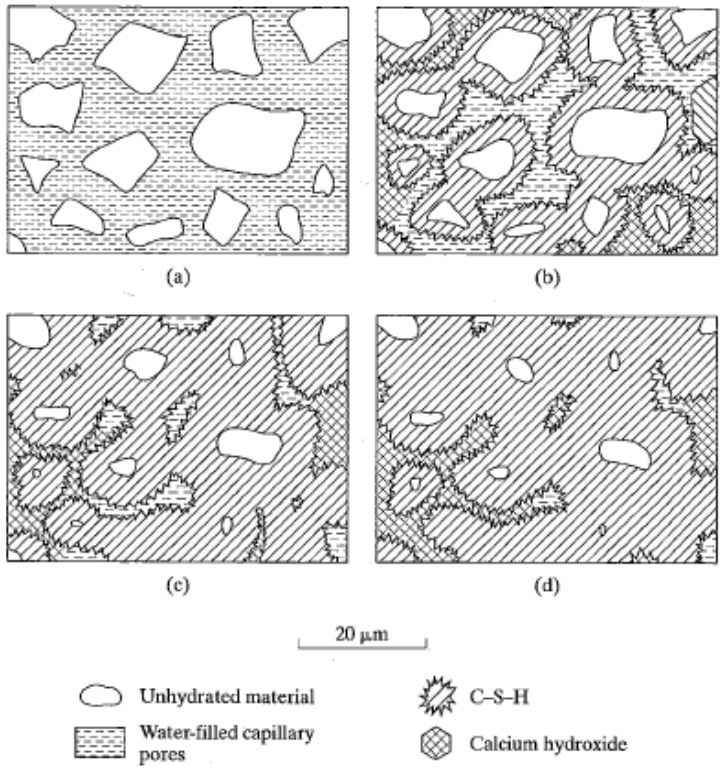

Figure 2.1: Schematic of microstructural evolution of cement paste. a) fresh mix, b) at 7 days, c) at 28 days, and d) at 90 days (Mindess et al. (2003)).

2.3.2. Classification of the Pore Structure in Cement Paste

The structure of a hydrated cement paste can be classified based on its pore size distribution of gel pores and capillary pores (Powers & Helmuth (1953)). Gel pores are attributed to the formation of the C-S-H gel and represent the smallest (approximately smaller than 2×10^{-7} cm) pore structure in cement paste. Capillary pores represent a class of larger pores (up to 5×10^{-4} cm) that form due to the existence of free water entrapped between partially hydrated cement grains. Capillary pores control permeability and diffusivity characteristics of the cement paste (Mindess et al. (2003)). Development of hydration products and subsequently capillary and gel pores within the cement paste depends on the availability of water (i.e. water/cement (w/c) ratio) required for the reactions described earlier, as well as the degree of hydration (i.e. fraction of the available cement being hydrated) as illustrated in Figure 2.2.

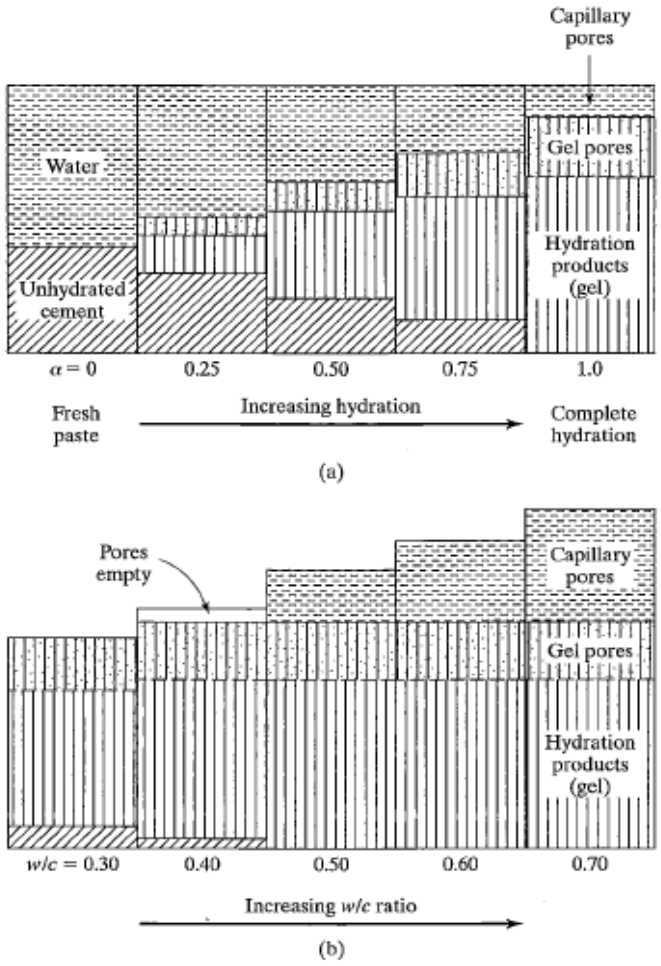

Figure 2.2: Influence of a) hydration process and b) w/c ratio on microstructure of cement paste (Mindess et al. (2003)).

In addition to gel pores and capillary pores, which are the smaller pore structures within the cement paste, larger air voids are also observed in cement-based materials. These voids may form due to the entrapment of air during the mixing process, or may be purposely included in the mix design using air-entraining agents to enhance f/t resistance. Air voids are distributed within the final structure and are surrounded by layers of cement paste containing gel pores and capillary pores.

2.3.3. Interfacial Transition Zone (ITZ)

It is known that the microstructure of cement paste in the vicinity of aggregates, a zone referred to as ITZ in the literature, is different from the bulk of cement paste matrix. This

is due to the inability of cement particles to pack efficiently at the aggregate interface, a phenomenon referred to as the "wall effect" (Mindess et al. (2003)). Since C-S-H forms around cement particles within the paste (i.e. at a distance from the "wall"), calcium hydroxide is the main hydration product that is present in the ITZ (Mindess et al. (2003)). The ITZ, usually 15 to 50 μm wide, also has a higher water content resulting in the reduction of the w/c ratio in the paste (Shane et al. (2000)). It is also shown that the maximum porosity of the ITZ may be up to three times higher than that of the bulk matrix. Higher porosity of ITZ might result in an adverse effect on the durability of cement-based materials (Shane et al. (2000)). Although the ITZ is very thin, calculations for a typical concrete shows that it may occupy 20 to 40 percent of the total volume of the cementitious matrix (Mindess et al. (2003)).

2.4. Applications and Objectives of Soil-Cement Stabilization

The majority of soil improvement projects require an increase in the bearing capacity (i.e. strength) and stiffness, and/or reduction in the frost susceptibility compared to the initial soil. Soil-cement used as base material for bituminous/concrete pavements, slope stability, and erosion control are a few examples of such applications (ACI (1990); ACI (1999)). In addition to improved mechanical properties, there are soil-cement applications where reaching and maintaining a target hydraulic conductivity is a concern. Examples include liners in wastewater treatment plant lagoons, vertical cut-off walls, and cement-based solidification/stabilization (s/s) remediation projects. Regardless of the strength requirement for a given soil-cement application, the hydraulic conductivity of the stabilized soil can greatly impact its long term performance, as it provides a potential pathway for environmental stresses such as leaching, chemical attack, w/d cycles, and f/t exposure (Hearn et al. (2006)).

Cement-based s/s, as a major soil-cement application requiring low hydraulic conductivity, is a well-established source-control remediation technology for the treatment of a wide range of contaminated materials (see Bone et al. (2004), Batchelor (2006), and Paria & Yuet (2006)). Monolithic s/s materials are usually designed to maintain a low hydraulic

conductivity (smaller than 10^{-8} m/s) to ensure slow diffusion-controlled release of contaminants to the environment (Stegemann & Côté (1990); ITRC (2010)). Solidification/stabilization is among the top three selected remediation techniques applied to in-situ and ex-situ remediation of Superfund sites in the United States (USEPA (2013)). In Canada, cement-based s/s was used for remediation of over one million tons of contaminated soils and sediments in the Sydney Tar Ponds and Coke Ovens remediation project (AECOM (2013)).

2.5. Soil-Cement Design Considerations

With the exception of organic soils, highly plastic clay, and poorly reacting sandy soils (i.e. sandy soil containing organic contents greater than 2 percent or pH less than 5), cement may be used for stabilization of a vast array of soils. Soil gradation is a crucial design consideration as it controls the amount of cement required in the mix design. For economic reasons in soil stabilization projects, the amount of fines (i.e. particles smaller than 0.08 mm) is normally limited to 5 to 35 percent to control the amount of the required cement (ACI (1990)).

As cement paste provides the binding capacity between soil particles, increases in the cement content normally results in improvements in the mechanical and hydraulic properties of the final product (Felt & Abrams (1957), ACI (1990)). The cement content typically ranges from 3 to 16 percent (i.e. weight of cement/weight of the dry soil) in soil-cement applications (BRAB (1969)).

Assuming the soil type and cement content are fixed for a mix design, the structure and performance of the final product is greatly influenced by the available water at the time of mixing (i.e. w/c ratio). In addition, the structure of soil-cement evolves with time due to cement hydration being a slow process, resulting in improvements in its performance. A brief description of the influence of water content and curing time on the mechanical (i.e. unconfined compressive strength (UCS)) and hydraulic (i.e. hydraulic conductivity) performance of soil-cement follows.

2.5.1. Mechanical Properties

2.5.1.1. Influence of Water Content in the Mixture

The influence of w/c ratio on the porosity of the cement paste and consequently strength development in concrete is well documented (Popovics & Ujhelyi 2008). According to Abram's theory (Abrams 1919), provided that a minimum w/c ratio required for the hydration of available cement and the workability of concrete is met, increases in the w/c ratio results in a reduction of strength in the paste.

Aderibigbe et al. (1985) showed a bell shape relation between w/c ratio and UCS for cement-treated compacted clay, with optimum w/c ratios ranging approximately from 0.4 to 2.6 depending on the cement content in the mix design. The relationship between the OWC to achieve maximum UCS and density in cement-treated compacted clay was studied by Horpibulsuk et al. (2010) and showed that the maximum UCS occurred at a water content about 1.2OWC measured from proctor test results (i.e. maximum density). For non-plastic cement-treated soils, however, observations by Felt (1955) showed that the maximum UCS occurs at dry of OWC obtained from standard proctor test on the soil-cement blend. Guney et al. (2006) reported similar observation on cemented non-plastic soils (i.e. foundry sand) for w/c ratios ranging from 2% dry of, to 2% wet of the OWC, showing a general decreasing trend for UCS values with the increase of water content in the mix design.

2.5.1.2. Influence of Curing Age

The structure of cement-based materials evolves with time as a result of the continuing cement hydration process. This results in an increase in the strength of the cement-treated soils because of the improved binding capacity of cement paste (ACI (1990)). Shihata & Baghdadi (2001a) studied the variation of UCS values for three compacted soil-cement mix designs (i.e. S1, S2, and S3 in Figure 2.3) for a curing (submerged in saline water) period of up to 180 days. Results showed a steep increase in the UCS values in the initial 28 days (similar to concrete), after which a much slower rate was observed.

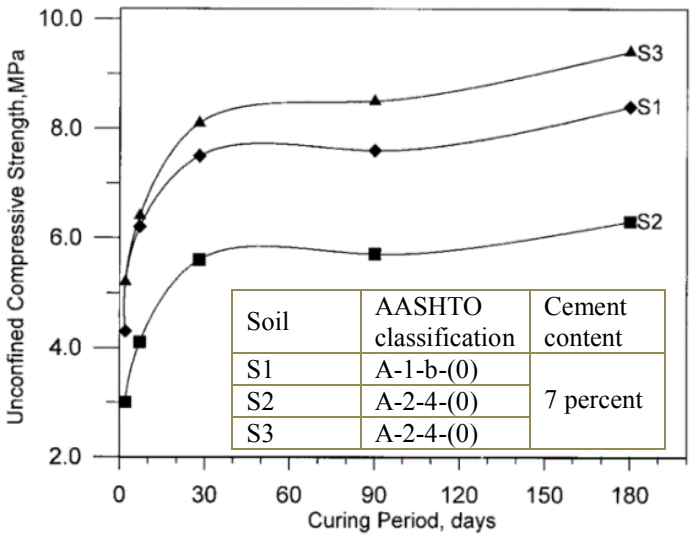

Figure 2.3: Changes in UCS values of compacted soil-cement over a curing period of 180 days (modified from Shihata & Baghdadi (2001a)).

2.5.2. Hydraulic Properties

2.5.2.1. Influence of Water Content in The Mixture

Studies on cement paste by Powers et al. (1954) showed that the permeability of cement paste can exponentially increase at w/c ratios above 0.4. In addition to its influence on the paste structure, the amount of water in a soil-cement mixture (i.e. w/c ratio) plays an important role in the mixing efficiency of the material and its final texture. At very low water contents (i.e. dry of OWC), air voids might form in the structure of hardened product due to the lack of lubrication between soil particles (and hence low compaction efficiency), resulting in possible increases in the hydraulic conductivity. Increased hydraulic conductivity for water contents dry of OWC has been previously reported for compacted clay by Mitchell et al. (1965) and Boynton & Daniel (1985). On the other extreme, high water contents in a soil-cement mixture may lead to bleeding in the paste. This can consequently create highly porous areas within the paste and essentially increase the hydraulic conductivity value of soil-cement.

Systematic studies available in the literature on the hydraulic performance of cement-treated soils are limited. Bellezza & Fratalocchi (2006) performed hydraulic conductivity measurements on cement-treated soils compacted slightly wet of OWC from standard proctor tests. Results were compared to the hydraulic conductivity values of un-cemented soils with similar water contents. Reductions in the hydraulic conductivity values were observed after addition of 5% cement to most soils, with the exception of the high plasticity clayey soils which exhibited increased hydraulic conductivity values. Hammad (2013) showed that the molding water plays an important role in the resulting hydraulic conductivity values. This study suggested the minimum hydraulic conductivity may occur in water contents ranging from 2 to 6 percent wet of OWC.

2.5.2.2. Influence of Curing Age

Permeation of water in cement paste predominantly occurs through capillary pores and air voids. During the progression of the hydration process, newly formed C-S-H gel products occupy parts of the capillary pores, resulting in a decrease in the effective porosity of the paste and subsequently its hydraulic conductivity. A reduction of over six orders of magnitude in the hydraulic conductivity of cement paste was reported by Powers et al. (1954) during the first 24 days of the curing process. Decreasing trends in the hydraulic conductivity of compacted soil-cement was also reported by Bellezza & Fratalocchi (2006) for a measurement period of up to 35 days.

2.6. Durability of Cement-Treated Soils

A successful soil-improvement process requires the final product to retain its properties over the service life of the project. Previous studies have shown several environmental factors such as chemical attack, cycles of w/d, as well as exposure to f/t cycles may influence the structure of stabilized soils (Klich et al. (1999); Fitch & Cheeseman (2003); PASSiFy (2010)). In the design of cement-treated soils, resistance to w/d and f/t cycles (resulting in creation of cracks in soil-cement structure due to shrinkage and expansion of

pore water during the freezing process, respectively) are routinely considered as an indicator of the durability of these materials.

Comparing the results of mass loss from w/d and f/t standard tests in previous studies (e.g. Felt (1955); Al-Tabbaa & Evans (1998)) suggest that f/t resistance may be a dominant factor in evaluating the durability of cement-treated materials. Shihata & Baghdadi (2001a) compared results of w/d and f/t experiments on compacted soil-cement according to standard methods (i.e. ASTM-D559 (1996) (withdrawn in 2012) and ASTM-D560 (2003)). After exposure to 12 cycles of w/d and f/t, specimens were tested for UCS values (i.e. residual UCS). Figure 2.4 shows that specimens with similar mix designs exhibited lower residual strength after f/t exposure compared to w/d tests. This also shows that f/t durability can be a stricter criteria in the design of cement-treated soils.

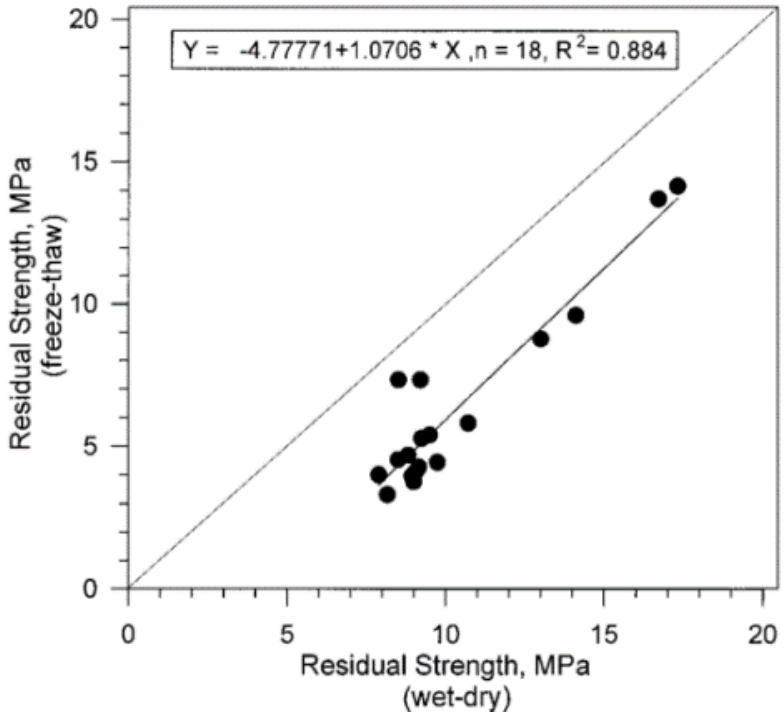

Figure 2.4: Comparison of changes in the residual strength for specimens exposed to f/t (ASTM-D560 (2003)) and w/d (ASTM-D559 (1996)) cycles (Shihata & Baghdadi (2001a)).

Damage due to f/t exposure can occur during the construction (i.e. early curing ages) of soil-cement or at a later time when the hydration process is near completion. As a result, evaluation of cement-treated materials in areas where exposure to f/t cycles are concerned should consider both exposure scenarios with regards to curing age.

2.7. Mechanisms of F/T Damage in Cement-Based Materials

Near-saturated cement-based materials are susceptible to degradation under exposure to f/t cycles, mainly due to the expansion of water during the freezing process. Initiation of damage depends on the tensile strength of the material and occurs through the "weakest link" in the structure (i.e. aggregates, cement paste, or ITZ). A photomicrograph of a concrete sample damaged due to frost action is shown in Figure 2.5 (Koskiahde (2004)). The micro-crack/crack formations can be seen (light lines in the image) meandering through different phases of the material.

It should be noted that the freezing temperature for the water in a porous system depends on the dimensions of the pores (Gibbs–Thomson law). For instance, in pores of 10^{-6} cm, water freezes at temperatures below -5ºC, while in pores of 3.5×10^{-7} cm a temperature below -20ºC is required for freezing the pore water. As a result, in practical construction weather conditions water in the gel pores doesn't freeze (Mindess et al. (2003)).

In this section, some of the popular theories developed in the concrete literature to explain mechanisms of damage development in cement paste and aggregates during f/t exposure are presented.

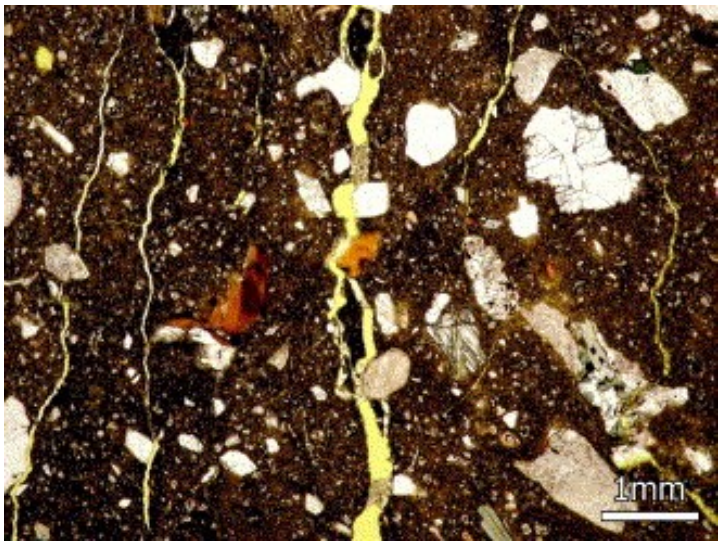

Figure 2.5: Photomicrograph of a frost damaged concrete (Koskiahde (2004)).

2.7.1. Damage Mechanisms in Cement Paste

2.7.1.1. Hydraulic Pressure Theory (Powers & Willis (1949))

Powers & Willis (1949) proposed one of the early theories in explaining frost damage in cement paste. According to this theory, when cement paste is subjected to sub-zero temperatures, a homogeneous formation of ice nuclides occur in the capillary pores with the proper size (as the freezing temperature in pores depends on the dimensions of the pore). Frozen water expands and under near-saturated conditions creates excess pore water pressures in the capillary pores. To release this created pressure, water in the capillary pores is pushed towards the adjacent pore structures. The magnitude of the resulting hydraulic pressure can be calculated using the following equation (Chatterji (2003)):

$$P = a\left(1.09 - \frac{1}{S}\right).\frac{uR}{k}.\left(\frac{L^3}{r_b} + \frac{3L^2}{2}\right) \qquad \text{Equation 2.3}$$

where:

P: hydraulic pressure, Pa

a: a factor mainly depending on the viscosity of the water, kg/m.s

S: degree of saturation for cement paste

u: the amount of water (kg) in one kilogram of cement paste which freezes when the temperature of the paste is reduced by 1 degree, kg/kg.^{o}C

R: freezing rate, ^{o}C/s

k: intrinsic permeability of the paste, m^2

r_b: average value for the radius of air bubbles, m

L: shortest distance between two air bubbles (spacing factor), m

Based on this theory, damage occurs when the induced pressure, P, exceeds the bursting strength of the material. Considering Equation 2.3, the highest degree of damage due to frost action can occur at full saturation of the matrix (i.e. S=1). Also if the saturation coefficient falls below 0.917, the value of P becomes negative, which means that no disruptive pressure can develop. This equation also suggests that air-entrainment may improve the performance of the paste under f/t exposure, by decreasing the shortest distance between air bubbles (L) (Chatterji (2003)).

2.7.1.2. Modified Hydraulic Pressure Theory (Powers & Helmuth (1953))

Powers & Helmuth (1953) realized that the proposed hydraulic pressure theory couldn't explain some observations such as continued dilation of non-air-entrained paste during the extended freezing of specimens at constant temperatures. They proposed a modified version of the hydraulic pressure theory to account for these observations.

According to Powers & Helmuth (1953) when cement paste is at 0^{o}C, the ice in capillary pores is in thermo-dynamic equilibrium with the water in gel pores. When the temperature drops, the energy balance between gel water and the ice in capillary pores is disturbed due to differences in energy loss between ice and water during temperature changes. To achieve thermo-dynamic equilibrium, gel water with higher free energy moves towards the ice with lower free energy. Movement of water towards the capillary pores causes the desiccation and thus shrinkage of the gel pores in the paste. In addition, it can contribute to the ice growth in capillary pores and development of hydraulic pressure in the paste. Since the

process of water expulsion from gel pores is very slow, extended exposure to freezing conditions may result in increased degradation of the paste.

2.7.1.3. Micro-Ice-Lens Model by Setzer (2001)

Setzer (2001) observed that in some cases, many cycles of f/t exposure are required to create damage in concrete specimens. This could not be explained by the available mechanisms at the time. He proposed a "pumping effect" in his micro-ice-lens model to explain these observations. He considered a three phase (i.e. ice, water and vapor) thermo-dynamic equilibrium model as the base of his theory. According to Setzer (2001), as the temperature is reduced below 0^{o}C, water in capillary pores starts to freeze resulting in movement of water from gel pores towards the ice. This causes an increase in the degree of saturation in capillary pores as well as desiccation and shrinkage of gel pores. Depending on the initial degree of saturation of capillary pore and the length of the freezing time, inflow of water and expansion of ice crystals may result in development of some damage in the paste.

As the temperature of the frozen paste increases (i.e. thawing process), ice on the exposed surface of the paste melts first. While ice in the large pores remains frozen in subzero temperatures, negative pressure in gel pores near the surface can draw water from exposed surfaces. This results in an increase in the degree of saturation of gel pores, while the degree of saturation in capillary pores remains unchanged. The whole process results in an increase in the total degree of saturation of the paste after one f/t cycle. As a result, the so called "pumping effect" makes the paste more susceptible to consequent f/t exposures.

2.7.2. Damage Mechanisms in Aggregates

Verbeck & Landgren (1960) suggested that the hydraulic pressure theory presented by Powers & Willis (1949) may also be applied to explain the mechanisms of aggregate damage during frost action. According to this theory, for damage to occur, an aggregate should be critically saturated (i.e. over 92 %) during the freezing process. Saturation of aggregates largely depends on their internal porosity and pore size distribution, as well as

permeability and thickness of the paste (i.e. distance to the wet surface) as the pathway for the inflow of water.

When a critically saturated aggregate is exposed to freezing conditions, hydraulic pressure may develop within its pore structure. Resistance of the aggregate to the developed hydraulic pressure depends on its tensile strength and its ability to transfer the hydraulic pressure to the surrounding paste. The latter parameter may be influenced by the size of the aggregate (i.e. affecting the travel distance), permeability of the aggregate (to transfer the pressure to adjacent pores), as well as the permeability of the surrounding paste to accommodate the inflow of excess water.

2.8. Standard Methods for Evaluation of F/T Resistance of Cement-Treated Soils

Soil-cement test methods have been mainly designed to satisfy the requirements for frost heave, bearing capacity, or other strength related parameters commonly used in the pavement industry as one of the major applications for these materials. For instance, ASTM-D560 (2003) suggests percent mass loss due to brushing as an indicator of f/t resistance of compacted soil-cement exposed to repeated f/t cycles. Apart from possible human induced errors resulting in reproducibility issues, this standard may be relevant to the changes in the mechanical performance of soil-cement as mass loss depends on tensile (and subsequently compressive) strength of the materials.

As the application of cement stabilization expanded into areas such as liner systems and contaminant containment/immobilization (e.g. cement-based s/s), percent mass loss has also been suggested as an indicator for assessment of these materials under f/t exposure. Examples include ASTM-D4842 (1996) (withdrawn standard) suggested by Stegemann & Côté (1996), ASTM-D560 (2003) suggested by Paria & Yuet (2006), and ASTM-C1262 (2010) suggested by ITRC (2010). However, mass loss doesn't adequately represent the internal damage (i.e. cracks/micro-cracks) responsible for changes in hydraulic conductivity and leaching properties of these materials (El-Korchi et al. (1989)).

A summary of methodologies suggested by ASTM-D560 (2003) and ASTM-D4842 (1996) is presented in this section.

2.8.1. ASTM-D560 (2003)

In this standard, 7-day cured compacted soil-cement specimens (prepared according to ASTM-D558 (2011)) are exposed to 12 cycles of freezing at -23ºC for 24 hours and subsequent thawing at 21ºC for 23 hours. Specimens are placed on 6 mm thick water-saturated pads to allow absorption of water during the test (i.e. open system conditions). At the end of each f/t cycle, specimens are brushed (18 to 20 strokes covering all the surfaces twice) and the mass changes are recorded. Percent mass loss based on the oven dried mass after the 12^{th} f/t cycle is reported at the end of the experiment. ASTM-D560 (2003) doesn't provide any acceptable limit of mass loss, however durability criteria for this test have been proposed by PCA (1992) and the Joint Departments of the Army and Air Force (1994) (with the condition of omitting wire brushing from the standard) for different soil types as presented in Table 2.2.

While simple, one of the problems associated with the use of this standard test method is the human induced variations due to brushing of the specimens at the end of each cycle.

Table 2.2: Durability requirements for f/t resistance of cement-stabilized soils.

Type of soil stabilized	Maximum allowable mass loss, percent	
	Joint Departments of the Army and Air Force (1994) (without brushing)	PCA (1992)
Granular, PI<10	11	14
Granular, PI>10	8	10
Silt	8	10
Clay	6	7

2.8.2. ASTM-D4842 (1996)

Intended to examine the f/t resistance of monolithic cement-treated wastes, ASTM-D4842 (1996) (withdrawn in 2006) suggested exposing 44 mm in diameter and 74 mm in length

cylindrical specimens to 12 cycles of freezing at -20°C for 24 hours and thawing (submerged) at 20°C for 23 hours. Specimens are either cut from a larger sample, or molded after mixing according to ASTM-C305 (2013). Molded specimens are cured for 28 days prior to f/t exposure. At the end of each thawing phase, loose particles are washed off the specimens by spraying water from a wash bottle. While this standard doesn't provide any acceptance criteria for mass loss, Stegemann & Côté (1996) suggested 10 percent mass loss as the maximum limit for f/t resistibility in cement-based s/s materials.

2.9. Strength and Hydraulic Performance Changes in Cement-Stabilized Soils Due to F/T Exposure

Due to the uncertainties and human induced errors attributed to mass loss measurement during f/t studies, many investigations have incorporated performance measurements in durability studies of soil-cement. Some examples of these studies are provided in the following sections for compacted and plastic soil-cement.

2.9.1. Compacted Soil-Cement

2.9.1.1. Strength Performance

Dempsey & Thompson (1973)

Dempsey & Thompson (1973) performed extensive laboratory studies to examine if the rapid and economical method of vacuum saturation could be used as an alternative test method for predicting changes in the performance of stabilized soils due to f/t exposure. Compacted cement, lime, or lime-fly ash stabilized soils (102×117 mm or 51×102 mm cylinders) cured for up to 7 days were subjected to 5 and 10 one-dimensional f/t cycles, with temperatures varying between -6°C and 4°C, for a total cycle length of 48 hours. UCS tests were performed on the specimens after f/t exposure. Another set of specimens, with similar mix designs, were vacuum saturated after the curing period and also tested for UCS. Dempsey & Thompson (1973) found a strong correlation between the UCS values from vacuum saturated and f/t exposed specimens as presented in Figure 2.6.

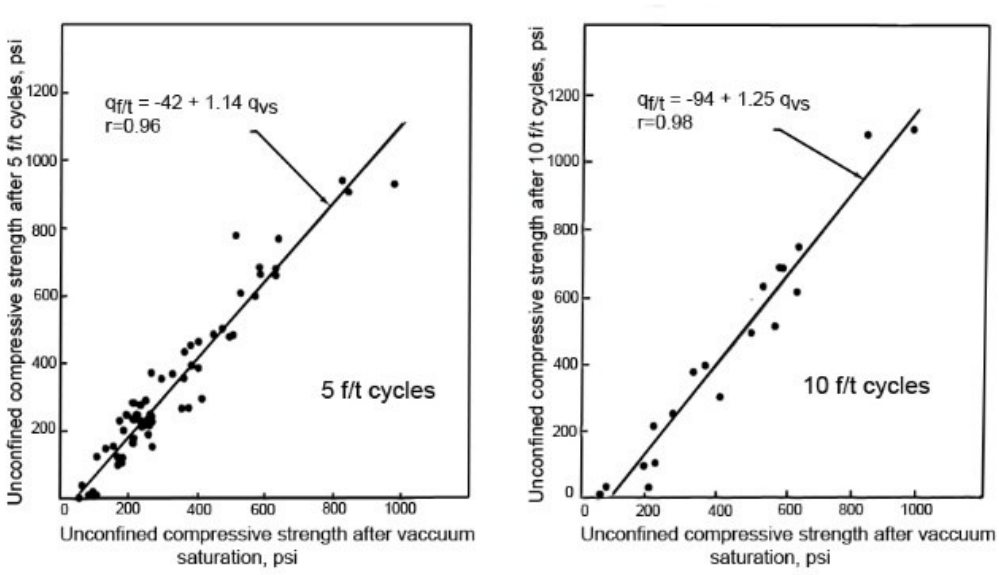

(a) (b)

Figure 2.6: Relationship between UCS values of vacuum saturated specimens and specimens exposed to a) 5 and b) 10 f/t cycles (modified from Dempsey & Thompson (1973)).

Dempsey & Thompson (1973) performed another set of tests to examine changes in UCS values of vacuum saturated soil-cement specimens after exposure to 3, 6, 9, and 12 f/t cycles. Results are presented in Figure 2.7 and show a 300 psi (2.1 MPa) reduction in UCS values after vacuum saturation without any f/t exposure (i.e. control conditions). After the f/t exposure, only specimens exposed to 9 cycles, exhibiting approximately 550 psi (3.8 MPa) reduction in UCS, showed significantly different values for UCS compared to the vacuum saturated conditions (with a reduction of about 300 psi (2.1 MPa)). For cycles 3, 6, and 12, a decrease of about 200 psi (1.4 MPa) in UCS values were observed, a value slightly less than the 300 psi (2.1 MPa) reduction observed after the vacuum saturation, indicating possible structural repair in the specimens.

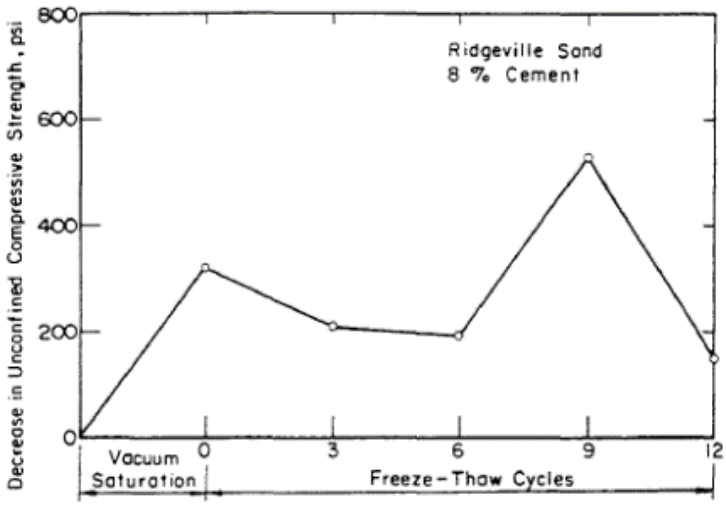

Figure 2.7: Reductions in the UCS value of vacuum saturated compacted soil-cement due to f/t cycles (Dempsey & Thompson (1973)).

Shihata & Baghdadi (2001a) and Shihata & Baghdadi (2001b)

Shihata & Baghdadi (2001b) compared the results of mass loss of the brushing test (ASTM-D560 (2003)) to UCS measurements on 7-day cured specimens, as well as to unbrushed residual UCS values. Unbrushed residual UCS was defined as the compressive strength of the specimens exposed to 12 f/t cycles (i.e. freezing at -10^{o}C and thawing at room temperature for a total cycle length of 44 hours), without performing the brushing test. Strong correlation between the results (Figure 2.8) showed UCS measurements may have the potential to replace the brushing test suggested by ASTM-D560 (2003).

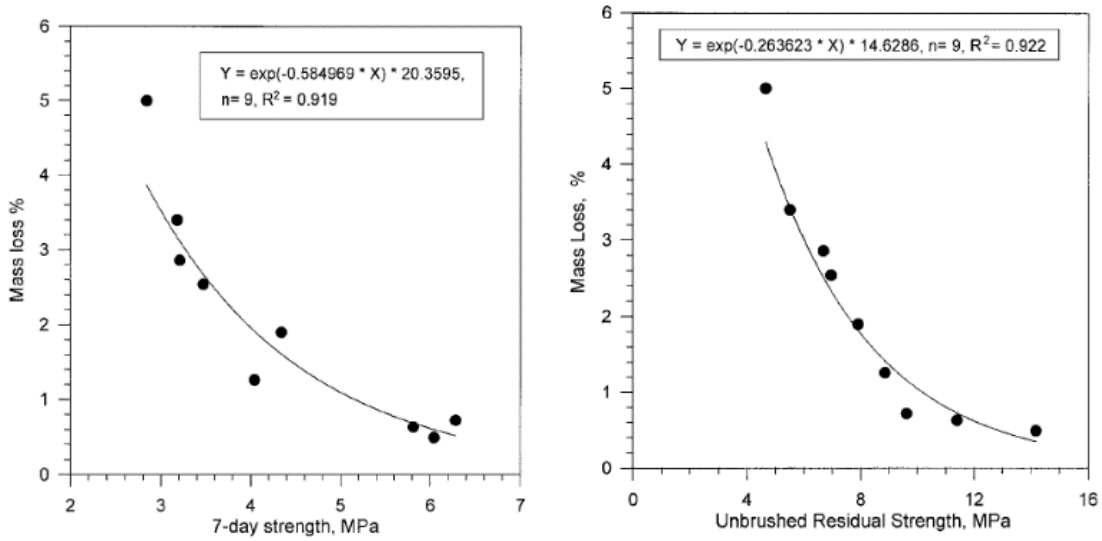

Figure 2.8: Correlation of mass loss after brushing test with 7-day UCS (left) and unbrushed residual UCS (right) for compacted soil-cement (Shihata & Baghdadi (2001b)).

Shihata & Baghdadi (2001a) also compared performance of compacted soil-cement specimens exposed to f/t cycles at various curing ages. Specimens were prepared by stabilizing three soils (i.e. S1, S2, and S3 classified as A-1-b(0), A-2-4(0), and A-2-4(0), respectively, according to AASHTO soil classification) using 7 percent Portland cement in the study. Specimens were immersed in saline water for 7, 270, and 360 days before f/t exposure. Percent mass loss due to the brushing, unbrushed residual UCS, and brushed residual UCS of specimens after f/t exposure according to ASTM-D560 (2003) were measured at each curing level. Figure 2.9 and Figure 2.10 present the results of the study showing that specimens cured for 7 days performed remarkably better, as compared to specimens cured for longer times.

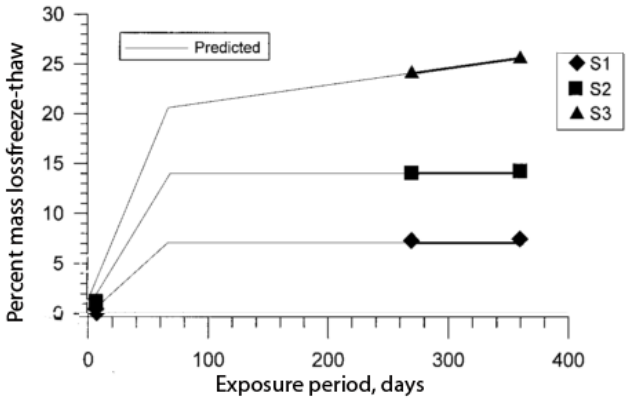

Figure 2.9: Influence of curing age (i.e. exposure period) on percent mass loss of specimens after exposure to 12 cycles of f/t (Shihata & Baghdadi (2001a)).

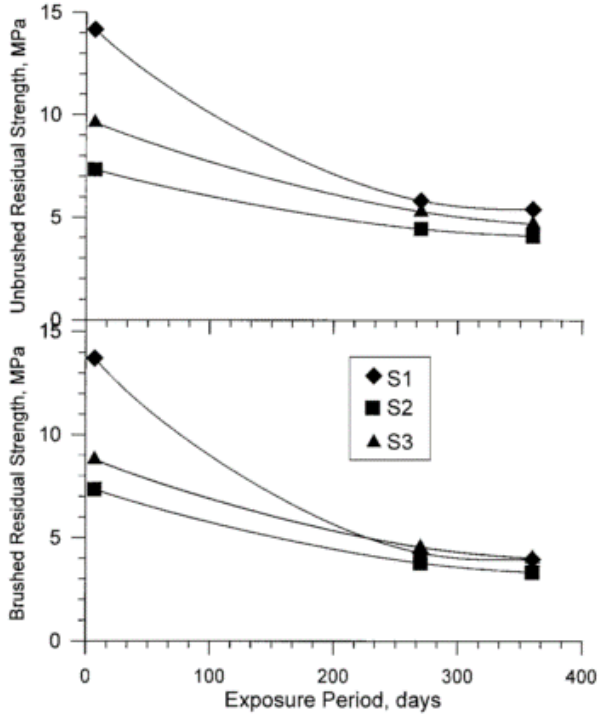

Figure 2.10: Influence of curing age (i.e. exposure period) on residual UCS (brushed and unbrushed) of specimens after exposure to 12 cycles of f/t (Shihata & Baghdadi (2001a)).

Guney et al. (2006)

Guney et al. (2006) conducted f/t studies on foundry sand stabilized by the addition of 5% cement and compacted at standard proctor OWC. F/t exposure consisted of exposing 7-day cured specimens to -23°C for 24 hours and thawing them at room temperature for 23 hours for a total of 8 f/t cycles. UCS measurements were performed for control conditions (i.e. cycle 0) and subsequently at cycles 1, 4, and 8. Results showed a reduction of about 40 percent in UCS values after the initial f/t cycle, with negligible changes from this initial decrease after subsequent f/t exposures.

2.9.1.2. Hydraulic Performance

Guney et al. (2006)

Guney et al. (2006) also examined changes in the hydraulic conductivity of compacted soil-cements at different f/t cycles. Similar to their observations for UCS, higher increases in hydraulic conductivity values were noted after the initial f/t exposure. Hydraulic conductivity values showed increasing trends, albeit at slower rates, at subsequent f/t cycles. For cement-stabilized specimens compacted at OWC with 5% cement, about 20 fold increase in hydraulic conductivity values were observed after the 8^{th} f/t cycle. Mass loss for the same mix designs were reported to be less than 14 percent.

Shea (2011)

Shea (2011) studied the f/t exposed hydraulic conductivity of six soils, each stabilized at three cement contents ranging from 1 to 14 percent in order to achieve target 7-day UCS values close to 200, 400, and 600 psi (1.4, 2.8, and 4.1 MPa, respectively). Specimens were compacted at standard proctor OWC and cured for 28 days prior to one cycle of f/t exposure. Freezing was performed in two phases. Initially, specimens were frozen one-dimensionally at a temperature of approximately -7°C for 10 days. Specimens were then transferred to a chest freezer at a temperature of -17°C for 24 hours to ensure complete freezing. At the conclusion of the freezing phases, specimens were thawed and tested for hydraulic conductivity under constant head conditions using a rigid wall permeameter.

Exposed hydraulic conductivity values were compared for different cement contents. Results showed both increasing and decreasing trends, depending on the soil type, as a result of increased cement content in the mix design.

Step-wise multivariable regression analysis was performed on the results, and a relation was proposed to predict the exposed hydraulic conductivity values after 1 f/t cycle based on basic soil characteristics, cement content, and the 7-day UCS value. The proposed equation based on the unified soil classification system (USCS) resulting in the best correlation coefficient compared to other proposed models is shown below:

$$k=184.91 - 137.94(P_{100}) - 11.786(Ln(UCS)) + 16.134(D_{10})(UCS) + 1089.9(D_{60})(SG) - 19.094(D60)(\gamma_d) + 12.822(Ln(P_{100}))(Ln(UCS)) + U \quad \text{Equation 2.4}$$

where:

K: hydraulic conductivity of exposed specimen, ft/day

P_{50}: material passing the No. 50 sieve, percent

UCS= 7-day unconfined compressive strength, psi

D_{10}: soil particle diameter at which 10 percent is finer, in

D_{30}: soil particle diameter at which 30 percent is finer, in

D_{60}: soil particle diameter at which 60 percent is finer, in

γ_d: dry density, lb/ft^3

SG: apparent specific gravity of the soil particles

P_{100}: material passing the No. 100 sieve, percent

U: USCS reference value (Table 2.3)

C: cement content, percent (dry weight)

Table 2.3: Suggested values for U in Equation 2.4 based on the USCS soil classification (Shea (2011)).

Classification	Coefficient
GP-GM	-50.392
GW	-128.80
ML	-62.353
SM	14.139
SP	0.00

2.9.2. Plastic Soil-Cement

Changes in the mechanical and hydraulic performance of plastic soil-cement after f/t exposure appears to have been the subject of very few studies. Results of laboratory studies performed by Pamukcu et al. (1994) are presented in this section.

Pamukcu et al. (1994)

Pamukcu et al. (1994) investigated the influence of f/t exposure on the performance of cement-stabilized dewatered sludge residues. Specimens, in the form of a thick slurry, were prepared at 16 and 20 percent (wet weight) cement contents and 0.78 to 1.2 water to cement (w/c) ratios. For unexposed specimens, UCS values ranged from 1.01 to 13.97 MPa and hydraulic conductivity values ranged from 6.6×10^{-9} m/s to 1.5×10^{-10} m/s after curing for 28 days. F/t studies were mainly focused on changes in the UCS values, as well as mass loss in accordance with ASTM-D4842 (1996). While UCS ratios (i.e. f/t exposed UCS divided by control UCS values) of 0.81 to 1.44 were reported after f/t exposure, percent mass loss data was below 1.3, with many cases exhibiting no changes. Four specimens tested for hydraulic conductivity after f/t exposure showed minor reductions as well as increases of up to two orders of magnitude compared to unexposed conditions. Although no correlation between UCS and hydraulic conductivity changes were presented, the authors suggested that a high initial strength may have the potential to mitigate the formation of cracks and micro-cracks attributed to changes in the effective porosity,

resulting in minimal increases in the hydraulic conductivity of the cement-treated materials.

2.10. Influence of F/T Exposure on the Hydraulic Conductivity of Compacted Clay

Compacted clay is often used as a low hydraulic conductivity material in various containment applications such as liners for landfills, ponds or lagoons, as well as covers to mitigate ingress of water into landfills or contaminated sites after the remediation. A maximum hydraulic conductivity of 1×10^{-9} m/s is typically considered necessary for the field performance of compacted clay (Benson et al. (1999)). Benson et al. (1995) showed that un-insulated compacted clay can undergo 1 to 10 cycles of f/t during a winter season in Wisconsin, USA. Changes in hydraulic conductivity of compacted clays exposed to f/t cycles have been the focus of many studies such as Kim & Daniel (1992), Othman & Benson (1992), and Othman & Benson (1993). A comprehensive review of the available literature in this field is presented by Othman et al. (1994).

While compacted clay is intrinsically different from soil-cement, in the absence of relevant studies on the influence of f/t exposure on hydraulic performance of soil-cement, available literature on compacted clay can provide some insight for the design of similar test methods to assess performance of cement-stabilized materials under f/t exposed conditions.

2.10.1. Mechanism of F/T Damage in Compacted Clay

In compacted clay, similar to cement paste, ice crystal nucleate at sub-zero temperatures and start to grow in larger pores within the clay structure. Due to the suction pressure developed adjacent to the ice phase, water moves towards the ice resulting in the formation of ice lenses in the clay. During this process, contrary to the case of stronger cement paste, the pressure applied to the clay particles causes them to move, rearrange, and consolidate (Kim & Daniel (1992)). The formation of ice lenses observed by Othman & Benson (1993) in thin sections prepared from frozen clay samples is presented in Figure 2.11. When ice lenses melt (during the thawing phase), micro-cracks/cracks remain in the clay's structure which can result in an increase in the hydraulic conductivity of the exposed materials.

Increases of up to three orders of magnitude in hydraulic conductivity of compacted clay exposed to f/t cycles have been reported in the literature (e.g. Kim & Daniel (1992), Othman & Benson (1992); Othman & Benson (1993)).

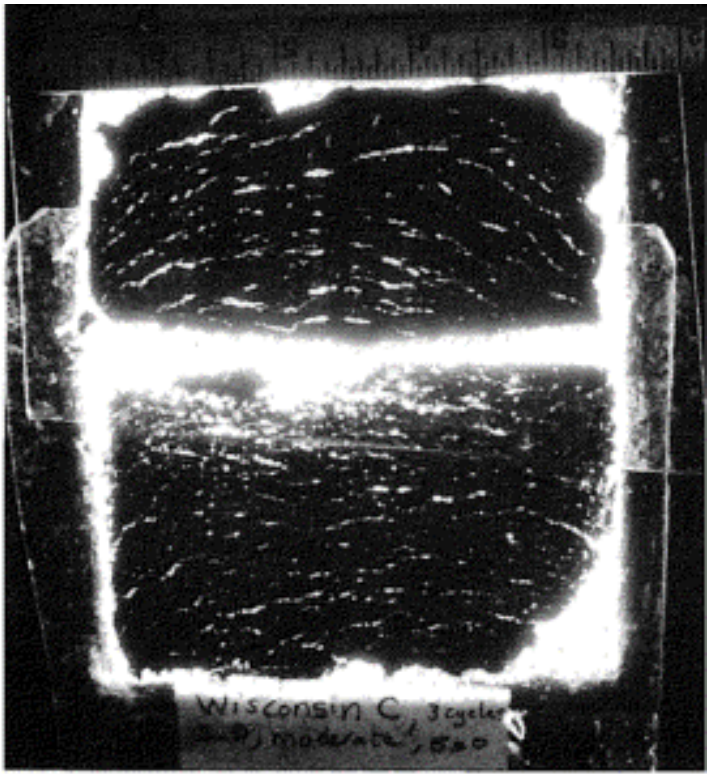

Figure 2.11: Ice lens formation shown on a thin section prepared from a frozen clay specimen (Othman & Benson (1993)).

2.10.2. Laboratory Investigation of F/T Effect on Compacted Clay

Several methods have been developed to perform f/t studies on clay specimens. These include (see Othman et al. (1994) for details): using the United States Army Cold Regions Research and Engineering Laboratory (CRREL) consolidometer (Chamberlain et al. (1990)); using a flexible wall permeameter set-up (ASTM-D6035 (2008)); covering the perimeter of specimens with fiberglass and styrene during the freezing process to enforce one-dimensional freezing; and placing the specimens directly in a temperature controlled environment without any thermal insulation. Advantages and disadvantages of each of these methods according to Othman et al. (1994) are presented in Table 2.4. The influence

of testing conditions on the observed changes in hydraulic conductivity of compacted clay is also discussed in great detail by Othman et al. (1994). A summary of these conclusions is presented in Table 2.5.

Table 2.4: Summary of advantages and disadvantages of different f/t testing methods for compacted clay (Othman et al. (1994)).

Method	Advantages	Disadvantages
CRREL Consolid-ometer	• minimal specimen disturbance • precise control of temperature gradient • one-dimensional freeze-thaw • closed- or open-system of freezing • simulates overburden pressure	• side-wall leakage possible under low overburden pressure • expensive • complicated
Flexible-Wall Permeameter	• minimal specimen disturbance • simulates overburden pressure • no side-wall leakage • inexpensive • commercially available	• temperature gradient is difficult to control • three-dimensional freeze-thaw • closed-system of freezing
Fiberglass and Styrene Wraps	• one-dimensional freeze-thaw • simple • inexpensive	• time consuming (takes few days for a single freeze-thaw cycle) • disturbance of specimen possible • closed-system of freezing • temperature gradient is difficult to control • zero overburden pressure
Freestanding Specimen	• simple • inexpensive • fast	• three-dimensional freeze-thaw • disturbance of specimen possible • closed-system of freezing • temperature gradient is difficult to control • zero overburden pressure

Based on the results of various published data, Othman et al. (1994) showed (see Figure 2.12) that compacted clay specimens with higher initial hydraulic conductivity values are less susceptible to damage during f/t exposure. It was contemplated that specimens with high initial hydraulic conductivity were likely compacted at dry of OWC conditions, which resulted in the presence of macroscopic pores in their structure. As a result, under exposed conditions, despite possible formation of cracks in these soils, changes in the pore size distribution were not significantly different from highly porous initial conditions (Othman et al. (1994)). Minor changes in the hydraulic conductivity of

f/t exposed clay compacted dry of OWC compared to materials compacted wet of OWC has been previously reported by Kim & Daniel (1992).

Table 2.5: Influence of various testing conditions on measured changes in hydraulic conductivity of compacted clay exposed to f/t cycles (summarized from the state-of-the-art review presented by Othman et al. (1994)).

Parameter	Observed effect on hydraulic conductivity changes
Number of f/t cycles	- Substantial increase after the initial cycle. - Increase continues at a slower rate at subsequent f/t exposure. - After 3 to 10 f/t cycles, changes become negligible at further exposures.
Availability of water	- No significant difference in hydraulic conductivity changes under closed- and open-system f/t exposure.
F/t dimensionality	- Insignificant difference in observed changes in hydraulic conductivity values for one- and three-dimensional f/t exposure.
Rate of freezing	- Higher freezing rates may result in higher changes in the hydraulic conductivity values. - Rapid freezing can result in higher number of ice lenses compared to slower freezing rates.
Ultimate freezing temperatures	- Minor increase in the hydraulic conductivity changes as the freezing temperature is reduced.
Overburden pressure	- Applying stress after or during f/t exposure can reduces the hydraulic conductivity values, compared to the cases when no pressure is applied.

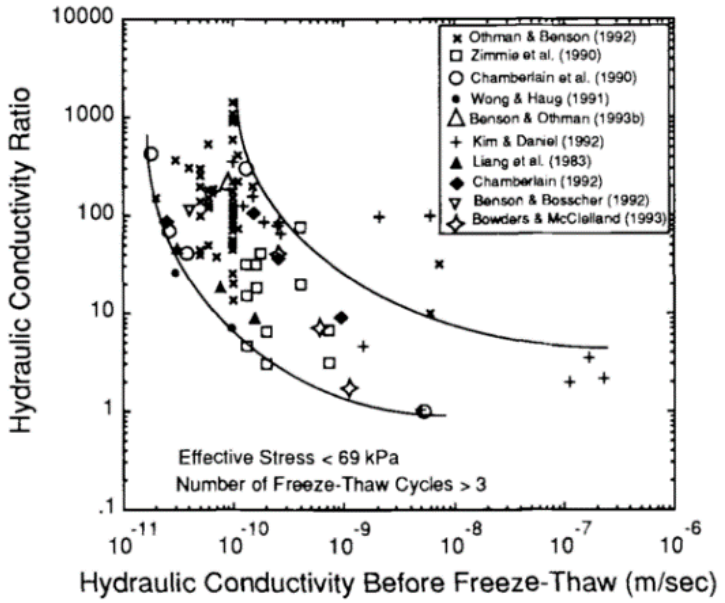

Figure 2.12: Influence of initial hydraulic conductivity on hydraulic conductivity changes observed after f/t exposure of compacted clay (Othman et al. (1994)).

2.11. Application of Non-Destructive Test Methods to Predict F/T Resistance of Cement-Treated Materials

Some of the drawbacks of f/t studies on cement-stabilized materials using available standards include the uncertainty associated with the mass loss measurement, evaluation of the surface damage as opposed to the changes in the internal structure, and the long testing time required. These have encouraged some researchers to examine the application of non-destructive test methods in the evaluation of cement-treated materials subjected to f/t cycles. Non-destructive tests are relatively quick and are routinely used for structural health monitoring purposes in various engineering applications. Studies performed by Kettle (1986) and El-Korchi et al. (1989) on evaluation of f/t exposed cement-treated materials are presented in this section.

2.11.1. Kettle (1986)

Kettle (1986) investigated the effect of 12 f/t cycles (ASTM-D560 (2003)) on compacted soil-cement specimens incorporating 5 to 15 percent cement in their mix design. Results of the brushing tests performed in accordance with the ASTM-D560 (2003) test method were compared to the changes in the resilient modulus of specimens after each f/t cycle. Resilient modulus was measured by applying small amounts of cyclic tension stresses (at 5% of the tensile strength of the material) on the specimens. Observations showed that the mix designs that failed the brushing experiment (i.e. mass loss measurements over 10 percent), exhibited over 40% reduction in the resilient modulus values after 3 cycles of f/t exposure. The proposed technique could significantly decrease the amount of time required to perform f/t durability studies by reducing the number of f/t cycles from 12 cycles (suggested by ASTM-D560 (2003)) to 3 cycles.

2.11.2. El-Korchi et al. (1989)

El-Korchi et al. (1989) used an acoustic continuous-wave non-destructive test (i.e. forced resonance procedure in ASTM-C215 (2008)) to compare the performance of cement s/s materials under various f/t exposure scenarios. Specimens used in this study were beams (2.54×2.54×14 cm) prepared according to ASTM-C305 (2013) by mixing synthesized sludge (with and without cadmium hydroxide as a contaminant) at a w/c ratio of 0.5. Specimens were cured for 28 days under two curing scenarios including moist curing and submersion under saltwater. Exposure included up to 18 f/t cycles following ASTM-C666 (2008), with temperatures ranging from -17.8 to 20^{o}C. Changes in the longitudinal resonant frequency (RF) and quality factor (i.e. damping characteristics) of the specimens were monitored for each mix design and curing condition at various f/t cycles.

An increase in both RF and quality factor of specimens was observed after the initial f/t cycles, suggesting increased integrity of the specimens. However, after 3 to 6 f/t cycles, a decreasing trend in the values was noted, indicating initiation of structural degradation.

2.12. Impact Resonance (IR) Method

Vibration-based non-destructive techniques are routinely used in concrete industry to evaluate the dynamic properties of materials, as well as changes in their structure due to various loading and environmental exposures (e.g. Swamy & Rigby (1971); El-Korchi et al. (1989); Nagy (1997); Shah et al. (2000); Jin & Li (2001); Gheorghiu et al. (2005)); Ababneh & Xi (2006)). ASTM-C215 (2008) suggests two test methods (i.e. forced and impact resonance method) for predicting the dynamic modulus of elasticity, dynamic modulus of rigidity, and dynamic Poisson's ratio of cylindrical or prismatic concrete specimens with a suggested length to transverse direction ratio of two. To perform the test using the IR method, specimens are placed on a support to facilitate easy vibration after excitation and are excited using an impactor (a metal or hard plastic) that can create a short duration impact on the specimen. Vibration signals are collected using an accelerometer attached to the specimen and are processed using a fast Fourier transformation (FFT) to calculate the resonant frequency (RF) values. Figure 2.13 presents the position of the accelerometer and the impact area on a specimen for measuring its dynamic properties under different excitation modes (i.e. transverse, longitudinal, and torsional).

Longitudinal (or transverse) dynamic modulus of elasticity (E_d) of a specimen is directly related to its mass, a constant (i.e. shape factor), and square of its longitudinal (or transverse) RF value:

$$E_d = D \times m \times (RF)^2 \qquad \text{Equation 2.5}$$

where:

E_d: Dynamic modulus of elasticity, Pa

D: Shape factor which equals 5.093 (1/m) in longitudinal mode (or 1.607 (ºC/m) in transverse mode) for cylinders

m: Mass of the specimen, Kg

RF: longitudinal (or transverse) RF of the specimen, Hz

Similarly, the dynamic modulus of rigidity (G_d) is proportional to the mass of the specimen, a shape factor, and square of the torsional RF value of the specimen.

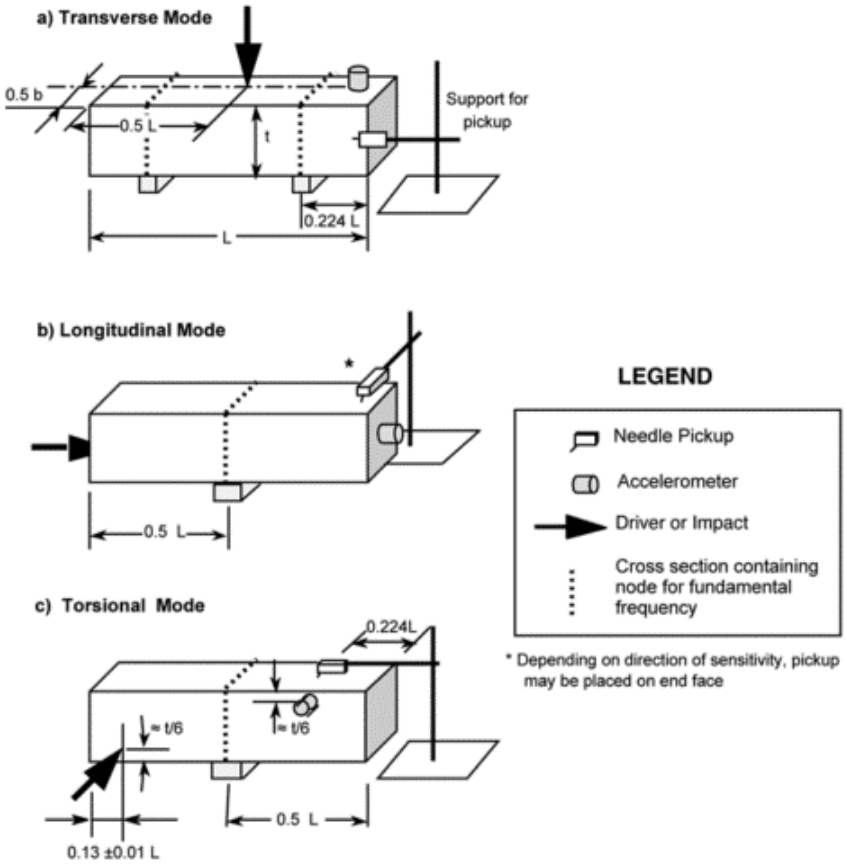

Figure 2.13: Position of the impact area and accelerometer for exciting different vibration modes of a beam as suggested by ASTM-C215 (2008).

Daniel & Kim (2001) used longitudinal RF measurements using the IR method to monitor changes in the dynamic modulus of elasticity of asphalt concrete mixtures exposed to elevated temperatures and cyclic loadings. Both reductions (as a result of the damage development due to fatigue and elevated temperatures) and increases (due to the healing of micro-cracks during rest periods in cyclic loading) in the dynamic modulus of elasticity were observed in the study.

Jin & Li (2001) used longitudinal RF measurements to monitor structural changes in concrete during early curing ages. RF values showed an increasing trend for the 28 day period of the testing, with the main portion of the increase happening in the initial 7 days of curing. Jin & Li (2001) also found a good correlation between the dynamic modulus of

elasticity calculated using the IR method and UCS test results based on the experiments performed on concrete specimens.

ASTM-C666 (2008) suggests monitoring changes in the dynamic modulus of elasticity, calculated using the transverse RF in ASTM-C215 (2008), as an indicator of changes in the integrity of concrete specimens exposed to rapid cycles of f/t.

Assuming the mass and geometric properties of the specimens do not change through f/t exposure (see Equation 2.5), the relative dynamic modulus of elasticity may simply be calculated by dividing the square of fundamental transverse frequency values (RF^2) for exposed specimens to the values measured under unexposed conditions:

$$P_m = \left(\frac{RF_m}{RF_0}\right)^2 \times 100 \qquad \text{Equation 2.6}$$

where:

P_m: relative dynamic modulus of elasticity after m cycles of f/t, percent

RF_0: fundamental transverse frequency before f/t exposure, Hz

RF_m: fundamental transverse frequency after m cycles of f/t, Hz

In ASTM-C666 (2008) the f/t cycling of specimens is terminated if either 300 f/t cycles are completed (i.e. pass), or the relative dynamic modulus of elasticity value of the specimens drops to a value less than 60 percent of the initial value prior to completion of the 300 f/t cycles (i.e. fail).

2.13. Healing Potential in Cement-Based Materials

In one of the earliest observations of autogenous (self) healing in cement-based materials, Abrams (1913) reported that concrete specimens tested for UCS at the age of 7 days, showed an appreciable increase in UCS values (higher than the initial measurements) when tested again at the age of 80 days. Different mechanisms, shown in Figure 2.14, have been reported to result in self-healing of damaged concrete. However, Edvardsen (1999)

suggested that crystallization of calcium carbonate may be the prevailing mechanism in the healing process.

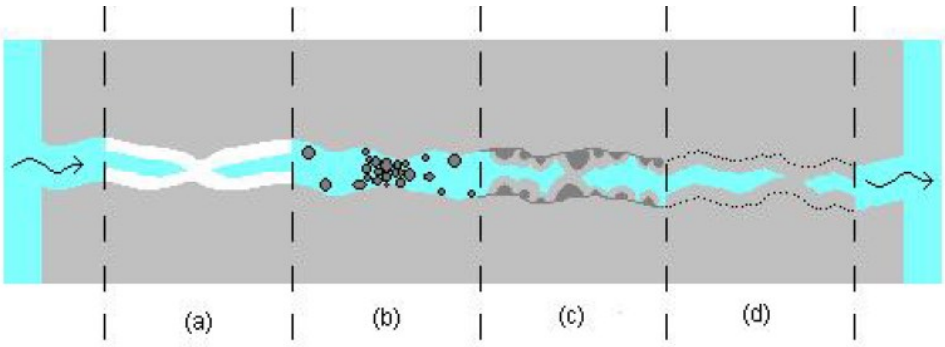

Figure 2.14: Possible mechanisms resulting in autogenous healing of concrete. a) crystallization of calcium carbonates, b) blockage of the flow path by loose particles, c) hydration of unreacted cement, and d) swelling of C-S-H gel (Heide (2005)).

Yang et al. (2009) evaluated the healing potential of concrete specimens (230 mm×76 mm× 13 mm beams) damaged under tensile stress after exposure to w/d cycles, by monitoring changes in the RF and permeability values. Results showed that cracks with widths smaller than 50 μm may gain full recovery, while partial recovery may be achieved for widths as high as 150 μm.

RF measurements were also used by Jacobsen & Sellevold (1996) to assess recovery potential of mature concrete specimens exposed to f/t cycles after up to three months of water submergence. Results were compared to the recovery measurements for UCS values (exposed and cured under similar conditions). Although a complete recovery of RF values for some specimens were observed in the study, UCS measurements showed only minor increases after the post exposure healing period.

2.14. Summary and Conclusions

From the preceding discussion in this chapter, it can be seen that the majority of the available literature on cement-treated materials revolves around compacted soil-cement. This is due to the prevailing application of cement-stabilization in the pavement industry, requiring the material to be compacted at near-optimum water content (OWC) conditions

from proctor tests. The required design objectives for such applications have also directed the performance and durability (i.e. f/t exposure) studies on compacted soil-cement towards mitigation of the frost heave, as well as monitoring strength related parameters such as UCS and the modulus of elasticity. With the increased application of cement-stabilized materials especially in the form of plastic soil-cement, there seems to be a need for the assessment of the treated materials on a wider range of water contents.

Among soil-cement applications, cement-based s/s, as well as cement-treated soils used for hydraulic and contaminant barrier systems require a target hydraulic conductivity value as part of their design and performance objectives. In the presented literature review, it was noted that there are limited systematic studies on the variations of the hydraulic properties of soil-cement at various mix designs and curing ages. Further, it was noted that durability studies for f/t resistance of materials in such applications also suggest percent mass loss as the criteria for monitoring changes during f/t exposure, even though correlations between mass loss and changes in the hydraulic conductivity have not been established.

In the durability studies on various forms of soil-cement (i.e. compacted and plastic) presented in the literature review, it was observed that f/t exposure is usually conducted on specimens cured for less than 28 days. This is potentially the result of an attempt to reduce the length of time required for such tests. However, since the progression of the hydration process in cement-based materials results in the transformation of the material into brittle conditions, conducting f/t tests at early curing ages might provide a false representation of the field conditions, where f/t may occur at later curing stages.

In the literature related to f/t durability of soil-cement, few studies suggested application of non-destructive tests to either reduce the required testing time, or eliminate the need for measuring mass loss as an indicator for changes in the structure of exposed specimens. While the results of these tests, mainly borrowed from the concrete industry, can be used to estimate possible changes in the strength related properties of these materials, no correlation was found to relate the results of non-destructive tests to changes in the hydraulic behavior of cement-treated soils exposed to f/t cycles.

Finally, based on the available literature on concrete, there seems to be a potential for f/t exposed soil-cement materials to recover some of the degraded performance after a period of post-exposure healing. While, it is known that the healing process can occur for small cracks, it may be beneficial to relate healing potential (specifically for hydraulic conductivity) to performance changes and exposure age of the material as a more practical tool for design of cement-treated materials in cold regions.

2.15. References

Ababneh, A.N. and Xi, Y., 2006. Evaluation of environmental degradation of concrete in cold regions. In *Proceedings of Cold Regions Engineering 2006: Current Practices in Cold Regions Engineering*. Edited by M. Davies & J. E. Zufelt. Orono, ME: American Society of Civil Engineers, pp. 1–10.

Abrams, D.A., 1919. *Design of concrete mixtures*, Chicago, IL: Bulletin No. 1, Published by Structural Materials Research Laboratory, Lewis Institute.

Abrams, D.A., 1913. *Test of bond between concrete and steel*, Urbana, IL: Bulletin No. 71, Published by the uinversity of Illinois.

ACI, 1999. *Controlled low-strength materials*, Farmington Hills, MI: Americal Concrete Institute (ACI) Committee 229, ACI229R-99.

ACI, 1990. *Report on soil cement*, Farmington Hills, MI: American Concrete Institute (ACI) Committee 230, ACI230.1R-90.

Aderibigbe, D.A., Akeju, T.A.I. and Orangun, C.O., 1985. Optimal water/cement ratios and strength characteristics of some local clay soils stabilized with cement. *Materials and Structures*, **18**(104):pp.103–108. doi:10.1007/bf02473376.

AECOM, 2013. Sydney Tar Ponds and Coke Ovens site remediation. *Accessed on April 8, 2014 at: http://www.aecom.com/vgn-ext-templating/v/index.jsp?vgnextoid=b5d743dfa94c5310VgnVCM100000089e1bacRCRD&cpsextcurrchannel=1*.

Al-Tabbaa, A. and Evans, C.W., 1998. Pilot in situ auger mixing treatment of a contaminated site. part 1: treatability study. *Proceedings of the Institution of Civil Engineers: Geotechnical Engineering*, **131**(1):pp.52–59. doi:10.1680/igeng.1998.30005.

ASTM-C1262, 2010. Standard test method for evaluating the freeze-thaw durability of dry-cast segmental retaining wall units and related concrete units. In *Annual Book of ASTM Standards*. West Conshohocken, PA: ASTM International. doi:10.1520/c1262-10.2.

ASTM-C215, 2008. Standard test method for fundamental transverse, longitudinal, and torsional resonant frequencies of concrete specimens. In *Annual Book of ASTM Standards*. West Conshohocken, PA: ASTM International. doi:10.1520/c0215-08.2.

ASTM-C305, 2013. Mechanical mixing of hydraulic cement pastes and mortars of plastic consistency. In *Annual Book of ASTM Standards*. West Conshohocken, PA: ASTM International. doi:10.1520/c0305-13.2.

ASTM-C666, 2008. Standard test method for resistance of concrete to rapid freezing and thawing. In *Annual Book of ASTM Standards*. West Conshohocken, PA: ASTM International. doi:10.1520/c0666.

ASTM-D4842, 1996. Standard test method for determining the resistance of solid wastes to freezing and thawing. In *Annual Book of ASTM Standards*. West Conshohocken, PA: ASTM International.

ASTM-D558, 2011. Standard test methods for moisture-density (unit weight) relations of soil-cement. In *Annual Book of ASTM Standards*. West Conshohocken, PA: ASTM International. doi:10.1520/d0558-11.

ASTM-D559, 1996. Standard test methods for wetting and drying compacted soil-cement mixtures. In *Annual Book of ASTM Standards*. West Conshohocken, PA.: ASTM International.

ASTM-D560, 2003. Standard test methods for freezing and thawing compacted soil-cement mixtures. In *Annual Book of ASTM Standards*. West Conshohocken, PA: ASTM International. doi:10.1520/d0560-03.

ASTM-D6035, 2008. Standard test method for determining the effect of freeze-thaw on hydraulic conductivity of compacted or intact soil specimens using a flexible wall permeameter. In *Annual Book of ASTM Standards*. ASTM International. doi:10.1520/d6035-08.2.

Batchelor, B., 2006. Overview of waste stabilization with cement. *Waste Management*, **26**(7):pp.689–98. doi:10.1016/j.wasman.2006.01.020.

Bellezza, I. and Fratalocchi, E., 2006. Effectiveness of cement on hydraulic conductivity of compacted soil–cement mixtures. *Ground Improvement*, **10**(2):pp.77–90. doi:10.1680/grim.2006.10.2.77.

Benson, C.H., Abichou, T.H., Olson, M.A. and Bosscher, P.J., 1995. Winter effect on hydraulic conductivity of compacted clay. *ASCE Journal of Geotechnical Engineering*, **121**(1):pp.69–79.

Benson, C.H., Daniel, D.E. and Boutwell, G.P., 1999. Field performance of compacted clay liners. *ASCE Journal of Geotechnical and Geoenvironmental Engineering*, **125**(5):pp.390–403.

Bone, B.D., Barnard, L.H., Boardman, D.I., Carey, P.J., Hills, C.D., Jones, H.M., MacLeod, C.L. and Tyrer, M., 2004. Review of scientific literature on the use of stabilisation/solidification for the treatment of contaminated soil, solid waste and sludges. *British Environmental Agency*, (SC980003/SR2).

Boynton, S.S. and Daniel, D.E., 1985. Hydraulic conductivity tests on compacted clay. *ASCE Journal of Geotechnical Engineering*, **111**(4):pp.465–478. doi:10.1061/(asce)0733-9410(1985)111:4(465).

BRAB, 1969. *Chemical soil stabilization*, Washington, DC: Building Research Advisory Board, US National Academy of Sciences.

Chamberlain, E.J., Iskandar, I. and Hunsicker, S.E., 1990. Effect of freeze-thaw cycles on the permeability and macrostructure of soils. In *Proceedings of International Symposium on Frozen Soil Impacts on Agricultural, Range, and Forest Lands*. Spokane, WA, pp. 145–155.

Chatterji, S., 2003. Freezing of air-entrained cement-based materials and specific actions of air-entraining agents. *Cement and Concrete Composites*, **25**(7):pp.759–765. doi:10.1016/s0958-9465(02)00099-9.

Daniel, J.S. and Kim, Y.R., 2001. Laboratory evaluation of fatigue damage and healing of asphalt mixtures. *ASCE Journal of Materials in Civil Engineering*, **13**(6):pp.434–440.

Dempsey, B.J. and Thompson, M.R., 1973. Vacuum saturation method for predicting freeze-thaw durability of stabilized materials. In *Highway Research Record 442*. Highway Research Board, US National Research Council, pp. 44–57.

Edvardsen, C., 1999. Water permeability and autogenous healing of cracks in concrete. *ACI Materials Journal*, **96**(4):pp.448–54.

El-Korchi, T., Gress, D., Baldwin, K. and Bishop, P., 1989. Evaluating the freeze-thaw durability of Portland cement-stabilized-solidified heavy metal waste using acoustic measurements. In *Environmental Aspects of Stabilization and Solidification of Hazardous and Radioactive Wastes (STP 1033)*. Edited by P. Côté & M. Gilliam. Philadelphia, PA: ASTM International, pp. 184–191. doi:10.1520/stp22878s.

Felt, E.J., 1955. Factors influencing physical properties of soil-cement mixtures. *Highway Research Board Bulletin*, (108):pp.138–162.

Felt, E.J. and Abrams, M.S., 1957. Strength and elastic properties of compacted soil-cement mixtures. In *Second Pacific Area Meeting Papers (STP 206)*. Philadelphia, PA: American Society for Testing Materials, pp. 152–178.

Fitch, J. and Cheeseman, C.R., 2003. Characterisation of environmentally exposed cement-based stabilised/solidified industrial waste. *Journal of Hazardous Materials*, **101**(3):pp.239–255. doi:10.1016/s0304-3894(03)00174-2.

Fleri, M. A., and Whetstone, G. T., 2007. In situ stabilisation/solidification: project lifecycle. *Journal of Hazardous Materials*, **141**(2):pp.441–56. doi:10.1016/j.jhazmat.2006.05.096

Gheorghiu, C., Rhazi, J.E. and Labossière, P., 2005. Impact resonance method for fatigue damage detection in reinforced concrete beams with carbon fibre reinforced polymer. *Canadian Journal of Civil Engineering*, **32**(6):pp.1093–1102. doi:10.1139/l05-064.

Guney, Y., Aydilek, A.H. and Demirkan, M.M., 2006. Geoenvironmental behavior of foundry sand amended mixtures for highway subbases. *Waste Management*, **26**(9):pp.932–45. doi:10.1016/j.wasman.2005.06.007.

Hammad, A., 2013. *Evaluation of soil-cement properties with electrical resistivity*. M.A.Sc. Thesis, Civil and Resource Engineering Department, Dalhousie Univesity, Halifax, NS.

Hearn, N., Hooton, R.D., and Nokken, M.R, (2006). "Pore structure, permeability, and penetration resistance characteristics of concrete." *Significance of tests and properties of concrete and concrete making.* Edited by: Lamond J.F. and Pielert J.H., The American Society for Testing and Materials, Philadelphia, ASTM STP 169B.

Heide, N., 2005. *Crack healing in hydrating concrete*. M.Sc. thesis, Faculty of Civil Engineering and Geosciences, Delft University of Technology, The Netherlands.

Horpibulsuk, S., Rachan, R., Chinkulkijniwat, A., Raksachon, Y. and Suddeepong, A., 2010. Analysis of strength development in cement-stabilized silty clay from microstructural considerations. *Construction and Building Materials*, **24**(10):pp.2011–2021. doi:10.1016/j.conbuildmat.2010.03.011.

ITRC, 2010. *Development of performance specifications for solidification/stabilization (technical/regulatory guidance)*, Washington, DC: The Interstate Technology & Regulatory Council, Solidification/Stabilization Team.

Jacobsen, S. and Sellevold, E.J., 1996. Self healing of high strength concrete after deterioration by freeze/thaw. *Cement and Concrete Research*, **26**(I):pp.55–62.

Jin, X. and Li, Z., 2001. Dynamic property determination for early-age concrete. *ACI Materials Journal*, **98**(5):pp.365–370.

Joint Departments of the Army and Air Force, 1994. *Soil stabilization for pavements*, Washington, DC: Joint Departments of the Army and Air Force, TM 5-822-14.

Kettle, R.J., 1986. The assessment of freeze-thaw damage in cement stabilized soils. In *Proceedings of Research on Transportation Facilities in Cold Regions (ASCE)*. Edited by O. B. Andersland & F. H. Sayles. Boston, MA, pp. 16–31.

Kim, W. and Daniel, D.E., 1992. Effects of freezing on hydraulic conductivity of compacted clay. *Journal of Geotechnical Engineering*, **118**(7):pp.1083–1097. doi:10.1061/(asce)0733-9410(1992)118:7(1083).

Klich, I., Batchelor, B., Wilding, L.P. and Drees, L.R., 1999. Mineralogical alterations that affect the durability and metals containment of aged solidified and stabilized wastes. *Cement and Concrete Research*, **29**:pp.1433–1440.

Koskiahde, A., 2004. An experimential petrographic classification scheme for the condition assessment of concrete in façade panels and balconies. *Journal of Materials Characterization*, **53**(2-4):pp.327–334. doi:10.1016/j.matchar.2004.09.004.

Mindess, S., Young, J.F. and Darwin, D., 2003. *Concrete;* Second Edi., Upper Saddle River, NJ: Pearson Education, Inc.

Mitchell, J.K., Hooper, D.R. and Campanella, R.G., 1965. Permeability of compacted clay. *Journal of Soil Mechanics & Foundations Division, Proceedings of the ASCE*, **91**(SM4):pp.41–65.

Nagy, A., 1997. Determintaion of E-modulus of young concrete with nondestructive method. *ASCE Journal of Materials in Civil Engineering*, **9**(1):pp.15–20. doi:10.1061/(asce)0899-1561(1997)9:1(15).

Othman, M.A. and Benson, C.H., 1993. Effect of freeze-thaw on the hydraulic conductivity and morphology of compacted clay. *Canadian Geothechnical Journal*, **30**:pp.236–246.

Othman, M.A. and Benson, C.H., 1992. Effect of freeze-thaw on the hydraulic conductivity of three compacted clay from Wisconsin. *Advances in Geotechnical Engineering, Transportation Research Record*, (1369):pp.118–125.

Othman, M.A., Benson, C.H., Chamberlain, E.J. and Zimmie, T.F., 1994. Laboratory testing to evaluate changes in hydraulic conductivity of compacted clays caused by freeze-thaw: state-of-the-art. In *Hydraulic Conductivity and Waste Contaminant Transport in Soil (STP 1142)*. Edited by D. E. Daniel & S. J. Trautwein. Philadelphia, PA: ASTM International, pp. 227–254. doi:10.1520/stp23890s.

Pamukcu, S., Topcu, I.B. and Guven, C., 1994. Hydraulic conductivity of solidified residue mixtures used as a hydraulic barrier. In *Hydraulic Conductivity and Waste Contaminant Transport in Soil (STP 1142)*. Edited by D. E. Daniel & S. J. Trautwein. Philadelphia, PA: ASTM International, pp. 505–520. doi:10.1520/stp23905s.

Paria, S. and Yuet, P., 2006. Solidification/stabilization of organic and inorganic contaminants using Portland cement: a literature review. *Journal of Environmental Reviews*, **14**:pp.217–255. doi:10.1139/a06-004.

PASSiFy, 2010. *Performance assessment of solidified/stabilised waste-forms, an examination of the long-term stability of cement-treated soil and waste*, A Joint Research Consortium.

PCA, 1992. *Soil-cement laboratory handbook*, Skokie, IL: Portland Cement Assosiation.

Popovics, S. and Ujhelyi, J., 2008. Contribution to the concrete strength versus water-cement ratio relationship. *ASCE Journal of Materials in Civil Engineering*, **20**(7):pp.459–464. doi:10.1061/(asce)0899-1561(2008)20:7(459).

Powers, T.C., Copeland, L.E., Hayes, J.C. and Mann, H.M., 1954. Permeability of portland cement paste. *Journal of American Concrete Institute*, **51**:pp.285–298.

Powers, T.C. and Helmuth, R.A., 1953. Theory of volume changes in hardened portland-cement paste during freezing. In *Proceedings of the Thirty-Second Annual Meeting of the Highway Research Board*. Edited by F. Burggra & W. J. Miller. Washington, D.C., pp. 285–297.

Powers, T.C. and Willis, T.F., 1949. The air requirement of frost-resistant concrete. In *Proceedings of the Twenty-Ninth Annual Meeting of the Highway Research Board*. Edited by R. W. Crum, F. Burggraf, & W. N. Carey. Washington, D.C., pp. 184–211.

Setzer, M.J., 2001. Micro-ice-lens formation in porous solid. *Journal of Colloid and Interface Science*, **243**(1):pp.193–201. doi:10.1006/jcis.2001.7828.

Shah, S.P., Popovics, J.S., Subramaniam, K. V. and Aldea, C., 2000. New directions in concrete health monitoring technology. *ASCE Journal of Engineering Mechanics*, **126**(7):pp.754–760.

Shane, J.D., Mason, T.O., Jennings, H.M., Garboczi, E.J. and Bentz, D.P., 2000. Effect of the interfacial transition zone on the conductivity of Portland cement mortars. *Journal of the American Ceramic Society*, **83**(5):pp.1137–1144.

Shea, M.S., 2011. *Hydraulic conductivity of cement-treated soils and aggregates after freezing*. M.A.Sc. thesis, Department of Civil and Environmental Engineering, Brigham Young University, Provo, UT.

Shihata, S.A. and Baghdadi, Z.A., 2001a. Long-term strength and durability of soil cement. *ASCE Journal of Materials in Civil Engineering*, **13**(3):pp.161–165.

Shihata, S.A. and Baghdadi, Z.A., 2001b. Simplified method to assess freeze-thaw durability of soil cement. *ASCE Journal of Materials in Civil Engineering*, **13**(4):pp.243–247.

Stegemann, J.A. and Côté, P.L., 1996. A proposed protocol for evaluation of solidified wastes. *Science of the Total Environment*, **178**(1996):pp.103–110. doi:10.1016/0048-9697(95)04802-2.

Stegemann, J.A. and Côté, P.L., 1990. Summary of an investigation of test methods for solidified waste evaluation. *Waste Management*, **10**(1):pp.41–52. doi:10.1016/0956-053x(90)90068-v.

Swamy, N. and Rigby, G., 1971. Dynamic properties of hardened paste , mortar and concrete. *Matériaux et Construction*, **1**(4):pp.13–40.

USEPA, 2013. *Superfund remedy report, Forteenth Edition*, USEPA Solid Waste and Emergrncy Respose, EPA 542-R-13-016.

Verbeck, G. and Landgren, G., 1960. Influence of physical characteristics of aggregate on frost resistance of concrete. In *ASTM Proceedings (Vol. 60)*. Phyladelphia, PA, pp. 1063–1079.

Yang, Y., Lepech, M.D., Yang, E.-H. and Li, V.C., 2009. Autogenous healing of engineered cementitious composites under wet–dry cycles. *Cement and Concrete Research*, **39**(5):pp.382–390. doi:10.1016/j.cemconres.2009.01.013.

CHAPTER 3: EXAMINING FREEZE/THAW CYCLING AND ITS IMPACT ON THE HYDRAULIC PERFORMANCE OF A CEMENT-TREATED SILTY SAND

3.1. Introduction

Solidification/stabilization (s/s) is a well-established remediation technology for the treatment of contaminated soils/sludge. This technology often involves mixing the contaminated material with a cement binder (cement-based s/s) or other supplementary materials such as fly ash, furnace slag, etc. to stabilize and/or solidify the contaminants in the structure of the resulting product (Bone et al. (2004); Batchelor (2006); Paria and Yuet (2006)). Depending on the desired treatment, the resulting material may be "soil-like" or in a monolithic physical form. Monolithic s/s materials are usually designed to have a significantly lower hydraulic conductivity compared to surrounding environment in order to ensure the contaminant release mechanism is a slower, diffusion-controlled process (ITRC (2010)). Hydraulic conductivity is also a measure of the connectivity of the pore structure and is an important factor in the durability of cementitious materials (Hearn (1998); Hearn et al. (2006); Antemir et al. (2010)).

Although considerable research has been performed to investigate the effectiveness of cement-based s/s for treatment of different types of contaminants and matrixes (see Bone et al. (2004) for a review), current knowledge on the possible changes in the performance of these treated soils under environmental stresses is limited. In northern regions of the world (e.g. Canada and parts of USA) the long term physical performance of a cement-treated monolith after freeze/thaw (f/t) conditions is an important factor governing the success of this technology. Freeze/thaw damage could occur either during the construction phase of the project (i.e. prior to placement of a cover system) or at some point during the design life of the treated material (i.e. when the cover system fails to fulfill its purpose as a thermal insulation barrier). The latter type of damage was observed by Klich et al. (1999) who used microscopic techniques on field samples to show how weathering processes such as f/t can cause cracking of these cement-treated materials.

Despite the lack of information on the long-term performance of monolithic cement-treated soils used in cement-based s/s projects subjected to f/t cycles, there is considerable research related to the f/t effects on the performance of soils and other types of cement-based materials. This includes examination of the formation of ice lenses and subsequent increase in the hydraulic conductivity of compacted clays for landfill applications (e.g. Othman and Benson (1992); Othman and Benson (1993)), degradation of mechanical performance (i.e. modulus of elasticity, compressive strength, etc.) in soil-cement for pavement applications (e.g. Kettle (1986); Shihata and Baghdadi (2001)), and changes in the physical performance (i.e. dynamic modulus of elasticity) of concrete (e.g. Penttala (2006); Micah Hale et al. (2009)).

Current engineering practice for the evaluation of f/t influence on s/s materials often considers percent mass loss of f/t exposed specimens as an indicator of the resistance (Stegman and Coté (1996); Paria and Yuet (2006); ITRC (2010)). However, mass loss does not necessarily correspond to changes in the internal structure of a solidified soil (El-Korchi et al. (1989)). It is these internal changes that control the hydraulic conductivity and inherently, the leaching potential of a cement-treated material (El-Korchi et al. (1989)). Any potential change in hydraulic conductivity under f/t exposure becomes an important consideration for the long term performance of monolithic cement-treated materials where solidification is the primary mitigation mechanism for the contaminant migration.

The objective of the current chapter is to investigate the influence of various f/t conditions on the performance of a saturated cement-treated monolithic silty sand. A laboratory-based testing program was developed to assess the impact of freezing temperature, number of f/t cycles, curing time, and mix design on the hydraulic conductivity and unconfined compressive strength (UCS) of individual specimens. In addition, impact resonance (IR) testing was used as a non-destructive method to monitor the changes in the structure of the specimens for additional exposure conditions than that used for hydraulic conductivity and unconfined compressive strength testing.

3.2. Materials and Methods

3.2.1. General

The majority of testing conducted in this paper was used for a "three factor"-"two level" factorial study (Brown and Berthouex (2002)). The factorial approach was used to examine the influence of freezing temperature (-10°C and -2°C), number of freeze/thaw cycles (4 and 12 cycles), and curing time ("immature" and "mature") on the hydraulic conductivity and unconfined compressive strength (UCS) of the cement-treated soil. In this chapter a curing time of 16 days prior to f/t exposure is referred to as "immature" and a curing time of over 35 days prior to f/t exposure is referred to as "mature". A summary of the different factors used in the factorial experiments and their levels is presented in Table 3.1. Test results obtained as part of the factorial experiments were analyzed using the Statistical Package for Social Science (SPSS) 18 software (SPSS Inc., Chicago, IL, USA) to quantify the significance of each factor. In addition to the factorial experiments, six additional tests (referred as complementary tests in this paper), were performed to further quantify the effect of lower freezing temperatures, lower water to solids ratios, and higher cement contents on the performance of "immature" and "mature" cement-treated soil.

Table 3.1: Factors and levels used in the factorial experiment.

Factors	Levels	
	Lower level	Upper level
Curing time	"Mature" (> 35 days)	"Immature" (16 days)
Freezing temperature	-10°C	-2°C
Number of cycles	12	4

A summary of exposure conditions and mix designs for all tests is provided in Table 3.2. In the names provided for each test series in this table, "I" refers to immature, "M" refers to mature, "04" and "12" refer to number of f/t cycles and "-2", "-10" and "-20" refer to freezing temperature. Also "20%" and "LWS" refer to 20% cement content (by mass of dry solids) and "lower water to solids ratio" conditions, for the complementary tests.

Table 3.2: Summary of mix designs and exposure conditions for the different tests performed.

Test group	Test series	Mix design			Exposure scenario		
		W/C[1]	W/S[2]	Cement content[3], %	Curing	Freezing temperature, °C	Number of f/t cycles
Factorial tests	I04-10	2.7	0.25	10	"Immature"	-10	4
	I12-10				"Immature"	-10	12
	I04-02				"Immature"	-2	4
	I12-02				"Immature"	-2	12
	M04-10				"Mature"	-10	4
	M12-10				"Mature"	-10	12
	M04-02				"Mature"	-2	4
	M12-02				"Mature"	-2	12
Complementary tests	M04-20	2.7	0.25	10	"Mature"	-20	4
	I04-20				"Immature"	-20	4
	M12-10(20%)	1.2	0.20	20	"Mature"	-10	12
	I12-10(20%)				"Immature"	-10	12
	M12-10(LWS)	1.6	0.15	10	"Mature"	-10	12
	I12-10(LWS)				"Immature"	-10	12

Note:

1. W/C: water to cement ratio.
2. W/S: water to solids ratio.
3. Cement content expressed per dry mass of soil.

3.2.2. Soil Characterization and Specimen Preparation

This study used a soil which classified as silty sand (SM) by the Unified Soil Classification System (USCS). The non-plastic soil had a maximum particle size of 10 mm, a coefficient of uniformity (C_u) of 17, a specific gravity of 2.7, and 30 percent passing the 75 μm sieve. General use Portland cement (ASTM Type I) was used as the binding agent for the soil-cement samples. A drill mounted paddle was utilized for mixing of the sample constituents. To prepare the test specimens, dry cement and water were first proportioned and then mixed to form a slurry in a 20 liter bucket. The soil was then incrementally added to the cement slurry and mixed to uniformity. Soil-cement mixtures were placed in three layers into cylindrical plastic molds, of 101 mm diameter by 118 mm height. Each layer was subjected to 20 strokes using a standard concrete slump testing rod to provide consistent consolidation. Molds were placed in a sealed plastic bag for 5 days before extrusion, after which the specimens were kept in a 100% humidity moist curing room prior to further testing.

3.2.3. F/T Conditioning for Exposed Specimens

All of the specimens to be tested under exposed conditions (described in the following sections) were saturated in a triaxial cell (ASTM-D5084 (2000) saturation phase). F/t cycling consisted of 24 hours of freezing at the required temperature (see Table 3.2), followed by thawing in a 100% humidity room at a temperature of 22±1ºC. Complete freezing and thawing of specimens in a typical f/t cycle was confirmed by monitoring the temperature in a dummy sample with a similar mix design to the specimens being tested. Specimens were allowed to absorb ambient moisture during the thawing phase and were exposed to three dimensional freezing conditions. Such conditions (i.e. open system and three-dimensional f/t exposure) are typical of those currently used in industrial practices for soil-cement and cement s/s materials (i.e. ASTM-D560 (2003) and withdrawn ASTM-D4842 (2001)). Studies by Othman and Benson (1993) showed that freezing dimensionality has little effect on the changes in the hydraulic performance of compacted

clays. The influence of one-dimensional freezing exposure on performance of cement-treated soils is discussed in chapter 6.

3.2.4. Performance Evaluation of Specimens

3.2.4.1. Hydraulic Conductivity Testing

The hydraulic conductivity of the specimens were measured according to ASTM-D5084 (2000) (i.e. flexible-wall method), using saturation, consolidation, and permeation stages. Back-pressure saturation (524 kPa) was performed under an effective confining pressure of 35 kPa, followed by consolidation under an effective confining pressure of 138 kPa. Subsequent permeation with de-aired water was performed under a hydraulic gradient of approximately 30. Specimens for the I12-10 and M12-10 tests which experienced higher degradation after the f/t exposure were subjected to a lower hydraulic gradient of approximately 6 due to the higher hydraulic conductivity of these samples. The tests were terminated according to the criteria of ASTM-D5084 (2000) (i.e. outflow to inflow ratio and steady hydraulic conductivity criteria). In some of the complementary tests where the hydraulic conductivity values were lower than 10^{-10} m/s, acceptable outflow to inflow rates were difficult to achieve in the time span of the tests, as a result those tests were terminated when consecutive measurements resulted in a steady hydraulic conductivity value.

Two replicates of each hydraulic conductivity test were performed to consider specimen variability. Hydraulic conductivity measurements were performed before (i.e. control) and after (i.e. exposed) f/t conditioning of each specimen. The average hydraulic conductivity ratio, defined as the average for hydraulic conductivity values of exposed specimens ($K_{exposed}$) divided by the values obtained prior to exposure (K_0) is utilized to compare different scenarios.

3.2.4.2. Compressive Strength

Unconfined compressive strength (UCS) testing was also performed on two replicates for each of exposed and control conditions. With respect to curing times, it was assumed that

no curing took place during freezing of the exposed specimens. Hence, specimens (control and exposed) were tested for UCS after at least 35 days of curing in the moist room (i.e. excluding freezing time). To ensure consistency, control and exposed specimens were tested on the same day. A total of four specimens (i.e. two as control and two exposed) were used for UCS measurements of factorial experiments. For the complementary tests, only one set of specimens were used to measure control values for immature and mature f/t exposure, thus a total of six specimens (i.e. two as control and four exposed (two for each of immature and mature exposure conditions)) were tested.

All specimens were sulfur-capped prior to testing to ensure that the specimens were tested under non-eccentric axial loading. UCS values were obtained using a vertical deformation rate of 0.5 mm/min. Changes in the UCS ratio, defined as the average UCS for exposed specimens divided by the average UCS values for control specimen, are reported in the results section.

3.2.4.3. Impact Resonance (IR) Testing

To further characterize the development of damage during the f/t process (i.e. intermediate cycles in addition to the 4^{th} and 12^{th} cycles), longitudinal IR testing was performed on selected tests (I12-02, I12-10, M12-02, M12-10, I12-10(LWS), and I12-10(20%) as specified in Table 3.2) to cover a wide range of observed f/t degradation. IR is a non-destructive test which has been widely used to predict the dynamic properties of cementitious materials (ASTM-C215 (2008)). ASTM-C666 (1997) suggests a similar technique to evaluate changes in the dynamic modulus of elasticity of concrete beams after exposure to rapid cycles of f/t.

To prepare the test specimens for the IR testing, an approximately 1 cm by 1 cm square tab of steel sheet metal (thickness of 1 mm) was glued to the axial centerline of each specimen on both ends, to enable the magnetic coupling of an accelerometer to the specimen at one end and a hard base upon which to create an impact at the other. The hardness of the steel tab ensured that a consistent frequency content was created for each impact event, while

impact on the damaged specimen surface could result in relatively plastic and longer duration contact. Longer contact duration may reduce and limit the available bandwidth of the forcing function and possibly influence the ability to detect the resonant frequency (RF) of the sample (Sansalone (1997)). During the test, the specimens were placed on a rectangular sponge measuring 23 by 9 by 7 cm to permit relatively unrestrained resonance under the impact load. Each specimen was excited using a steel ball with a diameter of 9.5 mm, glued to a plastic band (with a combined mass of approximately 5.3g). The response signal was acquired using a PCB model 353B02 accelerometer magnetically connected to the steel tab on the opposite end of the specimen which transferred the signals to an amplifier and a computer (Freedom NDT Data PC Platform, Olson Instruments Inc.) for signal processing. Data were sampled using a 500 kHz data acquisition card with a period of 2 micro seconds and a record size of 8192 in order to provide a frequency resolution of 61 Hz. During each test, signals were processed by the computer's software using a fast Fourier transform (FFT) to calculate the longitudinal RF of each specimen. Five replicates of the RF were measured and averaged for each of two different specimens at different f/t cycles.

The normalized changes in the longitudinal RF at the m^{th} f/t cycle (β_m), were calculated based on Equation 3.1, as follows:

$$\beta_m = \frac{RF_m}{RF_0} \qquad \text{Equation 3.1}$$

Where RF_m and RF_0 are resonant frequencies at the m^{th} and initial cycle of f/t, respectively. The average values for the normalized RF values of duplicate specimens are reported in the results section.

3.3. Results

Of the 14 sets of tests performed, the highest level of physical damage to the specimens was visually observed for the I12-10 and M12-10 test series. A high degree of surface degradation was observed for these tests and resulted in problems with handling and testing

of the specimens, especially at higher f/t cycles. As a result of the damage to these specimens, the method of measurement for the hydraulic conductivity and strength properties did not meet the requirements of available standard methods. Hence, the residual hydraulic conductivity and compressive strength of these specimens are presented in this paper only for the sake of a rough estimate for comparison between the scenarios and completion of the factorial experiment analysis.

A summary of hydraulic conductivity and compressive strength test results are presented in Figure 3.1 and Figure 3.2, respectively. Comparing the results for control and exposed conditions show that f/t cycles can greatly influence the expected performance of solidified soils. Increases of up to three orders of magnitude in hydraulic conductivity and decreases of up to 95% in UCS values were observed. In the following sections, the changes in the ratios of hydraulic conductivity and UCS values are separately discussed for each studied factor.

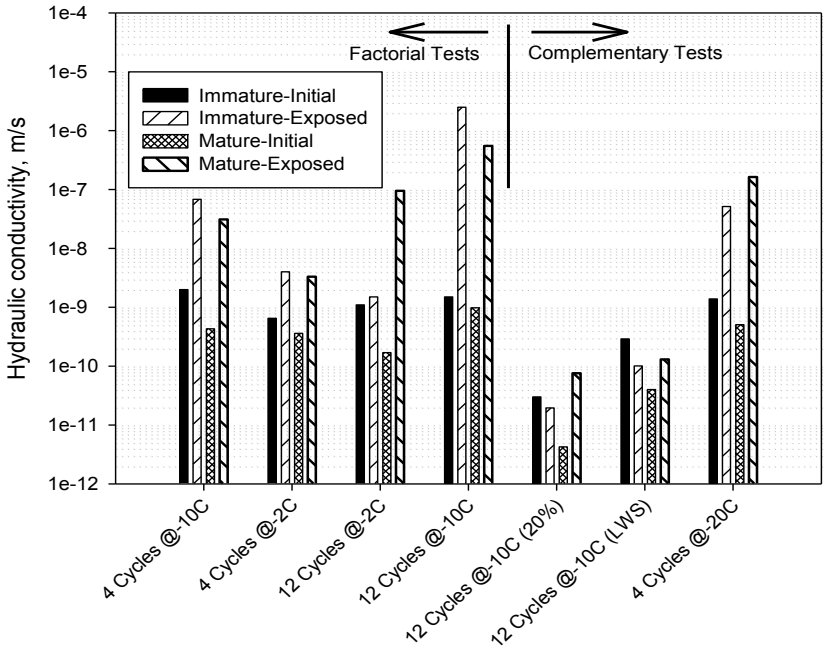

Figure 3.1: Summary of hydraulic conductivity results for different exposure scenarios and mix designs.

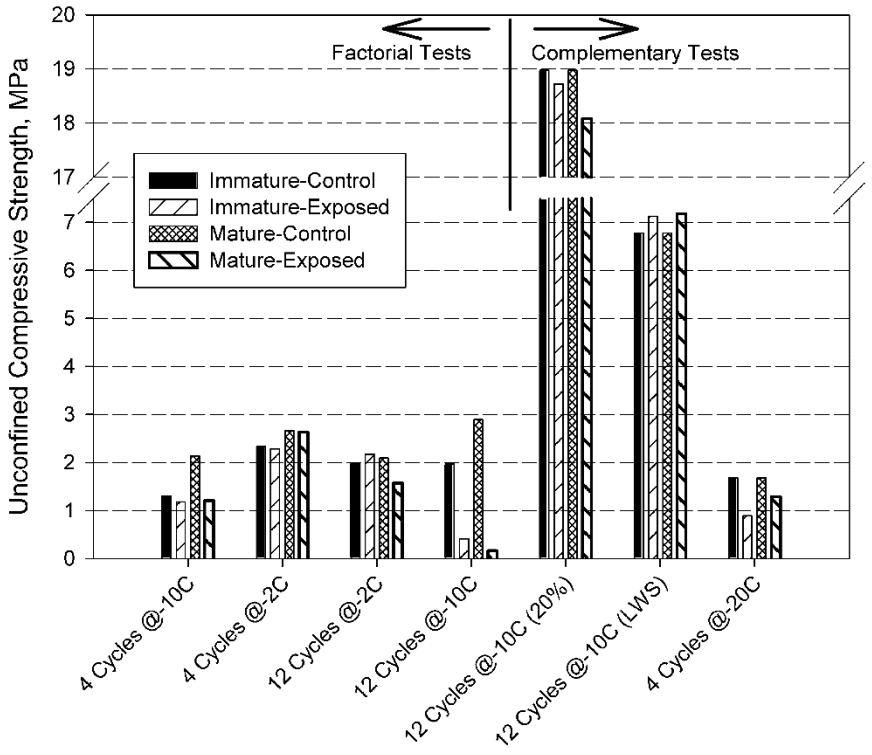

Figure 3.2: Summary of UCS test results for different exposure scenarios and mix designs.

3.3.1. Influence of F/T Cycles, Curing Time, and Freezing Temperature on Changes in the Performance of Soil-Cement

3.3.1.1. Number of F/T Cycles

The extent of f/t cycles expected in any exposed system depends on the local climate and depth of freezing (Benson and Othman (1993); Othman et al. (1994)). Previous studies on compacted clays show that a significant portion of total damage (in terms of increase in hydraulic conductivities) can occur at exposure to initial f/t cycles (Othman and Benson (1992)). In the current study, the performance of the cement-treated soils at 4 and 12 f/t cycles was investigated. Impact resonance testing was performed on selected specimens at intermediate cycles between 0, 4, and 12 cycles.

Figure 3.3 presents changes in the values of the hydraulic conductivity ratio ($K_{exposed}/K_0$) with respect to the number of f/t cycles performed. It can be observed that for both immature and mature specimens exposed to -10°C, a considerable increase in hydraulic conductivity (approximately 30 to 70 fold) occurs in the first 4 f/t cycles. The damage continues as the number of f/t cycles is increased to 12, resulting in hydraulic conductivity values of up to three orders of magnitudes higher than initial conditions. Mature specimens exposed to -2°C also see a continued increase in the hydraulic conductivity from 0 to 4 to 12 cycles (approximately 10 and 500 fold, respectively). This constant increase in the hydraulic conductivity at higher f/t cycles is in agreement to reported observations in the literature on soil-cement (Guney et al. (2006)).

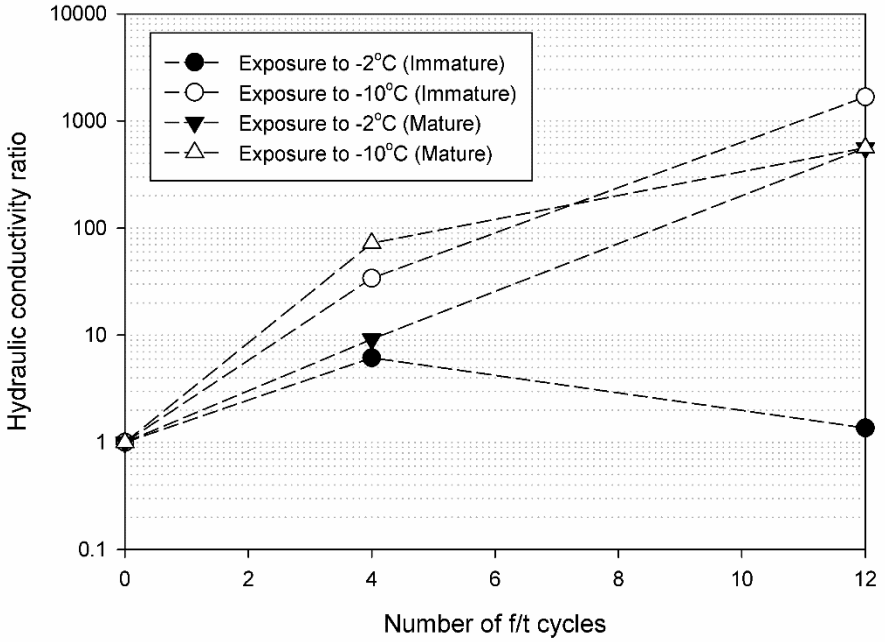

Figure 3.3: Changes in hydraulic conductivity ratios at different f/t cycles.

For immature specimens exposed to -2°C the approximately six-fold increase after 4 f/t cycles is followed by a slight decrease in hydraulic conductivity from 4th to 12th cycle, resulting in hydraulic conductivity values comparable to initial conditions. This reduction in hydraulic conductivity is likely a result of interaction between the self-healing processes

and the damage development in the solidified soil. A detailed explanation of these processes is presented by Hearn (1998).

Figure 3.4 shows the changes in UCS ratio at different f/t cycles based on the factorial experiments. A general trend of decreasing strength can be observed for specimens exposed to -10^{o}C as the number of f/t cycles increases from 0 to 4 to 12 (up to approximately 45 and 95% reduction, respectively). For the specimens exposed to -2^{o}C, at 4 cycles of f/t, the changes seem to be negligible, which is in contrast to the results of hydraulic conductivity ratios (approximately 6 to 10 times increase). This might imply the unsuitability of strength indicators for predicting the hydraulic performance of solidified soils subjected to f/t cycles at early stages of damage development. As the number of f/t cycles increases from 4 cycles to 12 cycles, a contrasting response is observed for immature and mature specimens. While mature specimens exposed to 12 cycles of f/t at -2^{o}C show a decrease of over 20% in the UCS values, immature specimens seem to reach higher strengths compared to control conditions (approximately 10%). This strength gain is consistent with the trends observed for hydraulic conductivity results described above (i.e. I12-02 series). The higher compressive strength values for f/t exposed specimens compared to control conditions may also be due to the conditioning (i.e. saturation) of the specimens prior to f/t exposure.

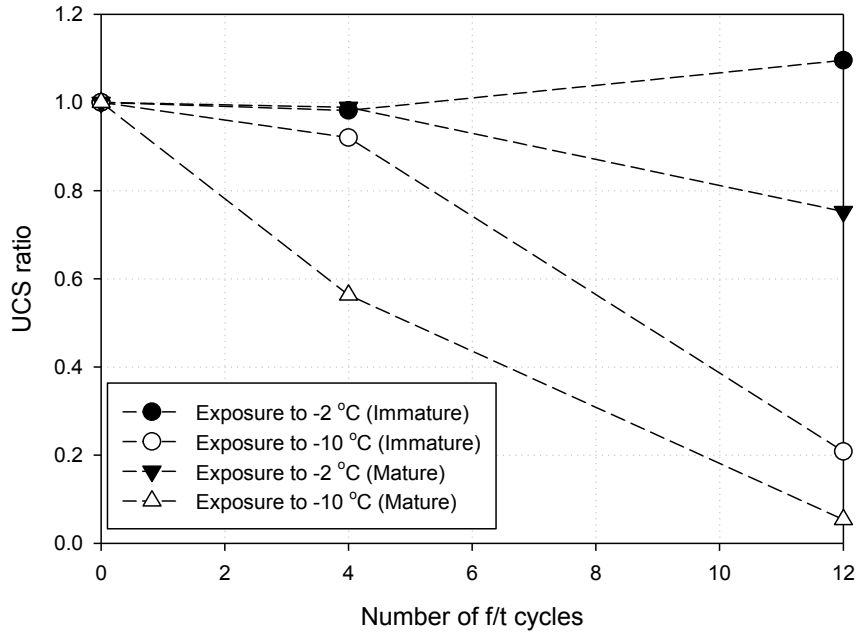

Figure 3.4: Changes in the UCS ratios due to exposure to different number of f/t cycles.

IR results shown in Figure 3.5 provide some further insight on the damage occurring during the successive f/t cycles. Shifts in the RF of specimens can represent changes in their structure which may be a result of mechanical damage or section loss (reduction in the frequency) or due to curing (increase in the frequency) as the RF is proportional to the modulus of elasticity of the material (ASTM-C215 (2008)). Based on the RF ratios at the end of the first f/t cycle, two distinct types of behavior were observed at further f/t exposures. For the exposed specimens in which the frequency reduction relatively small, the specimens seem to self-heal at further f/t cycles resulting in an increase in the RF ratio (I12-02, I12-10(LWS), and I12-10(20%) in Figure 3.5). These specimens showed a better performance in terms of hydraulic conductivity (less than an order of magnitude increase) and unconfined compressive strength (less than 10 percent decrease) changes. However, for the cases in Figure 3.5 where the decrease in the frequency at the end of the first cycle were large (i.e. more than 30%), the propagation of damage continues resulting in a considerable change in the performance of the specimens measured at the end of the 12th cycle (I12-10, M12-10, and M12-02 in Figure 3.5). Previous studies (e.g. Yang et al. (2009)) have shown that autogenous healing can happen up to a certain crack width, which

may explain the recovery in resonant frequency of certain specimens. Results imply that resistance of a solidified soil to the first cycle of f/t action may have the potential to be considered as a predictive tool for the performance of the samples at higher exposure levels. This hypothesis is further examined in chapter 5.

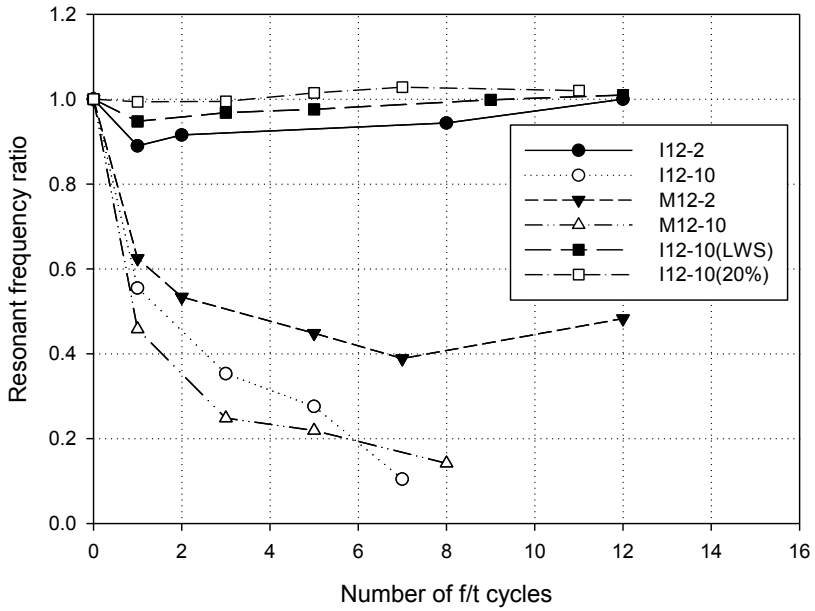

Figure 3.5: Changes in the resonant frequency ratio after exposure to different f/t scenarios.

3.3.1.2. Curing Time

Curing time is a factor that greatly influences the length of time required to perform experiments related to cement-based materials. Current practices for the examination of soil-cement under f/t cycles usually suggest short curing periods prior to f/t exposure (as low as seven days in ASTM-D560 (2003) for instance). This approach overlooks the differences in the structure of the soil-cement as a result of hydration progress and also neglects the possible interference of damage formation mechanisms during f/t exposure with the hydration of cement. In this chapter, the effect of curing time before f/t exposure was evaluated on specimens cured for 16 (i.e. immature) and over 35 days (i.e. mature). Visual observations showed that, in general, mature specimens undergo a higher degree of surface damage compared to immature specimens.

In Figure 3.6, changes in hydraulic conductivity values due to different f/t conditions are compared for exposure of immature and mature specimens. In general, a higher degree of change in the hydraulic conductivity (up to 410 times) was observed for mature specimens as compared to immature specimens. The results might suggest that immature specimens may have a higher capacity for self-healing compared to mature specimens. The exception to this was the case of exposure to 12 cycles at -10ºC (factorial experiments: I12-10 and M12-10). This slightly higher increase in immature specimens is likely due to the high degradation of specimens in both cases. Comparison of compressive strength test results for different scenarios of immature and mature f/t exposure (Figure 3.2), however, do not suggest any notable trend.

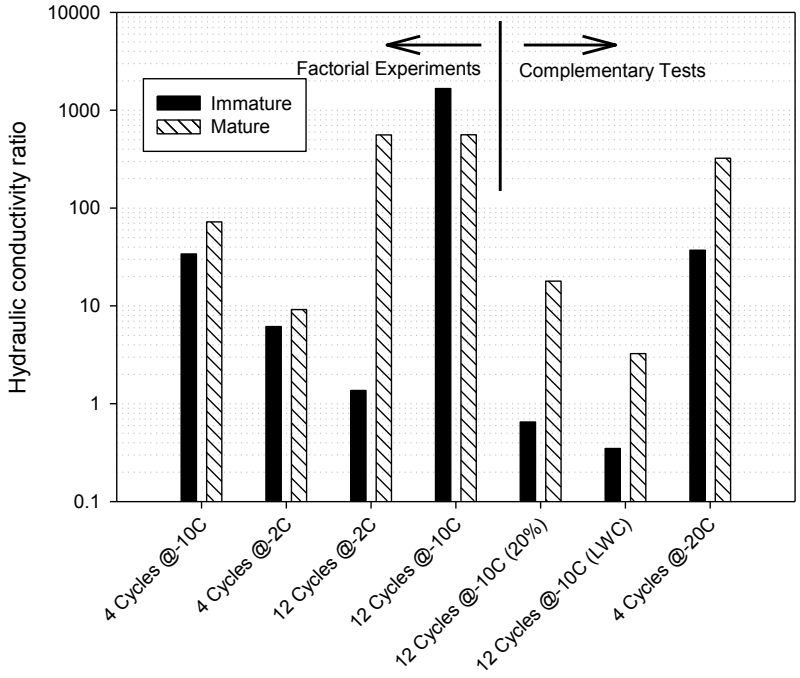

Figure 3.6: Comparison of the hydraulic conductivity changes for different scenarios of immature and mature conditions.

3.3.1.3. Freezing Temperature

One of the main concerns in the design of a testing procedure for examining the performance of cement-treated soils under f/t exposure is to estimate the conditions

expected in the field and attempt to replicate these conditions in the laboratory. Freezing temperature is an important factor with this regard as it controls the rate of freezing (Newton's law of cooling) and amount of freezable water (Nmai (2006)) within a material's structure. Choosing a freezing temperature for this purpose would greatly depend on the scenario which is investigated. For cases where exposure of the s/s material during the construction phase is concerned, freezing temperatures closer to 0°C might present a more realistic scenario. On the other hand, if the exposure in the service life of the product is of concern, harsher scenarios (lower freezing temperatures) could be preferable. Previous study by Othman and Benson (1992) on compacted clays show a slight increase in the hydraulic conductivity of exposed specimens as the freezing temperature is reduced from -1°C to -23°C.

In the current study, specimens were examined at three freezing temperatures (-2, -10, and -20°C). As shown in Figure 3.6, for mature specimens exposed to 4 f/t cycles, it was observed that the hydraulic conductivity ratio increased as the freezing temperature decreased from -2°C to -10°C and -20°C (approximately 8 and 35 times, respectively). For immature specimens exposed to 4 f/t cycles, although a six times increase in hydraulic conductivity ratio is observed for exposure to -10°C compared to -2°C, these values show no significant change as the freezing temperature is further reduced to -20°C.

An increase in the hydraulic conductivity ratio (approximately 3 orders of magnitudes) with the decrease in the freezing temperature (from -2°C to -10°C) was also observed for immature specimens exposed to 12 f/t cycles. However, as presented in the case of the mature specimens (12 cycles), relatively similar hydraulic conductivity ratios were observed at these freezing temperatures. The reason is likely the high degree of damage at these exposure conditions which could influence the expected trends for the results.

Exposed compressive strength values (Figure 3.2) also show a noticeable reduction when the freezing temperature drops from -2°C to -10°C for most of the cases studied. However, as the freezing temperature changes from -10°C to -20°C (for exposure to 4 f/t cycles) contradictory results were observed. For these cases, while immature specimens showed a

reduction in the UCS values, changes in the UCS values for mature specimens were negligible (see Figure 3.2). Therefore, the data currently available is not sufficient to suggest any trends at temperatures below -10^{o}C.

3.3.2. Statistical Analysis of Investigated Factors (Factorial Experiments)

A "three factor"-"two level" factorial experiment was performed to identify the effect of freezing temperature, curing time, and number of f/t cycles on the performance of solidified soil exposed to f/t cycles. Values for unconfined compressive strength ratio and logarithm of hydraulic conductivity ratio were chosen as the dependent variables in the analysis. For the hydraulic conductivity study, due to the high variability of the results in different test conditions, the logarithm of the hydraulic conductivity ratios was preferable as it helped to provide constant variance under the assumed normality of the data (Brown and Berthouex (2002)). As a result, the response, $\widehat{K}$, for each hydraulic conductivity test was calculated by:

$$\widehat{K} = \log(\frac{K_{exposed}}{K_0}) \qquad \text{Equation 3.2}$$

A summary of the testing conditions for different experiments and observed values for changes in the performance of replicate specimens (denoted as Trial 1 and Trial 2) are presented in Table 3.3. Analysis of Variance (ANOVA) was performed using the SPSS 18 software (SPSS Inc., Chicago, IL, USA), to examine the significance of each factor on changes in the hydraulic conductivity and UCS ratios, for which the results are presented in Table 3.4. The influence of a factor is usually considered significant when the corresponding p-value is less than 0.05 which means it can be claimed, with 95% confidence, that observed changes are a result of the different levels in the investigated factor (and not only due to the random error occurring between the tests). Based on the

Table 3.3: Testing program and results for the factorial experiments.

Testing conditions			Log($K_{exposed}/K_0$)				UCS ratio			
curing time	f/t cycles	Freezing temperature, °C	Trial 1, $\widehat{K_1}$	Trial 2, $\widehat{K_2}$	Average	Variance	Trial 1	Trial 2	Average	Variance
"Immature"	4	-2	0.82	0.77	0.80	1.6E-03	0.95	1.01	0.98	1.8E-03
"Mature"	4	-2	1.19	0.78	0.98	8.3E-02	0.96	1.02	0.99	1.8E-03
"Immature"	12	-2	0.06	0.20	0.13	9.3E-03	1.09	1.10	1.10	5.0E-05
"Mature"	12	-2	2.95	2.61	2.78	5.7E-02	0.77	0.74	0.75	4.5E-04
"Immature"	4	-10	1.34	1.68	1.51	5.5E-02	0.85	0.97	0.91	7.2E-03
"Mature"	4	-10	1.94	1.76	1.85	1.7E-02	0.62	0.50	0.56	7.9E-02
"Immature"	12	-10	3.50	2.34	2.92	6.7E-01	0.27	0.15	0.21	7.2E-03
"Mature"	12	-10	2.42	3.10	2.76	2.3E-01	0.02	0.09	0.05	2.5E-03

results, all of the studied factors are significant (with p-values less than 0.01) in observed changes for hydraulic conductivity and compressive strength. This is consistent with discussions presented in the previous sections. These results further emphasize the requirement for developing case specific f/t studies for cement-based s/s projects, based on the environmental conditions and specific project objectives.

Table 3.4: P-values based on the results of ANOVA test on hydraulic conductivity and UCS changes.

Factor	P-value	
	$Log(K_{exposed}/K_0)$	UCS ratio
Curing time	3.9×10^{-3}	1.1×10^{-4}
Number of f/t cycles	1.7×10^{-3}	3.7×10^{-6}
Freezing temperature	4.1×10^{-4}	1.1×10^{-7}

3.3.3. Discussion

The previous sections have focused on evaluating the influence of various testing factors on the resulting damage (i.e. hydraulic conductivity and UCS) of soil-cement samples. For the majority of the tests performed, differing degrees of damage were observed for both immature and mature specimens. From a practical perspective, this does not necessarily mean that all cement-based s/s materials undergoing f/t exposure are at risk to damage, but more so that it is important to evaluate a given mixture design for risk of f/t damage using some of the techniques outlined in this paper. The mixture design used throughout the factorial tests was held constant and had a high water content, hence explaining some of the excessive damage observed from the f/t exposure.

To demonstrate how the damage observed for this silty soil can be mitigated in a mix design for this particular soil, the complementary tests with higher cement content and reduced water to cement ratio (i.e. I12-10(20%) and M12-10(20%)) and lower water to solids ratio with 10 percent cement content (i.e. I12-10(LWS) and M12-10(LWS)) were performed. As is shown in Figure 3.1 and Figure 3.2, by increasing the cement content and decreasing the water to solids ratio, both mix design modifications may partially improve the

performance of solidified soil under the f/t exposure conditions adopted. When examining the absolute hydraulic conductivity values of both these mix designs in Figure 3.1, it can be seen that for both immature and mature specimens, the specimens all achieved a hydraulic conductivity of less than 10^{-9} m/s, which is often the lower limit of specification set for s/s projects. Similarly, high strengths are maintained after f/t, as shown in Figure 3.2. As shown in Figure 3.6, this does not mean that damage is prevented in the specimens, but rather that damage can be mitigated by changing the mix design. Lowering the water content (while keeping the cement content constant) seems to be an effective tool to improve the overall performance of solidified soil as it reduces the porosity, and consequently the amount of freezable water in the porous structure, and increases the strength of the soil-cement mixture. Influence of water to cement ratio on performance of cement-treated soils subjected to f/t cycles is further examined in chapter four.

3.4. Conclusions

In this study, physical performance of a cement-treated silty sand was evaluated under exposure to different f/t scenarios. A total of 14 sets of tests were performed. The results of hydraulic conductivity and unconfined compressive strength testing show that depending on the f/t exposure scenario, a considerable change was observed for the solidified soil tested. This included changes as high as 3 orders of magnitude increase in the hydraulic conductivity results and strength loss of up to 95 percent based on the residual UCS values. Based on the results of statistical analysis using ANOVA, the number of f/t cycles, freezing temperature, and curing time all are significant factors in observed changes in hydraulic performance and strength of the cement-treated soil examined. Monitoring of the RF changes in the specimens show that, changes in the structure can be expected as early as one f/t cycle exposure. Changes in hydraulic conductivity and compressive strength of specimens were studied after 4 and 12 f/t cycles in factorial experiments. Results show that for most cases higher damage happens at the end of 12^{th} cycle. This is with the exception of immature specimens exposed to -2^{o}C which (due to the hydration process) specimens seem to "self-heal" resulting in better performance compared to results of exposure at 4 cycles of f/t.

Specimens exposed to -10°C were shown to be considerably more damaged compared to specimens exposed to -2°C. However, observations due to further reduction of freezing temperature to -20°C (as discussed based on the results of complementary tests) were inconclusive.

It should be noted that the results presented herein are based on the experiments performed on a non-plastic soil. Further experiments is required to examine the performance of other types of soils (i.e. soils containing clay, organic materials, etc.) under the exposure scenarios investigated, as these soils may exhibit a different behavior during the f/t exposure.

3.5. References

Antemir, A., Hills, C.D., Carey, P.J., Gardner, K.H., Bates, E.R., Crumbie, A.K., (2010). "Long-term performance of aged waste forms treated by stabilization/solidification." *Journal of hazardous materials*, 181(1-3), 65-73.

ASTM-C215, (2008). "Standard test method for fundamental transverse, longitudinal, and torsional resonant frequencies of concrete specimens." In Annual Book of ASTM Standards. West Conshohocken, PA: ASTM International. doi:10.1520/c0215-08.2.

ASTM-C666, (1997). "Standard test method for resistance of concrete to rapid freezing and thawing." *Annual book of ASTM standards,* ASTM International. West Conshohocken, PA.

ASTM-D4842, (2001). "Standard test method for determining the resistance of solid wastes to freezing and thawing (Withdrawn 2006)." *Annual book of ASTM standards*, ASTM International. West Conshohocken, PA.

ASTM-D5084, (2000). "Standard test methods for measurement of hydraulic conductivity of saturated porous materials using a flexible wall permeameter." *Annual Book of ASTM Standards.* ASTM International, West Conshohocken, PA.

ASTM-D560, (2003). "Standard test methods for freezing and thawing compacted soil-cement mixtures." *Annual book of ASTM standards,* ASTM International. West Conshohocken, PA.

Batchelor, B. (2006). "Overview of waste stabilization with cement." *Waste management.* 26 (7), 689-98.

Benson, C. and Othman, M., (1993). "Hydraulic conductivity of compacted clay frozen and thawed in situ." *Journal of Geotechnical Engineering*, 119(2), 276-294.

Bone, B.D., Barnard L.H., Boardman D.I., Carey, P.J., Hills, C.D., Jones, H.M., MacLeon, C.L., Tyrer, M., (2004). *Review of scientific literature on the use of stabilisation/solidification for the treatment of contaminated soil, Solid Waste and Sludges*. British Environmental Agency. SC980003/SR2.

Brown L.C., and Berthouex P.M., (2002). *Statistics for Environmental Engineers,* Second Edition. Lewis Publishers.

El-Korchi, T., Gress, D., Baldwin, K., and Bishop, R. (1989). "Evaluating the freeze-thaw durability of portland cement-stabilized-solidified heavy metal waste using acoustic measurements". *Environmental Aspects of Stabilization and Solidification of Hazardous and Radioactive Wastes*, American Society for Testing and Materials, Philadelphia, ASTM STP 1033: 184-191.

Guney, Y., Aydilek, A.H., and Demirkan, M.M., (2006). "Geoenvironmental behavior of foundry sand amended mixtures for highway subbases." *Waste management*, 26(9), 932-45.

Hearn, N., (1998). "Self-sealing, autogenous healing and continued hydration: what is the difference?" *Materials and Structures*, 31, 563-567.

Hearn, N., Hooton, R.D., and Nokken, M.R, (2006). "Pore structure, permeability, and penetration resistance characteristics of concrete." *Significance of tests and properties of concrete and concrete making.* Edited by: Lamond J.F. and Pielert J.H., The American Society for Testing and Materials, Philadelphia, ASTM STP 169B.

ITRC (Interstate Technology & Regulatory Council), (2010). *Development of Performance Specifications for Solidification/Stabilization.* S/S-1.Washington, D.C.: Interstate Technology & Regulatory Council, Solidification/Stabilization Team. www.itrcweb.org.

Kettle, R.J., (1986), "Assessment of freeze-thaw damage in cement stabilized soils." Conference Proceeding*: Research on Transportation Facilities in Cold Regions*. Boston, Massachusetts, 16- 31.

Klich, I., Wilding, L.P., Drees, L.R., Landa, E.R. (1999). "Importance of microscopy in durability of solidified and stabilized contaminated soils." *Soil Science Society American Journal*, 63, 1274-1283.

Micah Hale, W., Freyne S., Russell B. (2009). "Examining the frost resistance of high performance concrete." *Construction and Building Materials*. 23(2), 878-888.

Nmai, C.K., (2006). “Freezing and thawing.” *Significance of tests and properties of concrete and concrete making.* Edited by: Lamond J.F. and Pielert J.H., The American Society for Testing and Materials, Philadelphia, ASTM STP 169B.

Othman, M.A. and Benson C.H. (1992). “Effect of freeze-thaw on the hydraulic conductivity of three compacted clay from Wisconsin.” *Transportation Research Board. Advances in Geotechnical Engineering,* 1369, 126-129.

Othman M.A. and Benson C.H., (1993). “Effect of freeze-thaw on the hydraulic conductivity and morphology of compacted clay.” *Canadian Geotechnical Journal*, 30, 236-246.

Othman, M.A., Benson, C.H., Chamberlain, E., and Zimmie, T., (1994). "Laboratory testing to evaluate changes in hydraulic conductivity of compacted clays caused by freeze-thaw: State-of-the-Art," *Hydraulic Conductivity and Waste Contaminant Transport in Soil*, American Society for Testing and Materials, Philadelphia, ASTM STP 1142.

Paria, S. and Yuet, P.K., (2006). “Solidification/stabilization of organic and inorganic contaminants using Portland cement: A Literature Review”. *Journal of Environmental Reviews,* 14, 217-255.

Penttala, V. (2006). “Surface and internal deterioration of concrete due to saline and non-saline freeze–thaw loads.” *Cement and Concrete Research.* 36, 921–928.

Sansalone, M. (1997). *Impact-echo nondestructive evalution of concrete and masonry*, Bulbrier Press, Jersey Shore, PA.

Shihata, S.A. and Baghdadi, Z.A. (2001). “Simplified method to assess freeze-thaw durability of soil cement.” *Journal of Materials in Civil Engineering*. 13(4), 243-247.

Stegemann, A. and Coté, P.L. (1996). “A proposed protocol for evaluation of solidified wastes.” *The Science of the Total Environment*. 178, 103-110.

Yang Y., Lepech M.D., Yang E., Li V.C., (2009). “Autogenous healing of engineered cementitious composites under wet–dry cycles.” *Journal of Cement and Concrete Research*, Volume 39, 382-390.

CHAPTER 4: HYDRAULIC AND STRENGTH PROPERTIES OF UNEXPOSED AND FREEZE/THAW EXPOSED CEMENT-STABILIZED SOILS

4.1. Introduction

Cement-based stabilization is widely used for improving the engineering properties of problematic soils. Although the majority of these soil improvement projects focus on increasing the strength related properties of the initial materials (e.g. soil-cement used as a base material for pavements, slope stability, etc.) (ACI 1990), there are many applications in which the hydraulic conductivity of the final product is a concern. Canal linings, vertical cut-off walls, and cement-based solidification/stabilization remediation projects are a few examples of such applications.

Hydraulic conductivity measurement of cement-stabilized soils has been the subject of studies by Ganjian et al. (2004), Bellezza & Fratalocchi (2006) and Hammad (2013). However, there has been few studies evaluating the influence of environmental exposures such as cycles of freeze/thaw (f/t) on the hydraulic performance of cement-treated materials. Based on evaluation of limited number of specimens, Pamukcu et al. (1994) showed minor reductions as well as increases of up to two orders of magnitude in the hydraulic conductivity of cement-stabilized dewatered sludge after 12 f/t cycles. To predict hydraulic conductivity of compacted soil-cement after one f/t exposure, Shea (2011) proposed an equation based on basic material characteristics, cement content, and the 7-day UCS value.

In absence of sufficient literature and reliable standards, many cement-stabilization projects (i.e. durability studies and project performance specifications) where changes in hydraulic conductivity may be critical to performance, suggest percent mass loss as an indicator for evaluating acceptance of performance under f/t exposure (e.g. Paria & Yuet (2006); ITRC (2010)). There are two drawbacks to this approach. Firstly, mass loss does not necessarily correspond to internal changes in the structure of cemented soils, which in essence controls the hydraulic conductivity of these materials (El-Korchi et al. (1989)).

Secondly, the actual performance degradation of the stabilized soil is not quantified, as the results do not provide any quantitative information on the changes in hydraulic conductivity of the material being tested. In other words, mass loss may be able to establish that there is damage to the specimen after f/t, but the extent of the damage will be unknown.

In the previous chapter, the effect of f/t testing conditions such as freezing temperature (-2, -10, and -20^{o}C), curing age at the time of first f/t cycle (16 and 35 days), and number of f/t cycles (4 and 12 cycles) were studied on hydraulic and strength performance of a cement-stabilized silty sand. Increases of up to three orders of magnitude in hydraulic conductivity as well as strength loss of up to 95 percent in the unconfined compressive strength (UCS) values were reported in the study. Statistical analyses performed on the results showed that all of the investigated testing factors were significant in the observed changes in the hydraulic conductivity and UCS values. It was also suggested that modifications in the mix design (i.e. increasing the cement content or reducing the water to cement (w/c) ratio) may result in better performance of cement-stabilized soils under f/t exposure.

The current chapter investigates the influence of a soil's grain size distribution (i.e. fines content), soil-cement w/c ratio, and curing age on the hydraulic and strength properties of cement-stabilized soils under control (i.e. unexposed) and f/t exposed conditions. Given the lack of literature on hydraulic performance of soil-cement, measurements on control conditions were necessary to better evaluate the influence of mix design on the f/t exposed specimens. The efficiency of the mass loss measurement in predicting changes in hydraulic performance of damaged specimens is also discussed. The potential healing capacity of f/t damaged specimens in recovery of their increased hydraulic conductive is also examined for some of the specimens that underwent damage during f/t.

4.2. Materials and Methods

4.2.1. Soil Materials

The three soils examined in this work were lab-manufactured by blending together "soil A" and "soil B" at different proportions, as presented in Table 4.1. Soil A consisted of a glacially derived silty sand (ASTM-D2487 (2011)) from Halifax, Nova Scotia that was initially sieved through a 9.5 mm (ASTM-D6913 (2004)) mesh-sized sieve to remove oversized material. The remaining soil was then passed through 4.75, 1.20, 0.30, and 0.08 mm sieves. The portion remaining on the 0.08 mm sieve was washed through this sieve (with wash water being discarded) in order to minimize the amount of fines content in this soil. Soil B was prepared by sieving a silt material derived from quarry operations through a 0.08 mm sieve and discarding the oversized portion. The graded materials from both soils were stored in plastic bags for future blending according to each mix design. The separation of the soils into specific gradation ranges provided some control on grain size distribution between different soil-cement mix designs.

Results of mineral oxides analyses for soil A and soil B are presented in Table 4.2. For both soils, silica and aluminum are the major oxides present, which account for more than 80% of the total composition. Ignition of the soil A and soil B at 1000^{o}C yielded a loss on ignition (LOI) of 2.41 and 1.17%, respectively, indicating the presence of small amounts of organic matter in these soils. X-ray diffraction tests performed on soil A and B samples (<0.044 mm size fraction) showed quartz and feldspars as the main mineralogical components of these materials.

Standard proctor compaction tests (ASTM-D558 (2011)) were performed on each soil (i.e. Soil I, II, and III) blended with 10% cement (i.e. under unhydrated conditions) to identify the optimum water content (OWC) of the resulting soil-cement. The three soils showed an OWC in the range of 8 to 11% and a maximum dry density ranging from 1976 to 2050 Kg/m^3. Slight increases in the OWC and slight decreases in the maximum dry density were observed with an increase in the fines content (passing 0.08 mm sieve) in the soils.

Table 4.1: Summary of soil particle size distributions and w/c ratios used for different mix designs.

Soil name	Mix designation	Water/cement ratio	Mixing method	Soil composition by dry weight, %					USCS classification of blended soil
				Soil A				Soil B <0.08 mm	
				9.5-4.75 mm	4.75-1.20 mm	1.20-0.30 mm	0.30-0.08 mm		
Soil I (SI)	SI(1)	1	Compaction	13	42	30	15	0	Well graded sand
	SI(1.5)	1.5	Self-consolidation						
	SI(2)	2	Self-consolidation						
Soil II (SII)	SII(1)	1	Compaction	11	36	25	13	15	Silty sand
	SII(1.5)	1.5	Compaction						
	SII(2)	2	Self-consolidation						
Soil III (SIII)	SIII(1)	1	Compaction	9	30	21	10	30	Silty sand
	SIII(1.5)	1.5	Compaction						
	SIII(2)	2	Self-consolidation						

Table 4.2: Mineral oxides analysis of the soils used in the study.

Mineral oxide	Soil A Wt. %	Soil B Wt. %
Al_2O_3	14.57	15.31
CaO	0.49	1.85
Fe_2O_3	2.66	5.66
K_2O	3.27	4.02
MgO	0.61	1.60
MnO	0.09	0.12
Na_2O	3.03	3.08
P_2O_5	0.23	0.39
SiO_2	71.82	65.65
LOI (1000°C)*	2.41	1.17
Total	99.18	98.85

*LOI: Loss on ignition

4.2.2. Soil-Cement Specimen Preparation

A total of nine mix designs were used in this research (see Table 4.1). Specimens were prepared by addition of 10% (i.e. cement/dry mass of soil) general use Portland-limestone blended cement (CSA type GUL) to each soil at different w/c ratios (i.e. 1, 1.5, and 2). Examination of the water content of the soil-cement mixture relative to the OWC, as well as some visual pre-assessment of the workability of the mixes, were performed to determine if specimens would be either compacted in standard compaction molds (ASTM-D558 (2011)) or placed into plastic molds for self-consolidation (Table 4.1). A brief description for each of these specimen preparation methods is provided in the following sections.

4.2.2.1. Compaction Method for Dry Soil-Cement Specimens

The required soil for each set of mix design was prepared by mixing soil A and B according to proportions presented in Table 4.1. Cement was then added to the soil and mixed until the mixture became homogeneous. The amount of water required to reach the target total w/c ratio, calculated by incorporating moisture content of the soil before mixing, was then

added to the soil-cement blend. Mixing was performed using a drill-mounted paddle until a uniform mixture was reached. The resulting soil-cement was compacted in standard proctor molds in three layers with each layer subjected to 25 blows of a 2.49 Kg standard hammer following ASTM-D558 (2011). After compaction, the molds were placed in sealed plastic bags (to minimize water evaporation) for 5 days prior to extrusion. Specimens were then stored in a 100% humidity moist room until the required age of testing.

4.2.2.2. Self-Consolidation Method for Wet Soil-Cement Specimens

For the wet mixing preparation of specimens, dry cement and water were first proportioned at the required w/c ratio and then mixed to form a slurry. The soil was then incrementally added to the cement slurry and mixed uniformly via a drill-mounted paddle. The given soil-cement mixture was then placed into cylindrical plastic molds with a nominal size of 101 mm diameter and 118 mm height. The soil-cement placement occurred in three layers, each layer being subjected to 20 strokes using a standard concrete slump testing rod to provide consistent consolidation. Similar to the dry mix preparation method, molds were placed in a sealed plastic bag for 5 days prior to extrusion. Specimens were then kept in a 100% humidity moist room prior to further testing.

4.2.3. F/T Conditioning of Soil-Cement Specimens

Specimens from each mix design were exposed to f/t cycles at immature and mature curing conditions. In this chapter, the first f/t cycle exposure occurred at the age of 16 days for immature and over 110 days for mature curing conditions. F/t cycling consisted of approximately 24 hours of freezing in a freezer set at -10±1^{o}C followed by thawing in a 100% humidity room at a temperature of 22±1^{o}C. All specimens were saturated under a minimum backpressure of 524 KPa (with a confining pressure of 558 to 593 KPa) for a minimum of seven days prior to f/t exposure (ASTM-D5084 (2010)).

4.2.4. Specimen Testing

The testing program was designed to evaluate the physical performance of both unexposed and exposed specimens for different mix designs and curing maturities. Figure 4.1 presents the sequence of testing for both immature and mature curing conditions. Tests performed on the 12 specimens from each mix design are also presented in Table 4.3. Details of the testing conditions used in the study are also discussed in the following sections.

4.2.4.1. Hydraulic Conductivity

Hydraulic conductivity measurements were performed on duplicate specimens following method A of ASTM-D5084 (2010) (i.e. constant head flexible-wall method). Permeation with de-aired water was performed under a hydraulic gradient ranging from 11 to 116 depending on the permeability of the specimens in order to control the length of experiments. Test durations ranged from 3 days for highly damaged specimens after f/t exposure, to 2 weeks for low permeable mature specimens. An outflow to inflow ratio of between 0.75 to 1.25 and a steady hydraulic conductivity value were considered as the test termination criteria. For specimens with very low hydraulic conductivity (i.e. less than 5×10^{-11} m/s), the outflow to inflow ratio was difficult to achieve in the two-week period of the testing, hence these tests were terminated when a steady hydraulic conductivity value was reached in consecutive readings.

For immature tests, control hydraulic conductivity values (K_0) were measured on specimens (specimens 1 and 2 in Figure 4.1 (a)) after approximately 9 days from specimen preparation. This test was completed before day 16, when the f/t cycling of these specimens began. At the end of the 12^{th} f/t cycle, these same specimens were tested for hydraulic conductivity values for exposed conditions ($K_{exposed}$). The hydraulic conductivity ratio, defined as the ratio of hydraulic conductivity values of exposed specimens to the values obtained prior to f/t exposure ($K_{exposed}/K_0$), are used subsequently to discuss changes in the hydraulic performance of specimens after f/t exposure.

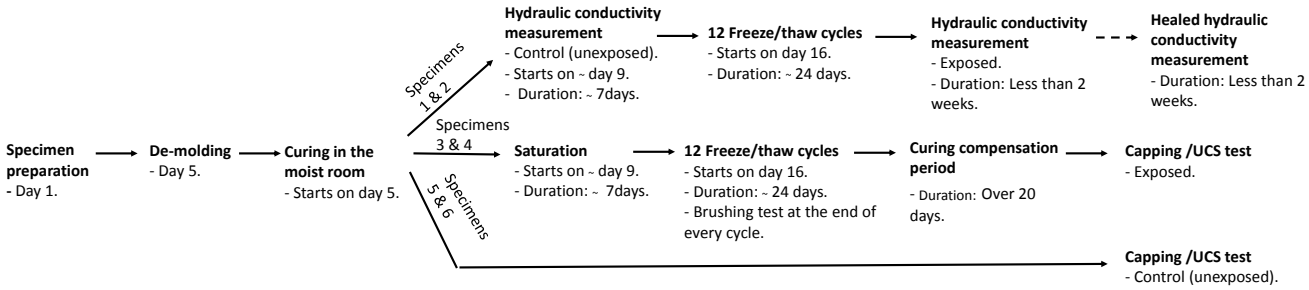

(a)

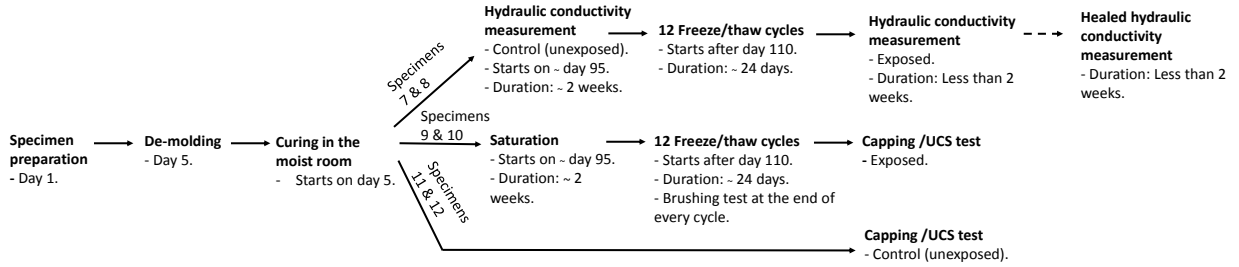

(b)

Figure 4.1: Summary of the testing procedures for a) immature b) mature tests.

Table 4.3: Details of testing on specimens from each mix design.

Specimen #	Immature exposure conditions						Mature exposure conditions					
	Hydraulic conductivity, unexposed	F/t exposure	Brushing test	Hydraulic conductivity, exposed	UCS, unexposed	UCS, exposed	Hydraulic conductivity, after healing	Hydraulic conductivity, unexposed	F/t exposure	Brushing test	Hydraulic conductivity, exposed	UCS, unexposed	UCS, exposed	Hydraulic conductivity, after healing
1 & 2	X	X		X			X							
3 & 4		X	X			X								
5 & 6					X									
7 & 8								X	X		X			X
9 & 10									X	X			X	
11 & 12												X		

For mature tests, control hydraulic conductivity values (K_0) were measured after about 95 days from specimen preparation (specimens 7 and 8 in Figure 4.1 (b)). At the completion of the test, specimens were exposed to 12 f/t cycles. Similar to immature specimens, hydraulic conductivity measurements were performed on exposed specimens and the hydraulic conductivity ratio was calculated to assess the changes in the performance of specimens after exposure to f/t cycles.

4.2.4.2. Percent Mass Loss

Current industry practice suggests percent mass loss as an indicator of resistance of cement-stabilized soils exposed to f/t cycles. To evaluate the reliability of this method in terms of predicting the changes in hydraulic performance of soil-cement, the brushing test (as suggested by ASTM-D560 (2003)) was performed on duplicate specimens (specimens 3 and 4 in Figure 4.1 (a), 9 and 10 in Figure 4.1 (b)) at the end of each f/t cycle and the specimens' mass was recorded. Brushing consisted of 20 strokes on the sides of the specimens (covering the perimeter twice) and 4 strokes on the top and bottom side of the specimens using a wire brush. Changes in the mass of the specimens were monitored by calculating the percent mass loss (Δ_m) using the following equation:

$$\Delta_m = \frac{m_0 - m_m}{m_0} \times 100 \qquad \text{Equation 4.1}$$

where m_0 and m_m are the initial mass and mass of the specimen after brushing at the end of the m^{th} f/t cycle, respectively.

4.2.4.3. Unconfined Compressive Strength (UCS)

Unconfined compressive strength (UCS) measurements were performed on duplicate specimens under unexposed (i.e. control) (specimens 5 and 6 in Figure 4.1 (a), 11 and 12 in Figure 4.1 (b)) and exposed conditions (specimens 3 and 4 in Figure 4.1 (a), 9 and 10 in Figure 4.1 (b)). For exposed conditions, the same specimens used for brushing tests were tested for UCS and as a result the reported values represent the residual compressive

strength of the specimens after the brushing test. The UCS ratio is calculated by dividing the average UCS values for exposed specimens by the average of values for unexposed specimens. In order to minimize variability between tests, UCS measurements for both exposed and unexposed specimens were performed on the same day. All specimens were sulfur-capped prior to the test to ensure concentric loading during the test. UCS values were obtained using a vertical deformation rate of 0.5 mm/min.

It is known that the hydration of cement occurs at a very slow rate at sub-zero temperatures (Kosmatka et al. (2003)). Comparing the testing procedures for measuring UCS values of control (unexposed) and exposed specimens in Figure 4.1 (a) and (b) shows that exposed specimens cure for about 12 days less than unexposed specimens due to the 12 f/t cycles (assuming minimal curing during each freezing period). For mature specimens, considering the length of the experiments (over 134 days), the curing age difference between control and exposed specimens will have a negligible effect on the observations. However, for immature specimens, to minimize the possible influence of this difference on UCS values, tests were performed approximately 20 days after completion of f/t cycles (curing compensation period in Figure 4.1 (a)). This ensured at least 48 days of curing for both control and exposed specimens in immature UCS tests. At this age it is assumed that differences observed in the results are due to the f/t cycling of exposed specimens as opposed to lack of curing in these specimens.

Considering the length of time required for f/t cycling and the curing compensation period (only for immature specimens), UCS tests for control conditions were performed at about 60 days after specimen preparation for immature tests and after 134 days for mature tests. To provide additional information on the effect of shorter and longer curing times on UCS than that described above, another specimen set was prepared for mixes SI(1), SI(2), SIII(1), and SIII(2) (selected as extreme mix designs for fine content and w/c ratio) and was tested for UCS values at the age of 16 days and 241 days.

4.2.5. Hydraulic Conductivity Recovery of Exposed Specimens

In contrast to exposure to f/t cycles, which is believed to damage the structural integrity of porous materials, autogenous healing has been reported to act positively in durability of cement–based materials (e.g. Jacobsen & Sellevold (1996)) and soils (e.g. Eigenbrod (2003)). To study the possibility for autogenous healing with respect to hydraulic conductivity changes after f/t exposure, ten immature and mature specimens (i.e. immature specimens from SI(1.5), SII(1.5), and SII(2) mix designs and mature specimens from SI(1.5) and SI(2) mix designs) which exhibited highest amounts of hydraulic conductivity changes during the experiments were re-tested for hydraulic conductivity values after a post-exposure curing period of at least 120 days in the moist room. Hydraulic conductivity ratios for healed specimens (i.e. K_{healed}/K_0) are calculated and compared to hydraulic conductivity ratios for the same specimens measured at the end of the 12^{th} f/t cycle (i.e. $K_{exposed}/K_0$).

4.3. Results and Discussion

Results of the testing described above are presented in following three sections. Firstly, the effect of mix design and level of curing on hydraulic and strength performance of cement-stabilized soils is presented (i.e. comparing the changes in the performance between unexposed specimens). Secondly, changes in hydraulic and strength performance of specimens after exposure to f/t cycles are presented and compared to values obtained from control conditions. This section also compares the changes in hydraulic conductivity values due to f/t exposure to the brushing tests results. Thirdly, the healing potential of exposed specimens are evaluated by presenting the changes in hydraulic conductivity values of damaged specimens after post-exposure curing.

4.3.1. Comparison of Performance Among Control Specimens

4.3.1.1. Influence of W/C Ratio on Hydraulic Conductivity and UCS

There is limited data in the literature related to the hydraulic conductivity of cement-stabilized soils and its relation to changes in the w/c ratio. Hammad (2013) performed laboratory studies on the effect of molding water content on hydraulic conductivity of a cement-stabilized silty sand. Hammad (2013) found that the lowest hydraulic conductivity for specimens cured for 28 days occurs at a water content ranging from 2 to 6 percent above the OWC measured from the standard proctor test. Extensive studies on compacted clays also exist in the literature that show the minimum hydraulic conductivity occurs at a water content slightly wet of OWC from standard proctor compaction effort (e.g. Boynton & Daniel (1985); Haug & Wong (1992)).

Based on the standard compaction test results for this study presented in Figure 4.2, specimens prepared at the w/c ratio of 1.5 (i.e. SI(1.5), SII(1.5), and SIII(1.5)) fall within the water content range of 2 to 6 percent wet of OWC (i.e. hatched areas in Figure 4.2). Figure 4.2 shows that, with the exception of the immature specimens for SI(1.5) and SII(1.5), these specimens have the lowest hydraulic conductivity values in comparison to other mix designs for both immature and mature conditions. Immature specimens for SI(1.5) and SII(1.5) both have hydraulic conductivity values higher than specimens with lower w/c ratio. This different behavior is likely due to high amounts of available water in the mix design of these specimens (due to the lower fines content of the initial soils) that delays the time required to disconnect the pore structure (Powers et al. (1959); Hearn et al. (2006)). Even for these specimens, at longer curing times (i.e. mature specimens), the lowest measured hydraulic conductivity occurs at w/c ratio of 1.5 (i.e. 2 to 6 percent wet of optimum water content).

Specimens from the SIII(1) mix design, which were compacted dry of optimum water content, exhibit hydraulic conductivity values of over two orders of magnitude higher than those compacted at slightly wet of optimum. This shows deviation from OWC towards a

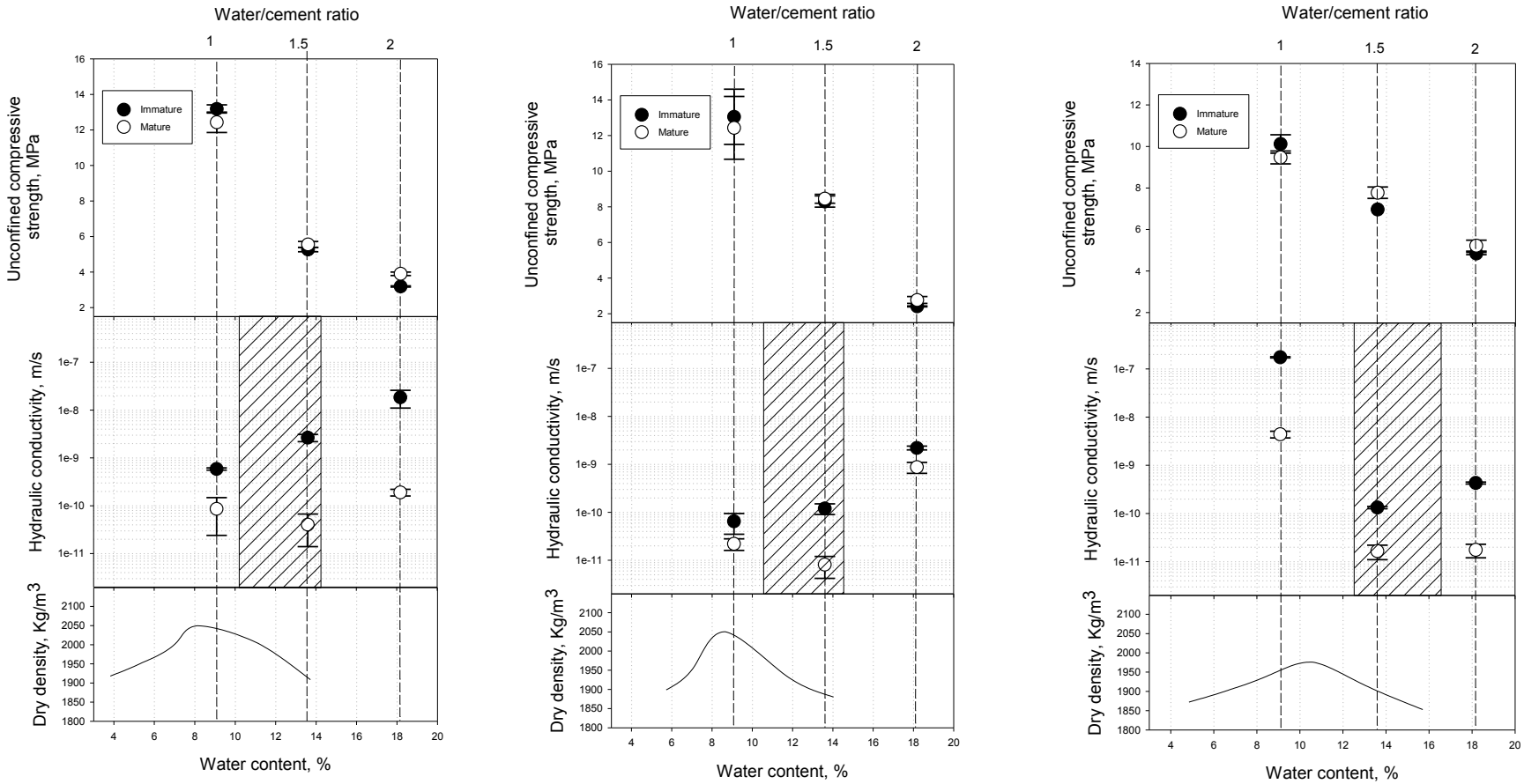

(a) Soil I: 0% fines **(b) Soil II: 15% fines** **(c) Soil III: 30% fines**

Figure 4.2: Effect of mix design on hydraulic and strength performance of cement-stabilized soils.
Note: hatched areas represent water contents that are 2 to 6% above optimum water content.

drier mix design can drastically increase the expected hydraulic conductivity values for both immature and mature conditions. Similar observations have been reported in previous studies on compacted clays (e.g. Mitchell et al. (1965); Boynton & Daniel (1985)). This is likely a result of insufficient lubrication of soil and cement particles during the compaction process at these low water contents which results in poor kneading compaction.

The w/c ratio and its importance as an indicator for mix design strength has been widely studied for concrete (Popovics & Ujhelyi (2008)). According to Abram's theory (Abrams (1919)), provided that a minimum w/c ratio required for the hydration of available cement and the workability of concrete is provided in a mix design, further increase in w/c ratio results in the reduction of compressive strength.

Results of UCS tests on cement-stabilized clays by Aderibigbe et al. (1985) showed a bell shape relation between w/c ratio and UCS. Optimum w/c ratios, to achieve the highest UCS, ranged from 0.4 to 2.6 for different ratios of cement/clay. Horpibulsuk et al. (2010) conducted some experiments to study the relation between the OWC for UCS and density (i.e. standard proctor test). Results showed that while for an un-cemented clay, the OWC for UCS and density were similar, for cemented samples the maximum strength occurred at about 1.2OWC from proctor test results. Horpibulsuk et al. (2003) also showed that Abram's equation is valid to predict the compressive strength of cemented clay with respect to w/c ratio at high water contents. Experiments by Guney et al. (2006) on cemented non-plastic soils (i.e. foundry sand) for w/c ratios ranging from 2% dry of to 2% wet of proctor test OWC, showed a general decreasing trend for UCS. This possibly suggests similarities between non-plastic soils and concrete in terms of w/c ratio-UCS behavior with respect to OWC from compaction tests (i.e. requiring minimum hydration water and workability as opposed to following the trends of proctor test OWC results).

For the three soils investigated in this study, all the w/c ratios, with the exception of SIII(1) specimens, are on the wet side of the material's OWC. UCS results (Figure 4.2) for the three soils show a general decreasing trend in compressive strength values as a result of an increase in the water content and a decrease in the dry density of the mix design.

4.3.1.2. Effect of Curing Age (Immature vs. Mature)

Cement-based materials have a dynamic structure that changes with time due to the ongoing process of cement hydration. According to Powers & Helmuth (1953) the pore size distribution within the structure of a cement paste can be divided into gel pores, capillary pores, and air voids. Water permeation in cement-based materials mainly occurs through a network of capillary pores and air voids. At the early stages of hydration, capillary pores are connected and provide a permeable medium. As the hydration process continues, some of the capillary pores change into gel pores and become disconnected, resulting in significant reduction in hydraulic conductivity. Powers et al. (1954) showed a reduction of over six orders of magnitude can occur in the hydraulic conductivity of cement paste from the time of specimen preparation (i.e. fresh paste) until 24 days of curing. The hydration process also causes an increase in the strength of the cemented soils because of the increased binding capacity of cement paste (ACI (1990)).

Comparing the hydraulic conductivity results for immature (16 days of curing) and mature (over 95 days of curing) conditions, Figure 4.2 shows a decrease of up to two orders of magnitude in the values at the longer curing age. However, UCS results in Figure 4.2 show a negligible difference between the values obtained for immature and mature control tests (with some cases immature specimens showing slightly higher UCS values compared to mature specimens). The reason for the minor difference between these cases is that, unlike the hydraulic conductivity specimens, UCS measurements for these control specimens were performed at an age of about 60 days for immature specimens (after completion of f/t cycling and curing compensation period (see Figure 4.1)), at which the main portion of hydration process is likely completed.

To provide some insight on the UCS values for shorter and longer curing ages, a parallel set of tests including mix designs from extreme conditions (lowest and highest w/c ratios and fines contents: i.e. SI(1), SI(2), SIII(1), and SIII(2)) was conducted. UCS measurements were performed on specimens at the age of 16 and 241 days. Results are presented in Figure 4.3, and show an increase of up to 52 percent in the UCS values between extreme curing ages (16 and 241 days). Considering the results of control

specimens (from immature and mature tests) presented in Figure 4.3, a general increasing trend can be observed for most of the mix designs. The exceptions are specimens from SIII(1), which show no obvious trend in the values. Considering that these specimens were cast at dry of OWC, this could be due to the low workability of this mix design resulting in a higher heterogeneity in the observed values.

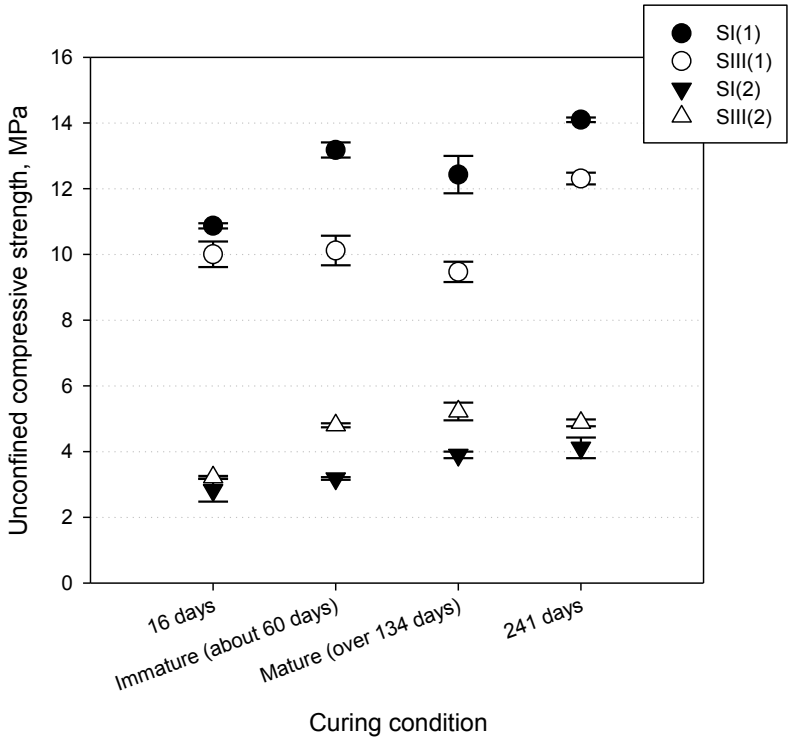

Figure 4.3: Effect of curing age on the compressive strength of cement-stabilized soils.

4.3.2. Influence of F/T Exposure on the Performance (i.e. Exposed Conditions)

Performance of specimens after exposure to f/t cycles are presented in the current section. In discussing the behavior of exposed specimens herein, immature and mature exposed specimens are referred as immature and mature specimens, respectively.

4.3.2.1. Hydraulic Conductivity

Figure 4.4 shows the results of hydraulic conductivity measurements for specimens after exposure to f/t cycles. In terms of hydraulic conductivity changes, Figure 4.4 shows both minor reductions for some immature specimens (i.e. hydraulic conductivity ratios less than 1) and increases of up to 5250 times. The increase in the hydraulic conductivity values can be attributed to the formation of cracks/micro-cracks within the structure of cement-stabilized soil during the freezing process. Any reduction in the hydraulic conductivity values after f/t is likely a result of the continuing hydration process in immature specimens that offsets any deteriorating effect of f/t cycles.

For soil I, specimens compacted near the OWC show the least amount of changes for both immature and mature conditions. It is expected that increase in water content in the mix design will result in higher f/t susceptibility of specimens (due to the reduced strength and increased porosity of the specimens) and hence increase in hydraulic conductivity ratios. According to Figure 4.4 (a), this trend is true with the exception of immature specimens at w/c ratio of 2. For these specimens, a reduction in hydraulic conductivity ratio was observed in comparison with the specimens prepared at w/c ratio of 1.5. This behavior could be due to interference of hydration process with deteriorating effect of freezing exposure in these specimens. Another possible reason for this behavior can be the high initial hydraulic conductivity of specimens from this mix design that can facilitate water transport through the soil-cement structure. This can prevent development of hydraulic pressure in the specimens during the freezing process and reduce the amount of observed damages (Powers & Willis (1949)).

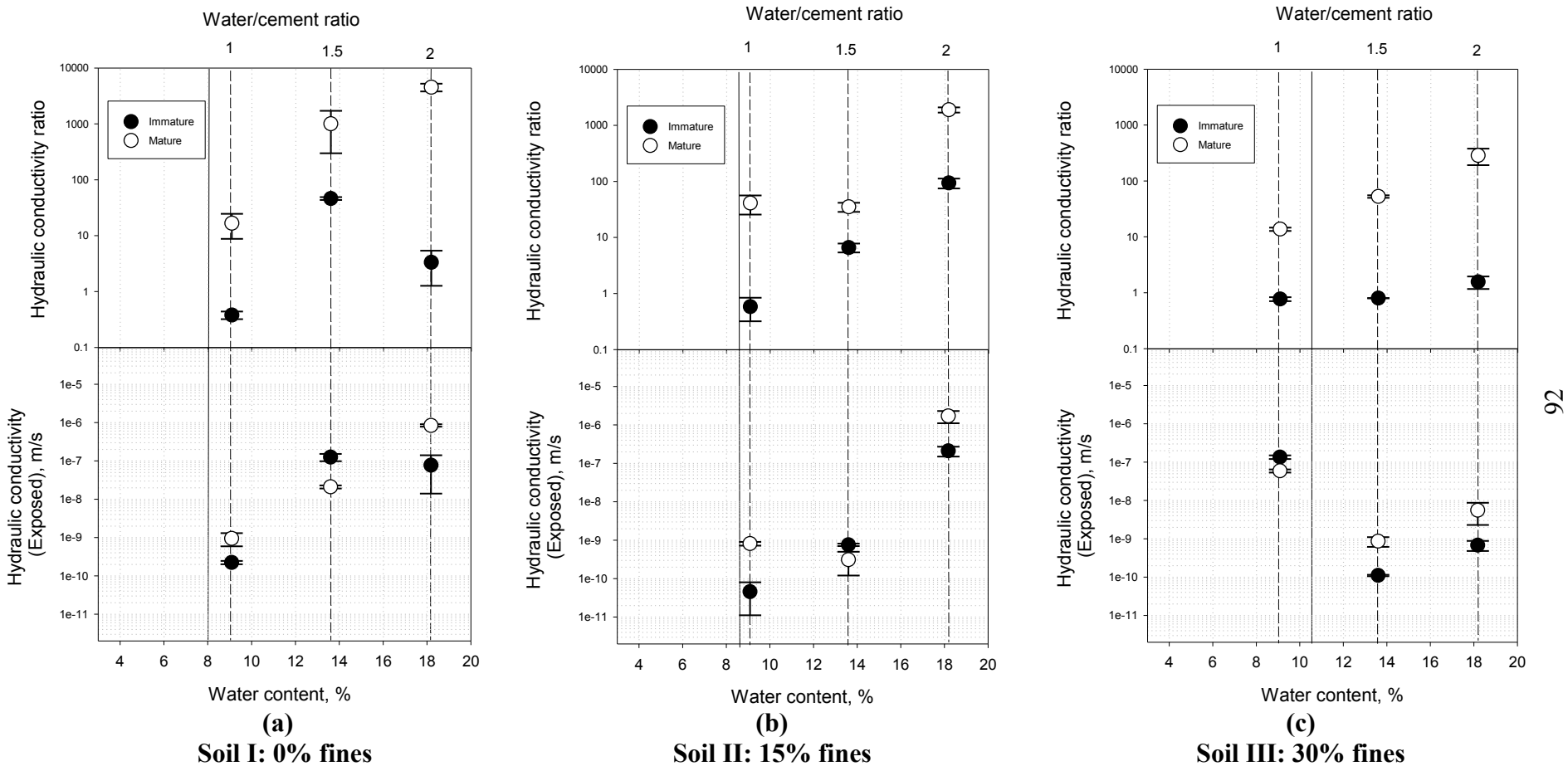

Figure 4.4: Hydraulic conductivity ratio (top) and exposed hydraulic conductivity (bottom) for exposed specimens.
Note: Vertical solid line represents the OWC conditions.

For soil II (Figure 4.4 (b)), an increase in the hydraulic conductivity ratio is evident as a result of increased w/c ratio in immature specimens. For mature specimens, while hydraulic conductivity ratio is noticeably higher for specimens prepared at w/c ratio of 2, specimens with w/c ratio of 1 and 1.5 exhibit relatively similar changes in hydraulic conductivity values.

For soil III (Figure 4.4 (c)), even though there are increasing trends in the hydraulic conductivity ratios for mature specimens with the increased w/c ratio, values of hydraulic conductivity for immature specimens are very similar to values measured for control conditions (i.e. hydraulic conductivity ratios close to 1). Comparing the hydraulic conductivity ratio for immature and mature specimens in Soil III to similar w/c ratios for Soil I and Soil II also shows better or relatively similar performance for this soil due to higher fines content.

From the results in Figure 4.4, it is also evident that mature specimens undergo a higher degree of damage (in terms of changes in hydraulic conductivity values) as compared to immature specimens. This is in agreement with observations in chapter three. Higher damage in mature specimens is likely a result of their increased brittleness due to the hydration process, which makes the material more sensitive to the deformations caused during the freezing exposure. The progressive hydration process in immature specimens may also offset the deteriorating effect of freezing, which can result in less changes in the observed hydraulic conductivity values.

Othman et al. (1994) showed that for compacted clays, specimens with higher initial hydraulic conductivity exhibit lower increases in hydraulic conductivity values after f/t exposure. For the specimens tested in this study, variation of hydraulic conductivity ratios after f/t exposure are plotted against initial hydraulic conductivity in Figure 4.5. While there is no obvious trend in the results, it seems that (although there are limited data points available) for initial hydraulic conductivity values higher than 1×10^{-8} m/s, relatively small changes in the hydraulic conductivity may occur after f/t exposure.

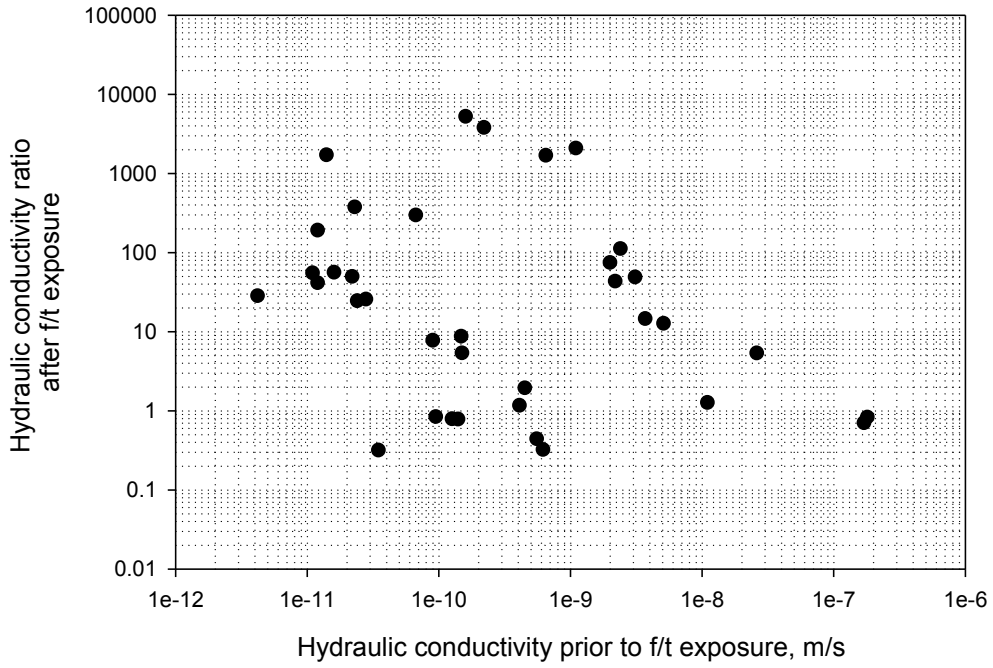

Figure 4.5: Variation of hydraulic conductivity ratios after f/t exposure compared to initial hydraulic conductivity values.

4.3.2.2. Brushing Test

The results of the brushing tests performed on exposed specimens at different f/t cycles is presented in Table 4.4. A mass loss (Δ_m) of between 0.72 to 23.4 percent was observed at the end of the 12th f/t cycle. However, it should be noted that all the experiments, with the exception of SII(2)-mature, showed a mass loss of less than 7 percent. This is despite hydraulic conductivity increases of up to three orders of magnitude for some of these mix designs. By comparing the mass loss data to the hydraulic conductivity changes presented in previous section, we can also conclude that the amount of mass loss in specimens is not proportional to the changes in the hydraulic conductivity values. For instance, specimens from SII(2)-immature and SII(1)-immature exhibit approximately equal mass loss at the end of the 12th f/t cycle, however, hydraulic conductivity ratios for these mix designs show about 100 times increase for SII(2)-immature and 15% reduction for SII(1)-immature. This difference is mainly because mass loss data represent the changes in the surface of the

exposed specimens, while hydraulic conductivity is controlled by internal changes in the specimens.

Comparing the results of mass loss at the end of the 12th f/t cycle for immature and mature curing conditions (Figure 4.6), shows a higher degree of surface damage in mature specimens after the brushing test. This is consistent with the observations for hydraulic conductivity changes (i.e. higher increases for mature specimens) presented in the previous section. Figure 4.6 also shows increase in w/c ratio seems to result in higher amount of mass loss for both immature and mature specimens. The exception to this observation being SII(1) and SII(1.5) specimens, which both have very low mass loss values of less than 3 percent. The increase in the mass loss due to the increased w/c ratio may partially be a result of decreased UCS values (and consequently tensile strength) of these specimens, which makes them more vulnerable to surface damages due to the brushing test.

4.3.2.3. Unconfined Compressive Strength

Figure 4.7 presents the results of UCS tests on specimens after exposure to f/t cycles. Reductions as high as 58 percent as well as increases as high as 14 percent were observed after f/t exposure. There is no clear trend in the changes in the observed values with regards to the mix design and water content. However, for most cases of immature and mature exposure (with the exception of SIII(1)-immature), compressive strength values still follow the same trend as control conditions (i.e. decreasing value with the increase in water content). SIII(1)-immature specimens showed 58 percent reduction in the compressive strength, resulting in UCS values smaller than SIII(1.5) and SIII(2) mix designs. This difference in the behavior suggests specimens compacted at dry of OWC may be more sensitive (in terms of UCS changes) to the exposure of freezing conditions at younger curing ages.

Table 4.4: Summary of percent mass loss data due to brushing of specimens at different f/t cycles.

SI												
	w/c=1				w/c=1.5				w/c=2			
	Immature		Mature		Immature		Mature		Immature		Mature	
f/t Cycles	Average Δ_m	SD	Average Δ_m	SD	Average Δ_m	SD	Average Δ_m	SD	Average Δ_m	SD	Average Δ_m	SD
0	0.00	0.00	0.00	0.00	0.00	0.00	0.00	0.00	0.00	0.00	0.00	0.00
1	0.72	0.03	0.93	0.08	0.14	0.04	0.44	0.10	0.51	0.16	0.39	0.12
2	0.84	0.05	1.23	0.22	0.34	0.09	0.60	0.09	0.89	0.22	0.70	0.30
3	0.91	0.08	1.46	0.33	0.48	0.10	0.83	0.19	1.25	0.14	0.97	0.50
4	0.95	0.11	1.69	0.38	0.68	0.09	1.45	0.00	1.62	0.20	1.47	0.81
5	0.86	0.17	1.97	0.24	0.87	0.04	1.74	0.00	1.92	0.21	1.81	0.96
6	0.92	0.17	1.98	0.38	0.99	0.08	2.03	0.00	2.07	0.24	2.45	1.38
7	0.90	0.21	2.20	0.44	1.19	0.11	2.39	0.00	2.38	0.24	2.66	1.58
8	0.99	0.20	2.38	0.50	1.33	0.17	2.59	0.00	2.70	0.33	2.91	1.72
9	1.02	0.21	2.43	0.49	1.41	0.12	2.74	0.00	2.82	0.27	3.18	1.97
10	1.05	0.21	2.56	0.52	1.59	0.19	2.98	0.01	3.02	0.27	3.41	2.04
11	1.08	0.28	2.70	0.57	1.71	0.13	3.21	0.01	3.60	0.52	3.78	2.32
12	1.15	0.28	2.88	0.59	1.83	0.14	3.36	0.01	3.87	0.27	4.17	2.66
SII												
	w/c=1				w/c=1.5				w/c=2			
	Immature		Mature		Immature		Mature		Immature		Mature	
f/t Cycles	Average Δ_m	SD	Average Δ_m	SD	Average Δ_m	SD	Average Δ_m	SD	Average Δ_m	SD	Average Δ_m	SD
0	0.00	0.00	0.00	0.00	0.00	0.00	0.00	0.00	0.00	0.00	0.00	0.00
1	0.66	0.04	0.76	0.35	0.09	0.01	0.54	0.05	-0.01	0.04	0.05	0.05
2	0.95	0.03	1.11	0.36	0.26	0.01	0.75	0.06	0.13	0.01	0.18	0.05
3	1.04	0.02	1.42	0.43	0.35	0.02	0.94	0.05	0.25	0.03	0.08	0.02
4	1.12	0.05	1.64	0.37	0.49	0.02	1.12	0.03	0.37	0.10	0.05	0.01
5	1.21	0.02	1.74	0.37	0.51	0.01	1.24	0.03	0.44	0.13	0.08	0.08
6	1.30	0.01	1.93	0.39	0.56	0.02	1.23	0.02	0.68	0.15	0.12	0.10
7	1.38	0.07	2.01	0.44	0.57	0.02	1.35	0.03	0.75	0.16	0.50	0.03
8	1.41	0.06	2.19	0.44	0.60	0.02	1.36	0.04	0.87	0.12	2.47	1.88
9	1.51	0.09	2.27	0.48	0.61	0.02	1.41	0.02	0.91	0.14	5.19	4.50
10	1.51	0.05	2.33	0.47	0.64	0.01	1.47	0.01	1.11	0.17	9.05	7.63
11	1.60	0.04	2.50	0.45	0.68	0.04	1.50	0.03	1.80	0.46	22.57	1.12
12	1.66	0.03	2.57	0.50	0.72	0.03	1.52	0.04	1.90	0.46	23.40	1.50
SIII												
	w/c=1				w/c=1.5				w/c=2			
	Immature		Mature		Immature		Mature		Immature		Mature	
f/t Cycles	Average Δ_m	SD	Average Δ_m	SD	Average Δ_m	SD	Average Δ_m	SD	Average Δ_m	SD	Average Δ_m	SD
0	0.00	0.00	0.00	0.00	0.00	0.00	0.00	0.00	0.00	0.00	0.00	0.00
1	0.38	0.11	0.61	0.10	0.72	0.01	0.90	0.14	0.56	0.04	0.51	0.01
2	0.47	0.12	1.06	0.27	0.87	0.03	1.08	0.16	0.68	0.04	0.90	0.08
3	0.56	0.15	1.30	0.31	0.98	0.09	1.26	0.18	0.81	0.05	1.21	0.12
4	0.70	0.16	1.44	0.29	1.12	0.08	1.36	0.20	0.97	0.08	1.43	0.22
5	0.80	0.20	1.50	0.24	1.15	0.09	1.46	0.20	1.05	0.07	1.47	0.27
6	0.88	0.25	1.64	0.23	1.20	0.13	1.60	0.21	1.15	0.08	1.59	0.31
7	0.94	0.28	1.68	0.29	1.29	0.14	1.66	0.19	1.29	0.07	1.78	0.36
8	0.93	0.28	1.74	0.73	1.32	0.16	1.80	0.18	1.33	0.08	1.84	0.40
9	0.98	0.20	1.83	0.74	1.40	0.19	1.84	0.13	1.43	0.09	1.89	0.41
10	1.13	0.34	1.85	0.76	1.43	0.20	1.85	0.15	1.41	0.11	1.99	0.47
11	1.12	0.37	2.00	0.78	1.43	0.20	2.04	0.11	1.47	0.12	2.18	0.53
12	1.23	0.45	2.01	0.77	1.47	0.21	2.07	0.13	1.54	0.11	2.29	0.58

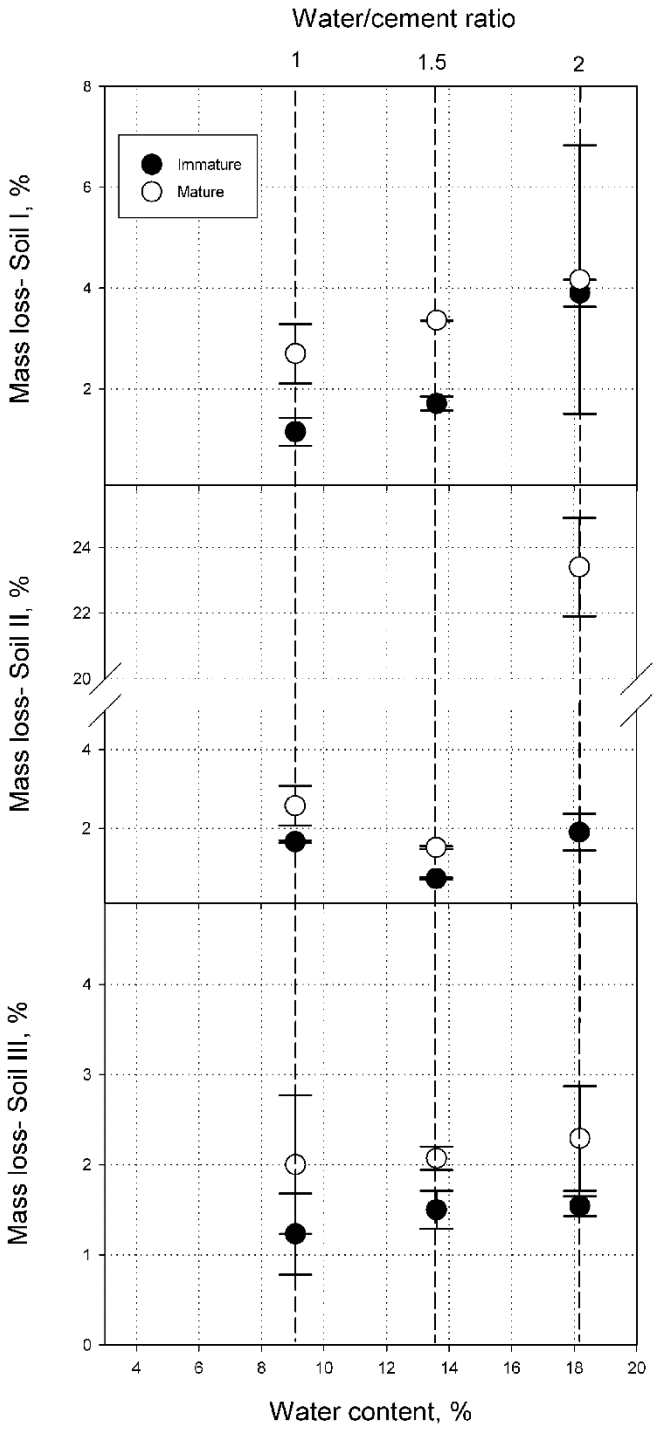

Figure 4.6: Mass loss of the exposed specimens at the end of the 12th cycle of freezing/thawing.

Considering the UCS ratios presented in Figure 4.7 (a) for soil I, specimens prepared at the w/c ratio close to the OWC resulted in minor changes after f/t exposure (UCS ratios close to 1). Also, an increase in w/c ratio in the mix designs for this soil seems to result in higher amounts of damage (i.e. lower UCS ratios) for both immature and mature cases with the exception of SI(2)-immature. This is in agreement with the changes in the hydraulic conductivity values for this mix design, which were presented in section 4.3.2.1.

For soil II (Figure 4.7 (b)), UCS ratios decrease (i.e. higher damage) as a result of increase in w/c ratio, with the exception of SII(1)-immature. For the SII(1) mix design, while mature specimens exhibited a UCS ratio of 1.14 (showing increase in the strength), immature specimens showed a decrease of approximately 30 percent (i.e. UCS ratio of 0.71) in the UCS values after f/t exposure. The poor performance of immature specimens for this mix design (compared to higher w/c ratios) is likely due to incomplete structure of these specimens at the time of exposure as a result of low w/c ratio. This is in agreement with the reductions observed in the hydraulic conductivity of SII(1)-immature after f/t exposure, which indicates continuation of curing process for these specimens.

For soil III (Figure 4.7 (c)), mature specimens compacted dry of OWC show an increase in UCS values after f/t exposure, while immature specimens from the same mix design exhibit about 58 percent reduction in UCS values compared to control conditions. Specimens prepared at higher w/c ratios exhibit UCS values similar to control conditions (i.e. UCS ratios close to 1), with the exception of mature specimens from SIII(1.5) that show about 20 percent reduction in UCS values after f/t exposure.

Dempsey & Thompson (1973) previously showed that there is a good correlation between UCS values for f/t exposed specimens (after 5 and 10 f/t cycles) and results of vacuum saturated UCS tests on unexposed specimens. The relation between exposed and unexposed UCS values in the current study is presented in Figure 4.8. A coefficient of determination (R^2) of 80 percent between the results suggests that unexposed UCS can be used to predict strength changes in the soil-cement after f/t exposure.

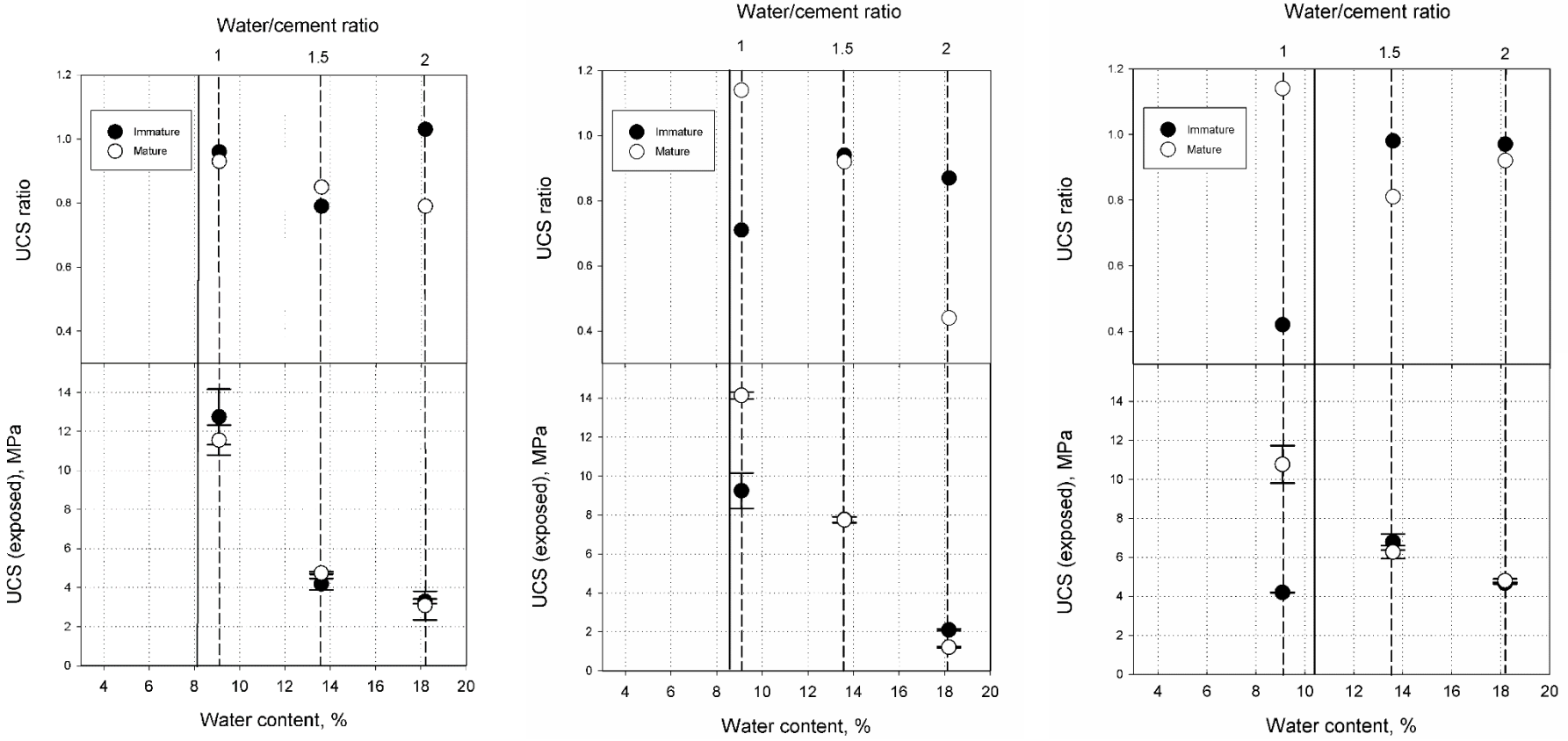

(a)
Soil I: 0% fines

(b)
Soil II: 15% fines

(c)
Soil III: 30% fines

Figure 4.7: Unconfined compressive strength ratio (top) and residual compressive strength (bottom) of specimens after f/t exposure. Note: Vertical solid line represents the OWC conditions.

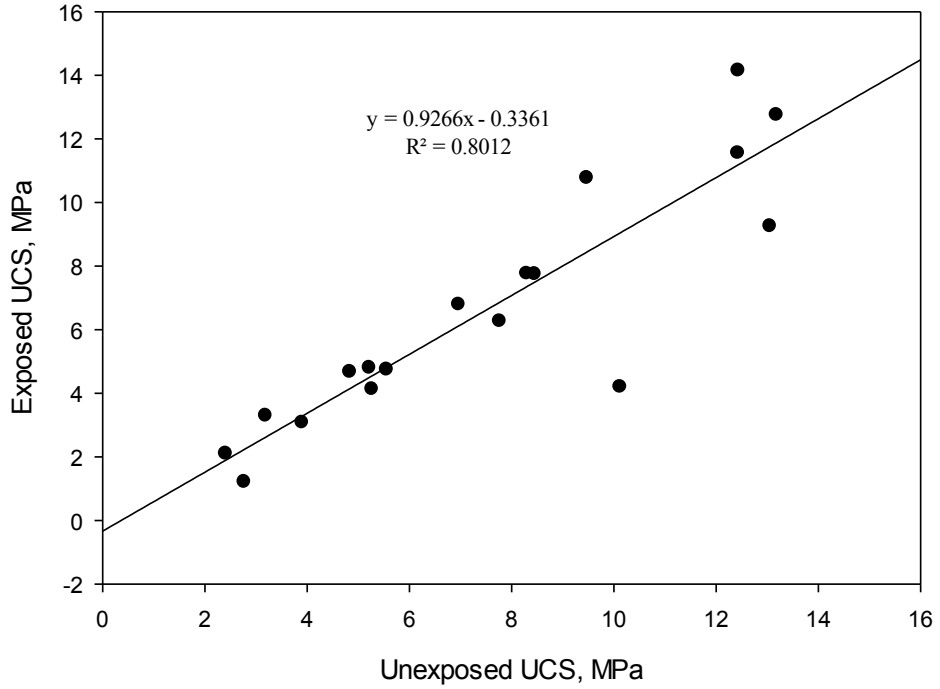

Figure 4.8: Correlation of UCS values for exposed and unexposed conditions.

Comparing the changes in the UCS and hydraulic conductivity values after exposure to f/t cycles doesn't show any correlation between the observed data. For instance, while SII(1)-mature specimens show an increase of about 50 times in hydraulic conductivity values after f/t exposure, specimens from the same mix design show a strength gain of about 14 percent. Similarly, while hydraulic conductivity of SII(1)-immature decreased after f/t exposure (i.e. improved performance), a reduction of approximately 30% is observed in UCS test results (i.e. performance degradation). These variations could be due to the different nature of these tests. For a specific mix design, f/t conditioning of the specimens may result in an increase in the porosity of the structure that can lead to a reduction in the compressive strength values. However, increase in the hydraulic conductivity, depends on the amount of connected porosity (including cracks and micro cracks) in the structure. Contrary, even a local crack can result in considerable increase in the hydraulic conductivity values, but possibly a smaller change in the observed UCS values.

4.3.3. Healing Potential for Exposed Specimens

Many mechanisms have been suggested to result in the self-healing of cement-based materials after f/t exposure. Those include further hydration of un-reacted cement, crystallization (calcium carbonate), or clogging of the cracks due to the impurities in the flow or moving of loose particles in the matrix (Edvardsen (1999)). A study by Jacobsen & Sellevold (1996) showed a partial regain of compressive strength of frost damaged concrete after a period of submersion in water. Scanning electron microscopy observations in that study showed presence of rehydration products (i.e. newly formed C-S-H), ettringite, and calcium hydroxide in the cracks. A study by Yang et al. (2009) on concrete suggests that the recovery of mechanical and transport properties of the samples can only be achieved under conditions of extremely tight crack widths. Under these conditions, full recovery for crack widths of less than 50 μm and partial recovery for crack width of up to 150 μm was achieved.

To study the potential for hydraulic conductivity recovery of specimens after f/t exposure, ten specimens (from both immature and mature curing conditions) that exhibited hydraulic conductivity ratios ($K_{exposed}/k_0$) ranging from 5.4 to 5250 were re-tested for hydraulic conductivity, after a post-exposure curing period of over 120 days in the moist room (K_{healed}). The healed hydraulic conductivity ratio was calculated by dividing values after the post exposure curing period by the control conditions (K_{healed}/K_0). Comparing the results to the values for control and exposed specimens (Figure 4.9) shows a wide range of healing potential for hydraulic conductivity values. Multiplier numbers next to the arrows on Figure 4.9 show the hydraulic conductivity ratios for exposed and healed specimens.

For immature conditions, SI(1.5) specimens which had hydraulic conductivity ratios of less than 50 times (49.2 and 43.5 for specimens #1 and # 2, respectively) after f/t cycles, recovered to hydraulic conductivity ratios of 5.5 and 2.0 after the healing period. SII(1.5)-immature specimens also healed from hydraulic conductivity ratios of 7.8 and 5.4 after f/t, to hydraulic conductivity ratios of 1.7 and 2.3, respectively. On the other hand, SII(2)-immature specimens which exhibited hydraulic conductivity ratios of 75 and 112.5 after

f/t exposure, reached to hydraulic conductivity ratios of 13.5 and 54.2 after the healing period, respectively.

Mature specimens from SI(1.5) and SI(2) mix designs showed hydraulic conductivity ratios of about 300 to 5200 after f/t exposure. After the post exposure healing period, even though these specimens exhibited some reduction in the hydraulic conductivity values compared to exposed conditions, results are still over two orders of magnitude higher than similar measurements for control conditions (Figure 4.9).

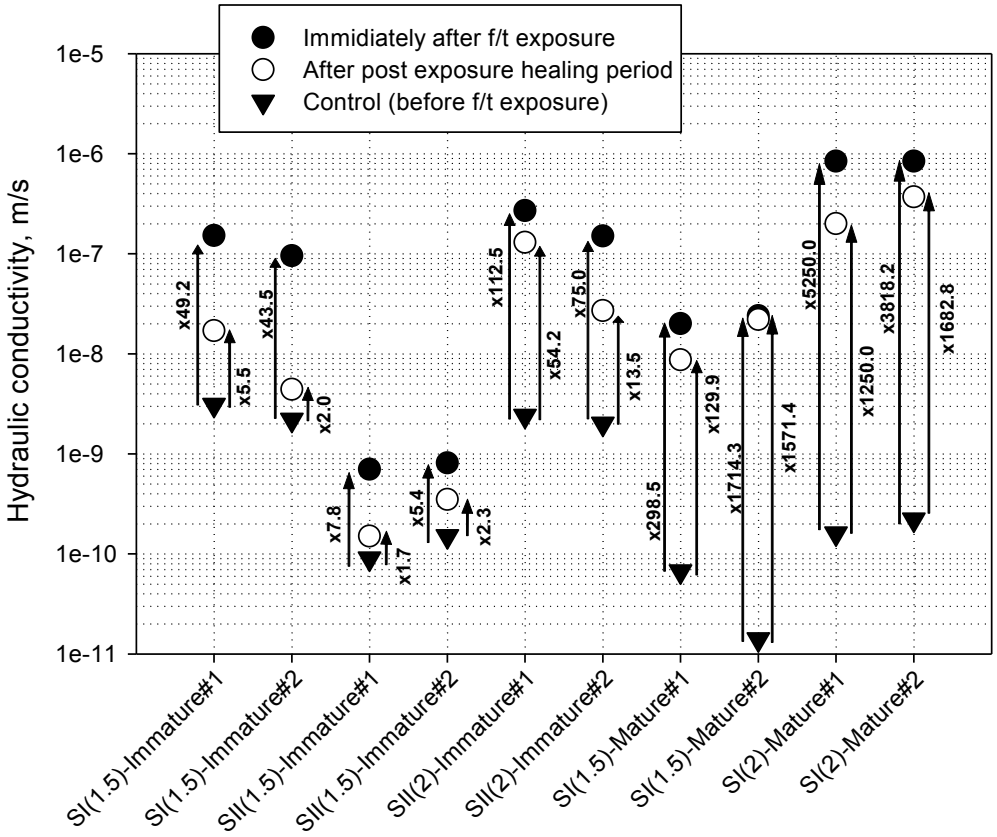

Figure 4.9: Hydraulic conductivity recovery of exposed specimens after post-exposure healing period.

Results of immature and mature specimens from Figure 4.9 could indicate that highly damaged specimens have less potential in recovery of lost hydraulic conductivity values,

potentially due to formation of larger crack widths in their structure similar to observations by Yang et al. (2009).

4.4. Summary and Conclusions

The current study investigated the influence of fines content in a soil, w/c ratio in soil-cement mix design, and curing conditions on performance of cement-stabilized soils prior to, and after, exposure to 12 cycles of f/t. A summary of the findings is as follows:

1. Hydraulic conductivity measurements for unexposed specimens showed that minimum values can likely be achieved at a w/c ratio slightly wet of OWC, as was previously suggested in the literature (Hammad (2013)). Also, comparing the results of immature and mature hydraulic conductivity measurements (16 days vs. over 95 days) showed a decrease of up to two orders of magnitude at the longer curing age.
2. For the mix designs investigated, UCS measurements on control specimens showed a decreasing trend, as a result of increase in w/c ratio. The difference between UCS values of immature and mature specimens were negligible. This was potentially because immature specimens were tested at an age of 60 days, when likely a considerable amount of hydration process was complete. A parallel test was conducted to compare the UCS values at short (16 days) and long (241 days) curing ages. These tests showed an increase of up to 52 percent in the values as a result of the curing process.
3. Both minor reductions and increases of up to 5250 times were observed in the hydraulic conductivity values after f/t exposure. While the increase in the hydraulic conductivity is a result of formation of cracks and micro-cracks in the specimens due to the freezing process, reduction in the hydraulic conductivity values may be a result of the continued hydration of cement that offsets the deteriorating effect of f/t cycles.
4. Mature specimens exhibited higher increases in the hydraulic conductivity values after f/t exposure as compared to immature exposed specimens. This is likely due

to brittleness of the specimens at mature conditions that makes them more susceptible to induced deformations during the freezing action. A continuing hydration process can also reduce the observed changes in the hydraulic conductivity of immature specimens after f/t exposure.

5. Brushing tests were performed at the end of each thawing phase, and the mass loss for each specimen was monitored for twelve cycles of f/t. Mass loss ranged from 0.72 to 23.4 percent, with most of the observed values under 7 percent. Mature specimens showed higher amount of surface damage (mass loss) compared to immature specimens exposed to f/t cycles. Comparing mass loss data with hydraulic conductivity changes after f/t cycles showed the changes are not proportional. This suggests mass loss is not a credible indicator for predicting changes in the hydraulic conductivity of cement-stabilized soils exposed to f/t cycles.
6. Changes in UCS values were monitored for different specimens exposed to f/t cycles. Decreases of up to 58 percent and increases of up to 14 percent were observed compared to control conditions. No obvious pattern in the changes was observed. Also comparing the results to the hydraulic conductivity measurements didn't show any correlation between the values.
7. Results of hydraulic conductivity measurements after a post exposure healing period of over 120 days showed that depending on the amount of initial damage, some reduction in hydraulic conductivity values can be expected over time. Specimens with lower amounts of damage (i.e. lower increase in hydraulic conductivity values) demonstrated a better potential in terms of reduction in the hydraulic conductivity values after the healing period. However, none of the specimens could achieve full recovery of the hydraulic conductivity values as compared to measurements performed for control conditions.

4.5. References

Abrams, D.A., 1919. *Design of concrete mixtures*, Chicago, IL: Bulletin 1, Structural materials research laboratory.

ACI, 1990. *Report on soil cement*, Farmington Hills, MI: Americal Concrete Institute (ACI) Committee 230, ACI230.1R-90.

Aderibigbe, D.A., Akeju, T.A.I. and Orangun, C.O., 1985. Optimal water/cement ratios and strength characteristics of some local clay soils stabilized with cement. *Materials and structures*, **18**(104):pp.103–108. doi:10.1007/bf02473376.

ASTM-D2487, 2011. Standard practice for classification of soils for engineering purposes (unified soil classification system). In *Annual Book of ASTM Standards*. West Conshohocken, PA: ASTM International. doi:10.1520/d2487-11.

ASTM-D5084, 2010. Standard test methods for measurement of hydraulic conductivity of saturated porous materials using a flexible wall permeameter. In *Annual Book of ASTM Standards*. West Conshohocken, PA: ASTM International. doi:10.1520/d5084-10.

ASTM-D558, 2011. Standard test methods for moisture-density (unit weight) relations of soil-cement. In *Annual Book of ASTM Standards*. West Conshohocken, PA: ASTM International. doi:10.1520/d0558-11.

ASTM-D560, 2003. Standard test methods for freezing and thawing compacted soil-cement mixtures. In *Annual Book of ASTM Standards*. West Conshohocken, PA: ASTM International. doi:10.1520/d0560-03.

ASTM-D6913, 2004. Standard test methods for particle-size distribution (gradation) of soils using sieve analysis. In *Annual Book of ASTM Standards*. West Conshohocken, PA: ASTM International. doi:10.1520/d6913-04r09.

Bellezza, I. and Fratalocchi, E., 2006. Effectiveness of cement on hydraulic conductivity of compacted soil–cement mixtures. *Ground Improvement*, **10**(2):pp.77–90. doi:10.1680/grim.2006.10.2.77.

Boynton, S.S. and Daniel, D.E., 1985. Hydraulic conductivity tests on compacted clay. *ASCE Journal of Geotechnical Engineering*, **111**(4):pp.465–478. doi:10.1061/(asce)0733-9410(1985)111:4(465).

Dempsey, B.J. and Thompson, M.R., 1973. Vacuum saturation method for predicting freeze-thaw durability of stabilized materials. In *Highway Research Record 442*. Highway Research Board, National Research Council, pp. 44–57.

Edvardsen, C., 1999. Water permeability and autogenous healing of cracks in concrete. *ACI Materials Journal*, **96**(4):pp.448–54.

Eigenbrod, K.D., 2003. Self-healing in fractured fine-grained soils. *Canadian Geotechnical Journal*, **40**:pp.435–449. doi:10.1139/t02-110.

El-Korchi, T., Gress, D., Baldwin, K. and Bishop, P., 1989. Evaluating the freeze-thaw durability of portland cement-stabilized-solidified heavy metal waste using acoustic measurements. In *Environmental aspects of stabilization and solidification of hazardous and radioactive wastes (STP 1033)*. Edited by P. Côté & M. Gilliam. Philadelphia, PA: ASTM International, pp. 184–191. doi:10.1520/stp22878s.

Ganjian, E., Claisse, P.A., Tyrer, M. and Atkinson, A., 2004. Selection of cementitious mixes as a barrier for landfill leachate containment. *ASCE Journal of materials in civil engineering*, **16**(5):pp.477–486. doi:10.1061/(asce)0899-1561(2004)16:5(477).

Guney, Y., Aydilek, A.H. and Demirkan, M.M., 2006. Geoenvironmental behavior of foundry sand amended mixtures for highway subbases. *Waste management*, **26**(9):pp.932–45. doi:10.1016/j.wasman.2005.06.007.

Hammad, A., 2013. *Evaluation of soil-cement properties with electrical resistivity*. M.A.Sc. Thesis, Civil and Resource Engineering Department, Dalhousie Univesity, Halifax, NS.

Haug, M.D. and Wong, L.C., 1992. Impact of molding water content on hydraulic conductivity of compacted sand-bentonite. *Canadian Geothechnical Journal*, **29**:pp.253–262. doi:10.1139/t92-029.

Hearn, N., Hooton, R.D. and Nokken, M.R., 2006. Pore structure, permeability, and penetration resistance characteristics of concrete. In *Significance of Tests and Properties of Concrete and Concrete-Making Materials (STP 169C)*. Edited by J. F. Lamond & J. H. Pielert. West Conshohocken, PA: ASTM International, pp. 238–252. doi:10.1520/stp36424s.

Horpibulsuk, S., Miura, N. and Nagaraj, T.S., 2003. Assessment of Strength Development in Cement-Admixed High Water Content Clays with Abrams' Law as a Basis (Technical Note). *Géotechnique*, **53**(4):pp.439–444.

Horpibulsuk, S., Rachan, R., Chinkulkijniwat, A., Raksachon, Y. and Suddeepong, A., 2010. Analysis of strength development in cement-stabilized silty clay from microstructural considerations. *Construction and Building Materials*, **24**(10):pp.2011–2021. doi:10.1016/j.conbuildmat.2010.03.011.

ITRC, 2010. *Development of performance specifications for solidification/stabilization (technical/regulatory guidance)*, Washington, DC.

Jacobsen, S. and Sellevold, E.J., 1996. Self healing of high strength concrete after deterioration by freeze/thaw. *Cement and Concrete Research*, **26**(I):pp.55–62.

Kosmatka, H., Kerkhoff, B. and Panarese, W.C., 2003. *Design and control of concrete mixtures* 14th editi., Skokie, IL: Portland Cement Assosiation.

Mitchell, J.K., Hooper, D.R. and Campanella, R.G., 1965. Permeability of compacted clay. *Journal of Soil Mechanics & Foundations Division*, **91**(SM4):pp.41–65.

Othman, M.A., Benson, C.H., Chamberlain, E.J. and Zimmie, T.F., 1994. Laboratory testing to evaluate changes in hydraulic conductivity of compacted clays caused by freeze-thaw: state-of-the-art. In *Hydraulic Conductivity and Waste Contaminant Transport in Soil (STP 1142)*. Edited by D. E. Daniel & S. J. Trautwein. Philadelphia, PA: ASTM International, pp. 227–254. doi:10.1520/stp23890s.

Pamukcu, S., Topcu, I.B. and Guven, C., 1994. Hydraulic conductivity of solidified residue mixtures used as a hydraulic barrier. In *Hydraulic Conductivity and Waste Contaminant Transport in Soil (STP 1142)*. Edited by D. E. Daniel & S. J. Trautwein. Philadelphia, PA: ASTM International, pp. 505–520. doi:10.1520/stp23905s.

Paria, S. and Yuet, P., 2006. Solidification/stabilization of organic and inorganic contaminants using portland cement: a literature review. *Environmental Reviews*, **14**:pp.217–255. doi:10.1139/a06-004.

Popovics, S. and Ujhelyi, J., 2008. Contribution to the concrete strength versus water-cement ratio relationship. *ASCE Journal of materials in civil engineering*, **20**(7):pp.459–464. doi:10.1061/(asce)0899-1561(2008)20:7(459).

Powers, T.C., Copeland, L.E., Hayes, J.C. and Mann, H.M., 1954. Permeability of portland cement paste. *Journal of American Concrete Institute*, **51**:pp.285–298.

Powers, T.C., Copeland, L.E. and Mann, H.M., 1959. *Capillary continuity or discontinuity in cement paste*, Skokie, IL: Bulletin no. 10, Portland Cement Association Research and Development Laboratories.

Powers, T.C. and Helmuth, R.A., 1953. Theory of volume changes in hardened portland-cement paste during freezing. In *Proceedings of the Thirty-Second Annual Meeting of the Highway Research Board*. Edited by F. Burggra & W. J. Miller. Washington, D.C., pp. 285–297.

Powers, T.C. and Willis, T.F., 1949. The air requirement of frost-resistant concrete. In *Proceedings of the Twenty-Ninth Annual Meeting of the Highway Research Board*. Edited by R. W. Crum, F. Burggraf, & W. N. Carey. Washington, D.C., pp. 184–211.

Shea, M.S., 2011. *Hydraulic conductivity of cement-treated soils and aggregates after freezing*. M.Sc. thesis, Department of Civil and Environmental Engineering, Brigham Young University, Provo, UT.

Yang, Y., Lepech, M.D., Yang, E.-H. and Li, V.C., 2009. Autogenous healing of engineered cementitious composites under wet–dry cycles. *Cement and Concrete Research*, **39**(5):pp.382–390. doi:10.1016/j.cemconres.2009.01.013.

CHAPTER 5: IMPACT RESONANCE METHOD AS A TOOL FOR PREDICTING CHANGES IN THE PERFORMANCE OF CEMENT-STABILIZED SOILS

5.1. Introduction

Cement-treatment of soils is an established method for improving their strength and hydraulic performance (ACI (1990); ACI (1999)). Previous studies (e.g. Klich et al. (1999); Fitch & Cheeseman (2003)) showed that despite improved mechanical properties after treatment, cement-treated materials can undergo degradation under environmental exposure such as freezing/thawing (f/t) cycles. Currently there is no standard method for assessing the hydraulic performance of cement-stabilized materials in cold regions. Durability studies for cement-treated materials intended for applications requiring low hydraulic conductivity values, such as cement-based solidification/stabilization, have suggested percent mass loss as an indicator of acceptability for performance under f/t exposure (e.g. Stegemann & Côté (1996); Paria & Yuet (2006); ITRC (2010)). While percent mass loss may sufficiently correlate with the changes in strength related parameters (e.g. Shihata & Baghdadi (2001b)), results in chapter four showed that it may not be a reliable indicator for predicting changes in the hydraulic conductivity of cement-stabilized soils exposed to f/t cycles. Further, conducting performance monitoring experiments, such as hydraulic conductivity measurement, prior to and after f/t exposure can add a significant amount of time to an already laborious testing process of these materials. Hence, development of quick predictive tools for assessment of hydraulic conductivity changes in cement-stabilized soils during freezing exposure seems to be beneficial.

Vibration-based non-destructive techniques are commonly used to evaluate the dynamic properties of structures incorporating different materials in civil engineering applications. These techniques have been used in evaluation of cement-based materials, mainly concrete, to predict dynamic modulus of elasticity (Swamy & Rigby (1971); Jin & Li (2001); ASTM-C215 (2008)), monitor changes due to progression of the hydration process (Nagy (1997); Jin & Li (2001)), or track damage formation during cyclic loads (Shah et al. (2000);

Gheorghiu et al. (2005)) and f/t exposure (El-Korchi et al. (1989); Ababneh & Xi (2006); ASTM-C666 (2008)). These techniques rely on the principle that the resonant frequency (RF) of a structure is related to its physical properties including density, shape, and the dynamic modulus of elasticity (Malhotra (2011)). Any changes in the physical properties of a structure will subsequently alter the measured RF of the system. Therefore, vibration-based non-destructive techniques are potentially efficient tools for monitoring degradation or improvement (e.g. curing processes) in cement-based materials.

Results in chapter three showed that the variations in the RF values measured using the impact resonance (IR) method during different f/t exposure scenarios was consistent with the observed changes in the hydraulic conductivity and UCS of a cement-stabilized silty sand. The purpose of the current study was to assess the suitability of the IR technique in replacing or supplementing the current industrial practice for evaluating the f/t performance of cement-stabilized soils. To achieve this objective, the IR method was used to monitor changes in the structure of cement-treated soils due to cement hydration (i.e. curing), f/t damage, and post f/t exposure healing processes. The results of the IR tests from the latter two experiments were compared to the hydraulic conductivity changes measured on the same specimens, presented in chapter four.

5.2. Experimental Program

The IR method testing conditions and experimental program is discussed in the current section. The majority of the IR experiments performed herein complement the performance characterization of specimens in chapter four. A comprehensive discussion on the materials used, specimens preparation, and f/t testing conditions were presented in chapter four. For the sake of completeness, only a summary of this information is presented in the current section.

5.2.1. Specimen Preparation

Three different soils (i.e. SI, SII, and SIII) were manufactured by blending “soil A” (size fraction between 0.08 mm and 9.5 mm of a glacially derived silty sand) and “soil B” (size

fraction smaller than 0.08 mm of a silt derived from quarry operations) according to the proportions presented in Table 5.1. X-ray diffraction tests performed on powdered samples (i.e. <0.044 mm) of soil A and B suggest quartz and feldspars as the main mineralogical components of these materials.

Table 5.1: Summary of soil particle distributions and w/c ratios used in different mix designs (chapter four).

Soil name	Mix designation	w/c ratio	Mixing method*	Composition by dry weight, %					USCS classification
				Soil A				Soil B <0.08 mm	
				9.50-4.75 mm	4.75-1.20 mm	1.20-0.30 mm	0.30-0.08 mm		
Soil I (SI)	SI(1)	1	C	13	42	30	15	0	Well graded sand
	SI(1.5)	1.5	S						
	SI(2)	2	S						
Soil II (SII)	SII(1)	1	C	11	36	25	13	15	Silty sand
	SII(1.5)	1.5	C						
	SII(2)	2	S						
Soil III (SIII)	SIII(1)	1	C	9	30	21	10	30	Silty sand
	SIII(1.5)	1.5	C						
	SIII(2)	2	S						

* C: Compaction, S: Self-consolidation

After blending, SI, SII, and SIII soils were stabilized by adding ten percent Portland-limestone blended cement (CSA type GUL) at different w/c ratios (i.e. 1, 1.5, and 2) resulting in nine different mix designs as presented in Table 5.1. Based on a visual assessment of the mix workability at the time of casting, specimens from each mix design were either compacted in standard compaction molds (ASTM-D558 (2011)), or placed into plastic molds (with a nominal size of 101 mm diameter and 118 mm height) for self-consolidation (Table 5.1). For all mix designs, the constituents were mixed using a drill-mounted paddle until uniformity was reached. After the soil-cement mixture was placed in the molds, they were sealed for 5 days in air-tight plastic bags to minimize water evaporation prior to extrusion. Specimens were then stored in a 100% relative humidity environment in a moist curing room until the required age for the start of each experiment.

5.2.2. Impact Resonance (IR) Test

A detailed procedure for conducting IR tests to measure fundamental transverse, longitudinal, and torsional RF of concrete specimens can be found in ASTM-C215 (2008). In the current study, the impact load was generated using a 9.5 mm in diameter steel ball attached to a plastic band, with a combined mass of 5.3 g, and was applied to the axial centerline of the specimens. An accelerometer (PCB model 352C68) was magnetically connected to a small piece of steel glued on the opposite side of the specimen. The vibration response of the specimen due to the impact was captured by the accelerometer and the signals were transferred to an amplifier and a computer data acquisition system (Freedom Data PC Platform, Olson Instruments Inc.) for recording and signal processing. A sampling rate of 500 kHz and record size of 8192 samples was used to provide a frequency resolution of 61 Hz for each test. A bandpass filter of 500 to 15000 Hz was applied during the test to isolate frequency components within the expected range of resonances. A fast Fourier transformation (FFT) was then used to transfer the signal to the frequency domain to determine the longitudinal RF of each specimen as the peak spectral amplitude within the response. Each test consisted of five replicate trials on the specimen and the average of the RF values were calculated for comparison in the results section. An average Relative Standard Deviation (RSD) value of less than 1 percent, with a range of 0 to 16.6 percent was calculated based on the five RF measurement trials on each specimen.

5.2.3. Testing Program

5.2.3.1. Monitoring the Curing Progress

Given that the hydration of cement becomes a slow diffusion-controlled reaction during its initial stages (Mindess et al. (2003)), the structure of cement paste continues to evolve over time as the process moves towards completion. Reductions in the hydraulic conductivity and increases in the strength are expected as a result of the curing progress in cement-based materials (e.g. Powers et al. (1954); ACI (1990)). Understanding the rate of evolution and the time span over which curing process occurs can be beneficial for implementation of cement-treatment projects in cold regions, as specimens cured for only 16 days have shown

slightly better performance under f/t exposure compared to specimens exposed at longer curing times (i.e. over 110 days) (chapter four). This may be due to the ductile behavior of specimens at early curing ages and/or the possible counteractive effect of the curing process with the development of f/t deterioration.

In this chapter, the curing progress of four different mix designs (i.e. SI(1), SI(2), SIII(1), and SIII(2)) was monitored using the IR method. Longitudinal RF measurements were performed on duplicate specimens at different specimen ages ranging from 5 days when they were de-molded, to 241 days after the specimen preparation. During this period, specimens were kept in a 100% humidity room in order to provide optimal curing conditions required for the hydration process. UCS tests were performed on duplicate specimens at curing times of 16 and 241 days for each mix design to evaluate the possible relationship between changes in the RF and strength development in the specimens.

5.2.3.2. Monitoring Specimens' Degradation Due to F/T Exposure

According to Powers' theory of hydraulic pressure (Powers (1945)), when water in the capillary pores of cement paste freezes, ice formation results in the water expanding nine percent from its initial volume. In near-saturated conditions, this process results in the development of excess pore water pressures in the structure that forces the water to escape to the nearest unsaturated voids/spaces. If the magnitude of the hydraulic pressure developed during this process exceeds the bursting strength of the material, it can result in development of cracks/micro-cracks within the structure (Powers (1945); Chatterji (2003)). Flaws which form during the freezing process can lead to an increase in the hydraulic conductivity, a reduction in the modulus of elasticity, and subsequently decrease in the RF of the material.

Specimens from different mix designs presented in Table 5.1 were exposed to f/t cycles at immature and mature curing conditions. In the current paper, immature and mature exposed specimens are simply referred as immature and mature specimens. For immature specimens, the initial f/t cycle occurred 16 days after specimen preparation; for mature

specimens, f/t cycling began after over 110 days of curing had occurred. It was assumed that after this age, changes in the soil-cement structure due to the curing process were negligible. For each f/t cycle, specimens were initially kept in a freezer at -10±1°C for approximately 24 hours, after which they were transferred to a 100% humidity room at a temperature of 22±1°C for thawing.

The IR testing was performed on each specimen prior to the initial f/t cycle (control conditions) and at the end of the thawing phase at different intervals through the f/t exposure.

The normalized changes in the longitudinal RF at the m^{th} f/t cycle (β_m), was calculated based on the following equation:

$$\beta_m = \frac{RF_m}{RF_0} \qquad \text{Equation 5.1}$$

where RF_m and RF_0 are longitudinal resonant frequency values at the end of the m^{th} f/t cycle, and at control conditions (i.e. unexposed), respectively.

Results of RF changes in this experimental study are compared to hydraulic conductivity measurements on the same specimens as presented in Table 5.2. Hydraulic conductivity measurements were performed prior to, and after f/t exposure following method A of ASTM-D5084 (2010) (i.e. constant head flexible-wall method) and results were discussed in chapter four. The hydraulic conductivity ratio in Table 5.2 is defined as the ratio of hydraulic conductivity values for exposed specimens measured at the end of the 12^{th} f/t cycle (K_{12}) to the values obtained prior to f/t exposure (K_0).

Table 5.2: Changes in hydraulic conductivity values of specimens due to f/t exposure (based on the data discussed in chapter four).

Soil	Mix design	Curing condition	Hydraulic conductivity, m/s				Hydraulic conductivity ratio (i.e. K_{12}/K_0)	
			Control		Exposed			
			Specimen #1	Specimen #2	Specimen #1	Specimen #2	Specimen #1	Specimen #2
SI	SI(1)	Immature	6.2e-10	5.6e-10	2.0e-10	2.5e-10	0.3	0.4
		Mature	2.4e-11	1.5e-10	5.9e-10	1.3e-9	24.6	8.8
	SI(1.5)	Immature	3.1e-9	2.2e-9	1.5e-7	9.5e-8	49.2	43.5
		Mature	6.7e-11	1.4e-11	2.0e-8	2.4e-8	298.5	1714.3
	SI(2)	Immature	1.1e-8	2.6e-8	1.4e-8	1.4e-7	1.3	5.4
		Mature	1.6e-10	2.2e-10	8.4e-7	8.4e-7	5250.0	3818.2
SII	SII(1)	Immature	3.5e-11	9.5e-11	1.1e-11	8.0e-11	0.3	0.8
		Mature	1.6e-11	2.8e-11	9.0e-10	7.2e-10	56.3	25.7
	SII(1.5)	Immature	9.0e-11	1.5e-10	7.0e-10	8.1e-10	7.8	5.4
		Mature	1.2e-11	4.2e-12	5.0e-10	1.2e-10	41.7	28.6
	SII(2)	Immature	2.4e-9	2.0e-9	2.7e-7	1.5e-7	112.5	75.0
		Mature	1.1e-9	6.5e-10	2.3e-6	1.1e-6	2090.9	1692.3
SIII	SIII(1)	Immature	1.8e-7	1.7e-7	1.5e-7	1.2e-7	0.8	0.7
		Mature	3.7e-9	5.1e-9	5.4e-8	6.5e-8	14.6	12.8
	SIII(1.5)	Immature	1.3e-10	1.4e-10	1.0e-10	1.1e-10	0.8	0.8
		Mature	2.2e-11	1.1e-11	1.1e-9	6.1e-10	50.0	55.5
	SIII(2)	Immature	4.1e-10	4.5e-10	4.8e-10	8.8e-10	1.2	2.0
		Mature	1.2e-11	2.3e-11	2.3e-9	8.7e-9	191.7	378.3

5.2.3.3. Recovery Potential for Exposed Specimens

Autogenous (self) healing in concrete structures was reported by Abrams (1913) over a century ago. Different mechanisms including the hydration of unreacted cement, swelling of C-S-H gel, blocking of flow paths by impurities, and crystallization of calcium carbonate may lead to autogenous healing, however the latter is believed to be the mechanism most responsible (Edvardsen (1999)). This healing process is believed to be more effective for crack widths smaller than 50 μm, while widths as high as 150 μm have been reported to exhibit partial recovery (Yang et al. (2009)).

To evaluate the healing potential under various exposure and mix design scenarios, specimens tested in the previous section were kept in a moist room for a period of at least 120 days after the 12th f/t cycle. IR testing was then performed on the specimens and RF values (i.e. RF_{healed}) were compared to the previous measurements on each specimen. Because of the interest in the variations of the RF values, all the measurements were normalized with respect to RF values measured for control conditions (i.e. β_{healed}). Results of the hydraulic conductivity measurements on specimens before and after the post-

exposure healing period presented in chapter four are also compared to the recovery potential for RF values in the current study.

5.3. Results and Discussions

Results of the current study are discussed in the following three sections. Section 5.3.1 describes the curing progression in specimens from selected mix designs evaluated by presenting the changes in the RF and UCS values over time. Section 5.3.2 describes damage development in specimens exposed to f/t cycles using the IR method. Results from this section are compared to hydraulic conductivity changes measured on the same specimens previously presented in chapter four. Finally, in section 5.3.3 the recovery potential for specimens from different mix designs evaluated using the IR method is discussed for f/t damaged specimens after a period of post-exposure curing in the moist room.

5.3.1. Assessment of the Curing Progress

Duplicate specimens from four mix designs (i.e. SI(1), SI(2), SIII(1), and SIII(2)) were tested for RF values at different time intervals ranging from 5 to 241 days after casting. Specimens were cured in a 100% humidity moist room during this period. Average RF values for each mix design are plotted in Figure 5.1. Immediately after de-molding, RF values ranged from 6700 to 11600 Hz for the different mix designs. Values increased sharply until a curing age of nearly 60 days, after which they reached about 80 percent of the total observed increase. After this age, the changes in the RF values continued, but at a reduced rate.

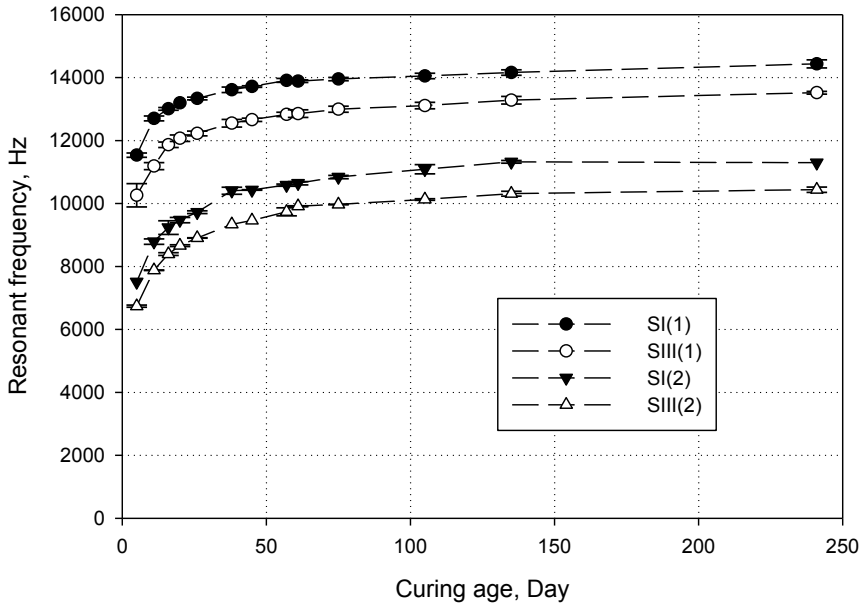

Figure 5.1: Variation of resonant frequencies at different curing ages.

Table 5.3 presents the average RF and UCS values for specimens cured for 16 and 241 days. UCS values ranged from 2.8 to 10.9 MPa for specimens cured for 16 days and from 4.1 to 14.1 MPa for specimens cured for 241 days, showing between a 23 to 52 percent increase in the values (i.e. UCS_{241}/UCS_{16} of 1.23 to 1.52). Comparing the RF between day 16 and 241 shows 11 to 25 percent increase (i.e. RF_{241}/RF_{16} of 1.11 to 1.25). Table 5.3 shows that within each soil type, specimens with higher RF ratios (RF_{241}/RF_{16}) exhibit higher increases in the UCS values (i.e. higher UCS ratio).

Comparing the results for each soil in Table 5.3 also shows that mix designs having a lower w/c ratio (i.e. SI(1) and SIII(1)) exhibit higher RF and UCS values. Further, these specimens exhibit smaller increases in RF and UCS values at the longer curing times, which may be due to the unavailability of sufficient amount of water for complete hydration in these specimens.

Table 5.3: Comparison of UCS and resonant frequency values at 16 and 241 days.

Soil type	Mix design	Day 16		Day 241		Frequency ratio (RF_{241}/RF_{16})	UCS ratio (UCS_{241}/UCS_{16})
		RF, Hz (RSD, %)	UCS, MPa (RSD, %)	RF, Hz (RSD, %)	UCS, MPa (RSD, %)		
Soil I	SI(1)	13006 (0.2)	10.9 (0.7)	14435 (0.6)	14.1 (0.5)	1.11	1.30
	SI(2)	9234 (1.7)	2.8 (12.4)	11292 (0.0)	4.1 (7.7)	1.23	1.45
Soil III	SIII(1)	11865 (0.5)	10.0 (3.9)	13520 (0.2)	12.3 (1.5)	1.14	1.23
	SIII(2)	8391 (0.4)	3.2 (1.4)	10437 (0.6)	4.9 (2.2)	1.25	1.52

Relative Standard Deviation (RSD) values for measurements in Table 5.3 show a maximum of 1.7 and 12.4 percent for IR and UCS tests, respectively. Noticeably smaller RSD values indicates strong reproducibility of results from IR test, as compared to those obtained from UCS testing under the conditions utilized in the current study.

5.3.2. Damage Progression Due to F/T Exposure

RF measurements were performed on duplicate specimens from different mix designs presented in Table 5.1 prior to f/t exposure (i.e. control conditions) and at subsequently increasing f/t cycles. Figure 5.2 shows the typical normalized acceleration responses of a specimen (i.e. SI(1.5)-mature) which was damaged through consecutive f/t cycles. It should be noted that damage is defined as an increase in the hydraulic conductivity value after f/t cycling. It can be seen that the damping dramatically increases after f/t exposure, resulting in a faster reduction of the acceleration amplitude (i.e. fewer oscillations) in signals from cycle 1 and 12 compared to the healthy signal obtained for control conditions. Applying a fast Fourier transformation (FFT) on the signals in Figure 5.2, one can plot the frequency spectrum of the SI(1.5)-mature specimen at different f/t exposure levels as presented in Figure 5.3. Results show a decrease in RF value as a result of damage progression in the specimen; dropping from about 11700 Hz for control conditions to less than 3000 Hz at the end of the 12^{th} cycle. Alterations observed in the acceleration-time domains and the corresponding frequency patterns are a result of the development of cracks/micro-cracks

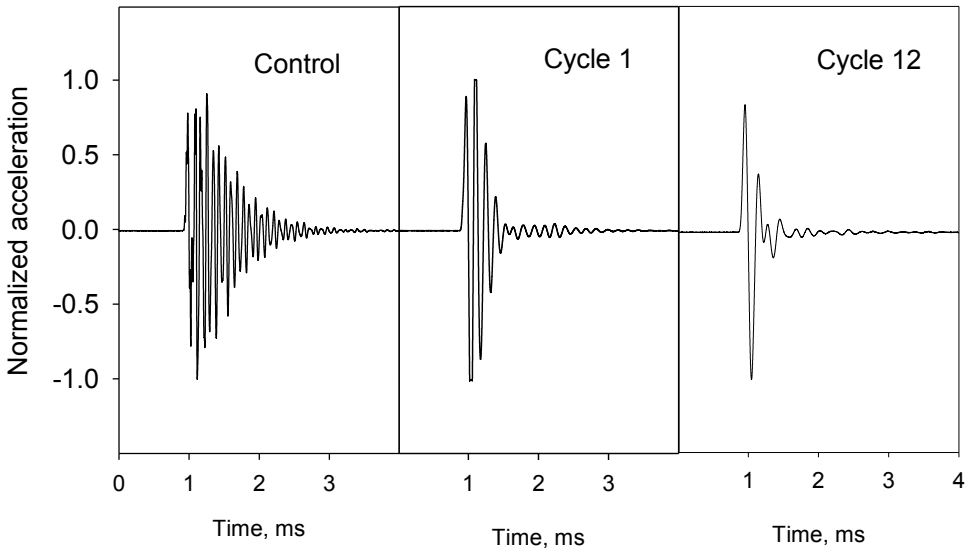

Figure 5.2: Changes in the frequency response signal as a result of progressive damage development in SI(1.5)-mature.

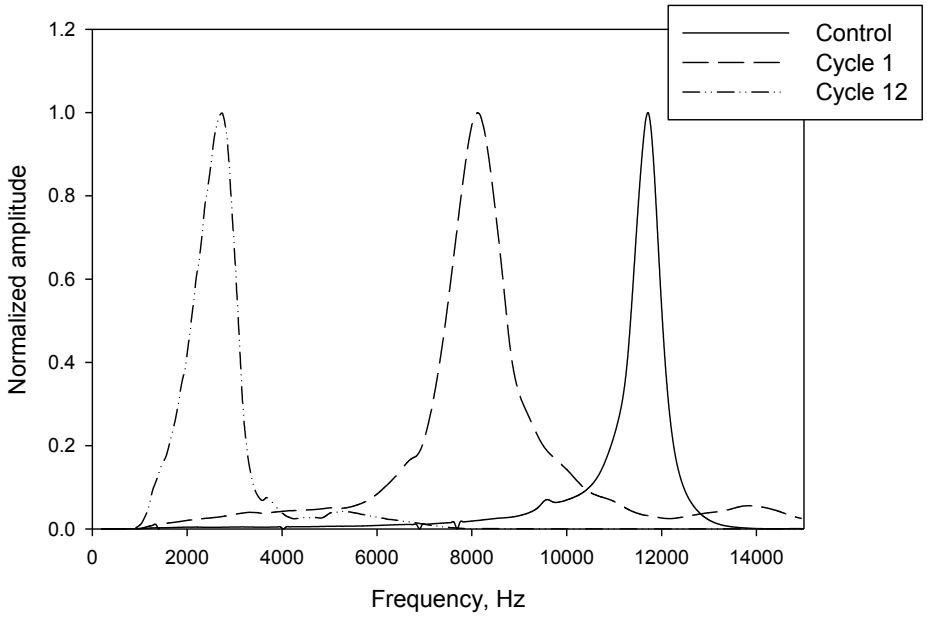

Figure 5.3: Changes in the frequency spectrum of SI(1.5)-mature as a result of progressive damage development due to f/t exposure.

within the specimen. In the damaged specimens, the impact-generated stress waves reflect from and are forced to travel around the newly formed cracks/micro-cracks (formed during f/t cycling), resulting in energy loss (i.e. increased damping) and reduction in the observed frequencies (Sansalone (1997)).

Figure 5.4 shows the RF measurements for control conditions (RF_0) as well as RF ratios at the end of the 12^{th} f/t cycle for different mix designs in this study. Since the obtained RF values depend on both dynamic modulus of elasticity of the material and the mass of each specimen (ASTM-C215 (2008)), results of the standard proctor tests (ASTM-D558 (2011)) on each soil-cement blend is also presented in Figure 5.4 in order to provide an insight on the density variations between the mix designs. An optimum water content (OWC) in the range of 8 to 11% and a maximum dry density in the range of 1976 to 2050 Kg/m^3 was observed for the three soils. It can be seen that all the mix designs in Figure 5.4 are on the wet side of the optimum water content with the exception of SIII(1) which is slightly dry of OWC.

Figure 5.4 shows that, for the mix designs being investigated, RF values for both immature and mature control specimens decrease as the w/c ratio is increased. Results in chapter four showed that an increase of w/c ratio in mix designs in Table 5.1 also resulted in a reduction in the UCS values. Also, RF measurements in Figure 5.4 show a higher value for mature conditions compared to immature specimens. Considering results from the previous section, this is a result of increase in the stiffness of the specimens due to the progression of the hydration process.

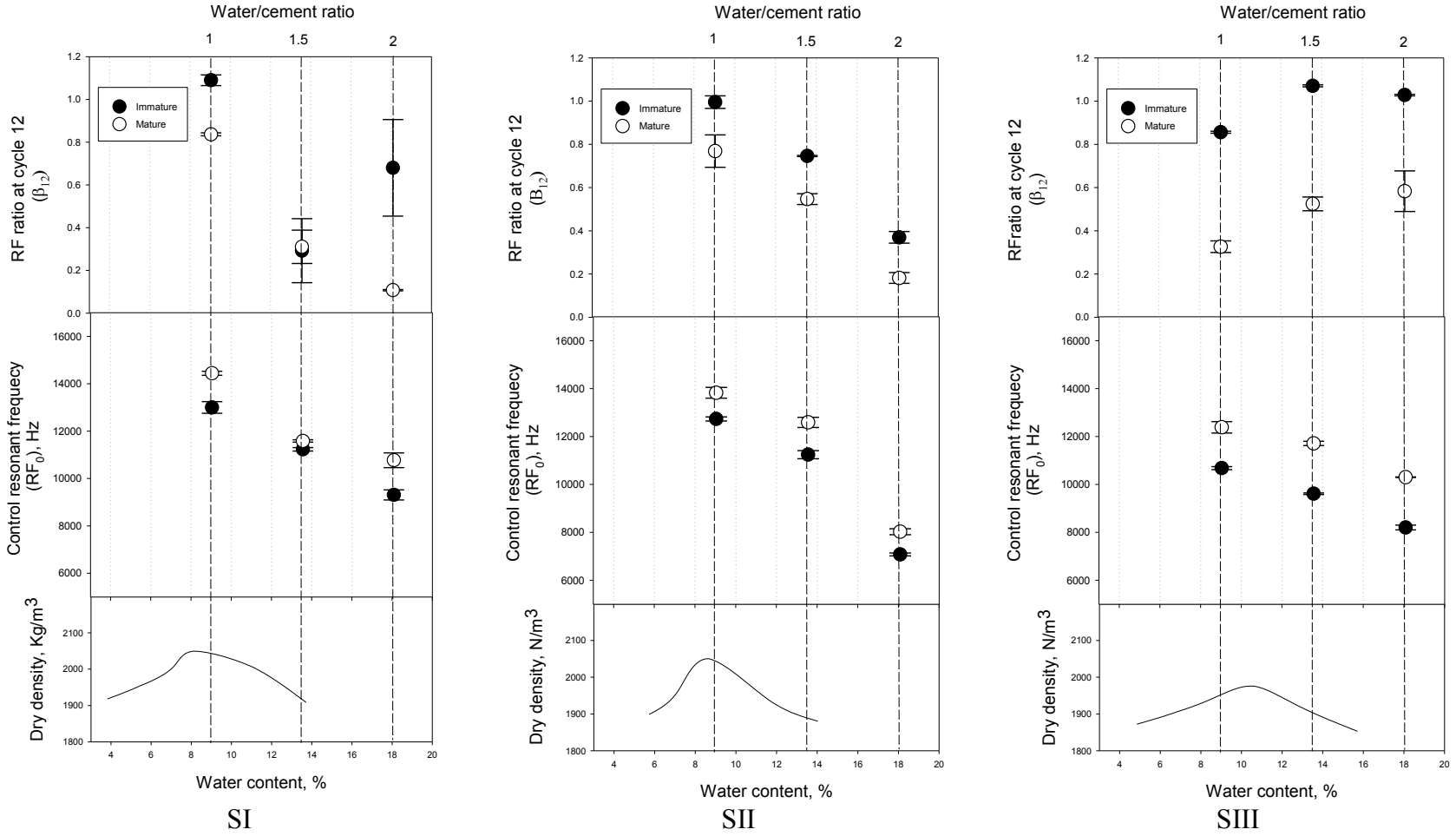

Figure 5.4: Variation of RF_0, RF ratio at 12th f/t cycle (β_{12}), and density-water content relations for different mix designs and soils.

Results of RF ratios at the end of the 12th f/t cycle (β_{12}) in Figure 5.4 show reductions as high as 90 percent and increases as high as 11 percent in the values. There is no clear trend in the changes of RF ratios (i.e. β_{12}) with respect to the variations in the mix design and soil type. However, within each mix design, mature specimens generally exhibit lower RF ratios (i.e. β_{12}) as compared to immature specimens, indicating a higher degree of structural degradation for mature specimens. This is in agreement with observations reported in chapter four for hydraulic conductivity changes of immature and mature specimens, which showed higher increases in the hydraulic conductivity values for mature specimens after exposure to f/t cycles (Table 5.2).

Immature specimens from some mix designs in Figure 5.4 (i.e. specimens prepared at the w/c ratio of 1 using soil SI and SII, as well as specimens prepared using soil SIII at w/c ratios of 1.5 and 2), exhibited some increase in the RF values after exposure to 12 f/t cycles (i.e. $\beta_{12}>1$) compared to values obtained for control conditions (i.e. β_0). This is likely due to the counteractive interference of the hydration process in these specimens, given that f/t exposure occurred at an early curing age, compared to the deteriorating effect of f/t damage. The same specimens exhibited hydraulic conductivity ratios ranging from 0.3 (decrease) to 2 (minor increase) after 12 f/t cycles as presented in Table 5.2.

Changes in the RF ratios at different f/t cycles (β_m) are presented in Figure 5.5. Results show that exposure to the initial f/t cycle has a significant influence on the creation of damage. For most cases, even specimens that exhibit higher RF values at the end of the 12th cycle (i.e. $\beta_{12}>1$) show minor drops in values at the end of the first cycle (β_1). This can be explained by the fact that specimens are in near saturated conditions before the initial f/t exposure due to the permeation process during the hydraulic conductivity tests prior to f/t exposure. Considering Power's theory of hydraulic pressure (Powers (1945)), after the initial f/t cycle, the possible cracks/micro-cracks developed in the specimens can create a pressure relief opportunity similar to air entrainment in concrete. Because specimens probably did not fully re-saturate during the thawing phase in the moist room, cracks/micro-cracks can reduce the travel distance for releasing the excess pore water

pressures developed during the subsequent freezing phases. Therefore, less damage can be expected in the following f/t cycles as compared to the initial exposure.

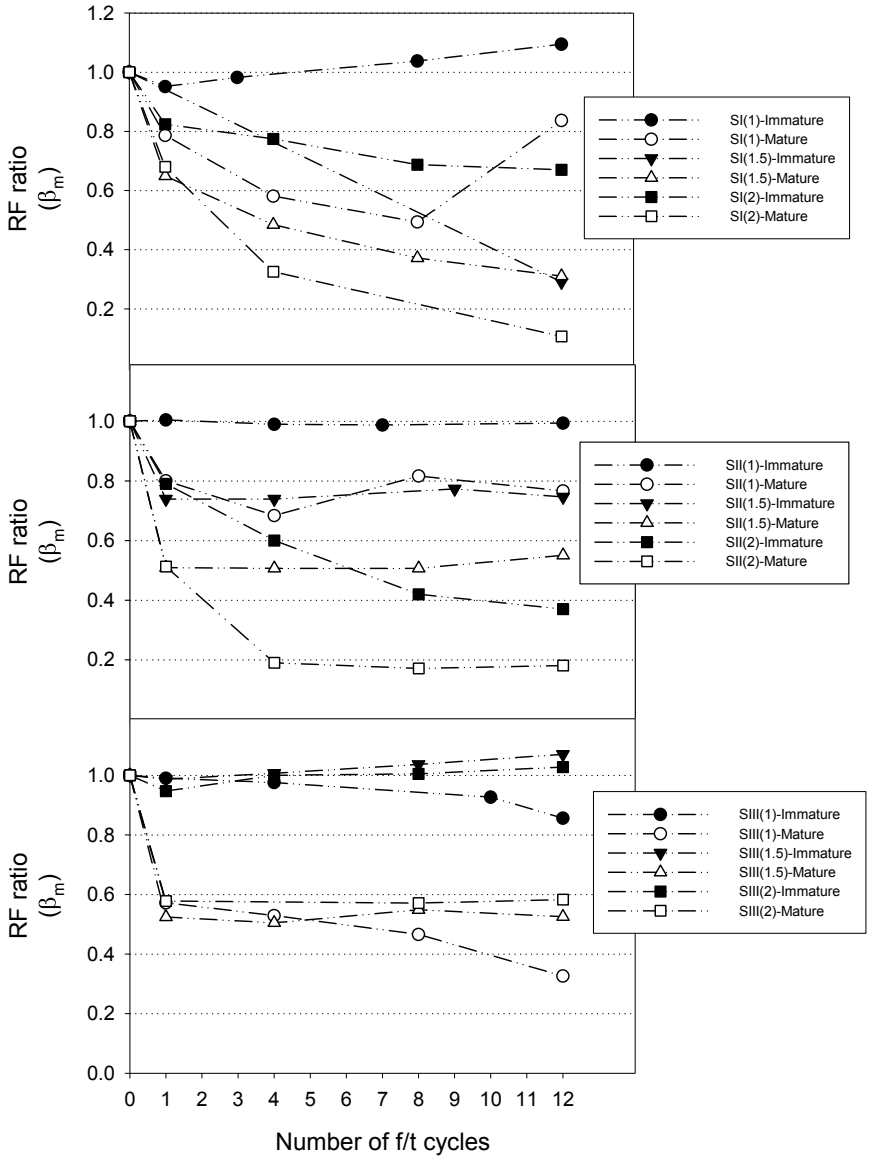

Figure 5.5: Changes in the RF ratio (β_m) values as a result of consecutive f/t cycles.

After the initial cycle, varying behaviors were observed for specimens at subsequent f/t exposures as noted in Figure 5.5. Those include:

- Some specimens exhibited small changes in the RF values after the initial f/t cycle (β_1), with an increase or minor reduction in the frequency values at further f/t exposure. Immature specimens from SI(1), SII(1), SIII(1.5), and SIII(2) fall into this category.

- Some specimens showed a substantial reduction in the RF values after the initial f/t cycle (β_1), but exposure to subsequent cycles resulted in only minor changes in the RF. Immature specimens from SII(1.5), and mature specimens from SII(1), SII(1.5), SIII(1.5), and SIII(2) are in this category.

- Some specimens exhibited a continuous drop in RF values even after the initial f/t cycle. This includes immature specimens from SI(2), SII(2), and SIII(1), and mature specimens from SI(1.5), SI(2), and SIII(1).

Some of the specimens in Figure 5.5 did not follow any of the previously mentioned patterns. For instance, RF measurements for SII(2)-mature shows some reduction between cycle 1 and 4, however, no significant variation was observed at subsequent f/t cycles. Also, mature specimens from SI(1) showed an unusual increase in the RF ratios between cycle 8 and cycle 12. For SI(1.5)-immature, due to the unavailability of equipment, RF values were only measured for control conditions and cycle 12. No trend in RF changes can be concluded from these measurements.

Results of RF ratios at the end of the 12^{th} f/t cycle (β_{12}) are plotted against hydraulic conductivity ratios obtained at the end of the 12^{th} cycle (i.e. K_{12}/K_0) in Figure 5.6 (a). As previously noted, measurements were performed on the same specimens for both tests. A distinctive behavior was observed for the RF ratio of approximately 0.85. Most specimens having a RF ratio higher than this value, exhibit minor increases or reductions in the hydraulic conductivity values after 12 f/t cycles (i.e. K_{12}/K_0 values close to or smaller than 1). However, specimens with frequency ratios less than approximately 0.85 appeared to exhibit a higher degree of degradation in terms of hydraulic conductivity changes. Similar behavior was observed for RF ratios at the end of the first f/t cycle (i.e. β_1) as presented in Figure 5.6 (b).

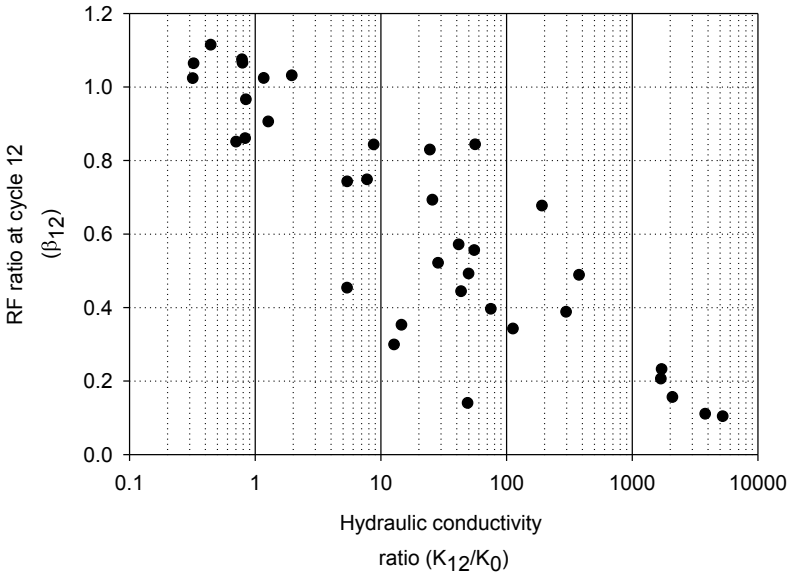

(a)

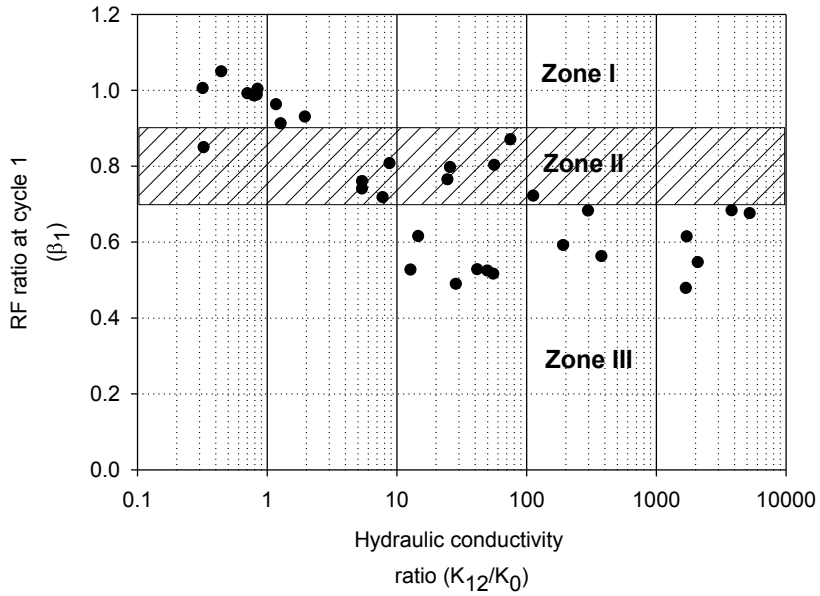

(b)

Figure 5.6: Variation of frequency ratio at the end of the a) 12th and b) 1st f/t cycle compared to the hydraulic conductivity ratio (i.e. K_{12}/K_0) measured after 12 cycles of f/t exposure.

As mentioned earlier, one of the drawbacks of current test methods for durability assessment of cement-stabilized soils is the long testing time required for f/t cycling of the specimens. This is in addition to an already long curing process, and the need to conduct

performance (e.g. hydraulic conductivity) measurement for these materials. A practical application of findings presented in Figure 5.6 (b) is to develop a pre-screening scheme based on RF measurements at the end of the initial f/t cycle (i.e. β_1) to enable the prediction of possible hydraulic conductivity changes (in terms of the magnitude) in specimens after exposure to 12 f/t cycles (i.e. K_{12}/K_0). According to the RF ratios, Figure 5.6 (b) has been divided into three zones designated as I, II and III. In zone I, for specimens with RF ratios greater than 0.9 at the end of the first f/t cycle (i.e. $\beta_1>0.9$), one can conclude with a great certainty, that there will be minor changes in the hydraulic conductivity values after 12 f/t cycles. As a result, all the specimens in zone I would "pass" the f/t tests performed under conditions demonstrated earlier in the study, if less than an order of magnitude change in hydraulic conductivity values is desired. In zone III, specimens with RF ratios less than 0.7 at the end of the first f/t cycle (i.e. $\beta_1<0.7$), all the specimens seem to show a significant increase (over one order of magnitude) in the hydraulic conductivity values at the end of the 12^{th} cycle, and hence would fail the f/t study tests. For specimens in zone II, with RF values between 0.7 and 0.9 at the end of the initial f/t cycle (i.e. $0.7<\beta_1<0.9$), IR test results are inconclusive and further testing (i.e. exposure to 12 cycles and measurement of hydraulic conductive changes) would be necessary to predict the hydraulic performance of specimens. The proposed pre-screening scheme can eliminate the need for completing the 12 f/t cycling of the specimens in zones I and III in order to predict the acceptability of changes in the hydraulic conductivity values as a result of f/t exposure under the conditions demonstrated in this study. It should also be noted that, at this point these conclusions are the result of a qualitative analysis of RF measurements. Further experiments combined with statistical analysis would provide some estimate of the reliability of this approach.

5.3.3. Recovery Potential After the Post-Exposure Healing Period

After exposure to the 12^{th} f/t cycle, previously tested specimens were kept in a moist room for over 120 days. Figure 5.7 shows that all specimens exhibited some improvement in their structure after the post-exposure healing period (i.e. $\beta_{healed} > \beta_{12}$). For most cases of immature specimens, with the exception of SI(1.5) and SII(2), average RF values at the end of the healing period reached or exceeded the values obtained as control measurements

prior to f/t damage (i.e. $\beta_{healed} \geq 1$). SI(1.5) and SII(2) specimens also showed a noticeable increase in the RF values after the healing periods resulting in an average β_{healed} value of about 0.6 for each mix design.

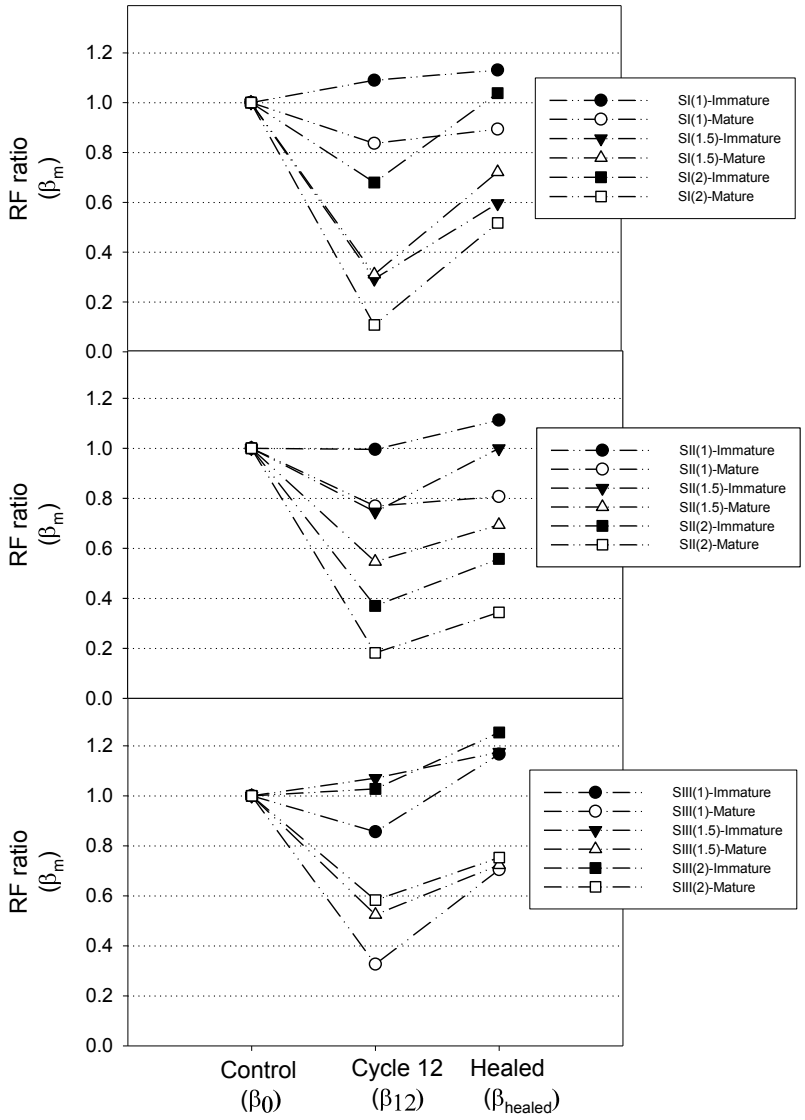

Figure 5.7: Frequency ratio after 12th f/t cycle and post-exposure healing period.

Considering the case of mature specimens, it can be assumed that the hydration process of cement is nearly complete at the end of the 12th f/t cycle (at the age of over 134 days). In

addition, hydraulic conductivity measurements prior to and after f/t cycling minimizes the potential for presence of unreacted cement in the specimens as a result of water permeation within the pore structures. Interestingly, in Figure 5.7, mature specimens still exhibit a considerable amount of healing potential as suggested by increases in the RF ratios after the healing period.

Figure 5.7 shows that specimens with similar RF ratios after the 12^{th} f/t cycle (β_{12}) do not necessarily exhibit similar recovery potential after the healing period. SII(1)-mature and SII(1.5)-immature both showed a RF ratio of about 0.8 at the end of the 12^{th} cycle; but after the healing period, the RF ratio (β_{healed}) of SII(1.5)-immature increased to a value of about 1, while the RF ratio of SII(1)-mature showed only a small increase. Also, mature specimens from SIII(1), SIII(1.5), and SIII(2) had a RF ratio (β_{12}) ranging from 0.3 to 0.6 at the end of the 12^{th} cycle, however after the healing period, all these specimens reached an average RF ratio (β_{healed}) of about 0.7.

The recovery of hydraulic conductivity values for selected f/t damaged specimens from mix designs in Table 5.1 after the post-exposure healing period was discussed in chapter four. Results are presented in Table 5.4 and are compared to the changes in the RF values for the same specimens. Based on the results in Table 5.4, the healing potential for the hydraulic conductivity and RF values do not seem to be proportional. For most of the specimens tested, increases in the RF values after the healing period are significantly more than the improvements in the hydraulic performance. This is potentially a result of the nature of the IR test which involves applying low stress levels to specimens for measurement of the RF values. As a result, it is possible that during the healing process minor improvements in the structure of the damaged specimens can improve the RF values, while the overall performance of the specimens remains unchanged. Jacobsen & Sellevold (1996) previously showed only minor increases in UCS values for f/t exposed concrete, despite noticeable recovery of RF values after the healing period.

Table 5.4: Comparison of the healing potential between RF and hydraulic conductivity of the damaged specimens.

Curing condition	Mix design	Specimen #	After the 12th f/t cycle		After the post-exposure healing period	
			Hydraulic conductivity ratio, K_{12}/K_0	RF ratio, β_{12}	Hydraulic conductivity ratio, K_{healed}/K_0 (% decrease)	RF ratio, β_{healed} (% increase)
Immature	SI(1.5)	1	49.2	0.14	5.5 (89)	0.63 (350)
		2	43.5	0.44	2 (95)	0.56 (27)
	SII(1.5)	1	7.8	0.74	1.7 (78)	0.98 (32)
		2	5.4	0.75	2.3 (57)	1.0 (33)
	SII(2)	1	112.5	0.34	54.2 (52)	0.62 (82)
		2	75.0	0.40	13.5 (82)	0.51 (28)
Mature	SI(1.5)	1	298.5	0.39	129.9 (56)	0.74 (90)
		2	1714.3	0.23	1571.4 (8)	0.70 (204)
	SI(2)	1	5250.0	0.10	1250.0 (76)	0.52 (420)
		2	3818.2	0.11	1682.8 (56)	0.51 (364)

The recovery ratio, defined as the ratio of RF after the healing process (RF_{healed}) divided by RF measured at the end of the 12th f/t cycle (RF_{12}), was calculated and plotted against the hydraulic conductivity ratios (i.e. K_{12}/K_0) in Figure 5.8. There seems to be a scattered trend suggesting that specimens with higher hydraulic conductivity ratios (K_{12}/K_0), which indicates higher amount of damage in their structure, also show a higher potential for healing (in terms of recovery of RF values). This observation is likely due to the presence of more cracks/micro-cracks in the highly damaged specimens, which creates a better potential for RF gain during the healing period. However, it should be noted that the superior recovery potential of highly damaged specimens does not necessarily result in a better final performance of these specimens. Considering the case of immature and mature specimens in Figure 5.7, mature specimens have an inferior performance under f/t exposure, compared to immature specimens within each mix design. Despite the higher recovery rate for some of the mature specimens (for instance about five times increase in RF for SI(2)-mature between healed conditions and cycle 12), they still exhibit lower RF

ratios at the end of the healing period (β_{healed}) as compared to similar conditions for immature specimens exhibiting less initial damage.

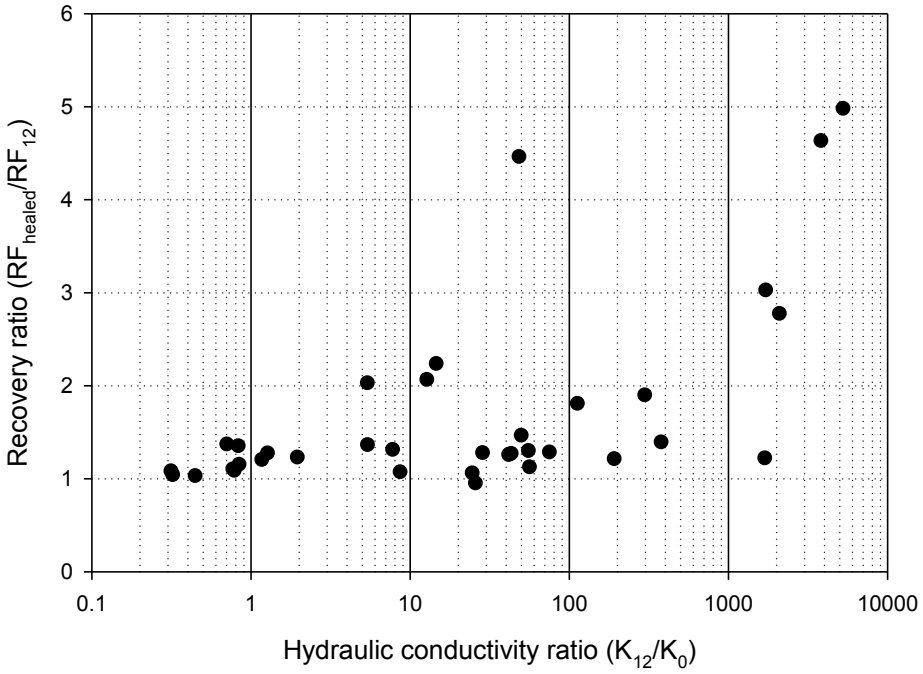

Figure 5.8: Recovery ratio of specimens compared to the hydraulic conductivity ratio measured after 12th f/t cycle.

5.4. Summary and Conclusions

The IR method was used as a non-destructive tool to monitor curing progress, f/t damage, and healing process in soil-cement specimens prepared at different mix designs. Results of the RF measurements using this technique were compared to the strength and hydraulic performance of the same specimens. Results showed that IR can provide an effective tool in predicting changes in the performance of cement-treated soils. A summary of the specific conclusions from the experimental studies discussed in the previous sections is as follows:

1. RF changes were monitored for specimens from four different mix designs for curing ages ranging from 5 to 241 days. A rapid increase in RF values was

observed in the initial 60 days of curing, after which the changes in the RF continued at a slower rate. Comparing RF and UCS measurements for specimens cured for 16 and 241 days showed that within each soil type, specimens with higher increases in RF values exhibited higher UCS gains.

2. RF measurements on specimens exposed to 12 cycles of f/t showed that the initial cycle has a significant effect in the degradation of the structure. At the end of the 12^{th} f/t cycle, a wide range of behaviours was observed varying from minor increases to decreases of up to 90 percent in the RF values as compared to control measurements performed before f/t exposure.
3. RF ratios at the end of the first (β_1) and 12^{th} (β_{12}) f/t cycles were compared to the hydraulic conductivity ratio (K_{12}/K_0) measurements on the same specimens. Results show IR may have the potential to be used as a non-destructive tool in predicting changes in the hydraulic conductivity of cement-stabilized soils exposed to f/t cycles. Based on the RF measurements at the end of the first f/t cycle, three zones (I, II, and III) were proposed. Specimens in zones I ($\beta_1 > 0.9$) would likely to pass the hydraulic performance requirements after 12 cycles of f/t exposure. Specimens in zone III ($\beta_1 < 0.7$) would likely fail the hydraulic performance requirements and would result in significant increases in the hydraulic conductivity values after 12 f/t cycles. The test on specimens with RF ratios between 0.7 and 0.9 ($0.7 < \beta_1 < 0.9$) in zone II is inconclusive, and further f/t cycling and performance monitoring would be required. Using the proposed scheme can significantly reduce the testing time in f/t studies on cement-stabilized soils intended to be used for applications that requires low hydraulic conductivity over the life span of the material. Further experiments along with appropriate statistical analysis is required to evaluate the reliability of the proposed scheme.
4. Increases in the RF values were observed for both immature and mature specimens after a post-exposure healing period. Specimens with higher degree of damage seemed to exhibit a higher potential for RF recovery, which is possibly due to the higher number of cracks in these specimens. Healing potential for RF

values was not proportional to the recovery of the hydraulic conductivity values for the specimens tested in this study.

5.5. References

Ababneh, A.N. and Xi, Y., 2006. Evaluation of environmental degradation of concrete in cold regions. In *Proceedings of Cold Regions Engineering 2006: Current Practices in Cold Regions Engineering*. Edited by M. Davies & J. E. Zufelt. Orono, ME: American Society of Civil Engineers, pp. 1–10.

Abrams, D.A., 1913. *Test of bond between concrete and steel*, Urbana, IL: Bulletin No. 71, Published by the uinversity of Illinois.

ACI, 1999. *Controlled low-strength materials*, Farmington Hills, MI: Americal Concrete Institute (ACI) Committee 229, ACI229R-99.

ACI, 1990. *Report on soil cement*, Farmington Hills, MI: American Concrete Institute (ACI) Committee 230, ACI230.1R-90.

ASTM-C215, 2008. Standard test method for fundamental transverse, longitudinal, and torsional resonant frequencies of concrete specimens. In *Annual Book of ASTM Standards*. West Conshohocken, PA: ASTM International. doi:10.1520/c0215-08.2.

ASTM-C666, 2008. Standard test method for resistance of concrete to rapid freezing and thawing. In *Annual Book of ASTM Standards*. West Conshohocken, PA: ASTM International. doi:10.1520/c0666.

ASTM-D5084, 2010. Standard test methods for measurement of hydraulic conductivity of saturated porous materials using a flexible wall permeameter. In *Annual Book of ASTM Standards*. West Conshohocken, PA: ASTM International. doi:10.1520/d5084-10.

ASTM-D558, 2011. Standard test methods for moisture-density (unit weight) relations of soil-cement. In *Annual Book of ASTM Standards*. West Conshohocken, PA: ASTM International. doi:10.1520/d0558-11.

Chatterji, S., 2003. Freezing of air-entrained cement-based materials and specific actions of air-entraining agents. *Cement and Concrete Composites*, **25**(7):pp.759–765. doi:10.1016/s0958-9465(02)00099-9.

Edvardsen, C., 1999. Water permeability and autogenous healing of cracks in concrete. *ACI Materials Journal*, **96**(4):pp.448–54.

El-Korchi, T., Gress, D., Baldwin, K. and Bishop, P., 1989. Evaluating the freeze-thaw durability of Portland cement-stabilized-solidified heavy metal waste using acoustic measurements. In *Environmental Aspects of Stabilization and Solidification of Hazardous and Radioactive Wastes (STP 1033)*. Edited by P. Côté & M. Gilliam. Philadelphia, PA: ASTM International, pp. 184–191. doi:10.1520/stp22878s.

Fitch, J. and Cheeseman, C.R., 2003. Characterisation of environmentally exposed cement-based stabilised/solidified industrial waste. *Journal of Hazardous Materials*, **101**(3):pp.239–255. doi:10.1016/s0304-3894(03)00174-2.

Gheorghiu, C., Rhazi, J.E. and Labossière, P., 2005. Impact resonance method for fatigue damage detection in reinforced concrete beams with carbon fibre reinforced polymer. *Canadian Journal of Civil Engineering*, **32**(6):pp.1093–1102. doi:10.1139/l05-064.

ITRC, 2010. *Development of performance specifications for solidification/stabilization (technical/regulatory guidance)*, Washington, DC: The Interstate Technology & Regulatory Council, Solidification/Stabilization Team.

Jacobsen, S. and Sellevold, E.J., 1996. Self healing of high strength concrete after deterioration by freeze/thaw. *Cement and Concrete Research*, **26**(I):pp.55–62.

Jin, X. and Li, Z., 2001. Dynamic property determination for early-age concrete. *ACI Materials Journal*, **98**(5):pp.365–370.

Klich, I., Batchelor, B., Wilding, L.P. and Drees, L.R., 1999. Mineralogical alterations that affect the durability and metals containment of aged solidified and stabilized wastes. *Cement and Concrete Research*, **29**:pp.1433–1440.

Malhotra, V.M., 2011. Nondestructive tests. In *Significance of Tests and Properties of Concrete and Concrete-Making Materials (STP 169D)*. Edited by J. F. Lamond & J. H. Pielert. West Conshohocken, PA: ASTM International, pp. 314–334.

Mindess, S., Young, J.F. and Darwin, D., 2003. *Concrete;* Second Edi., Upper Saddle River, NJ: Pearson Education, Inc.

Nagy, A., 1997. Determintaion of E-modulus of young concrete with nondestructive method. *ASCE Journal of Materials in Civil Engineering*, **9**(1):pp.15–20. doi:10.1061/(asce)0899-1561(1997)9:1(15).

Paria, S. and Yuet, P., 2006. Solidification/stabilization of organic and inorganic contaminants using Portland cement: a literature review. *Journal of Environmental Reviews*, **14**:pp.217–255. doi:10.1139/a06-004.

Powers, T.C., 1945. A working hypothesis for further studies of frost resistance of concrete. *Bulletin no. 5, Portland Cement Association. Research and Development Laboratories.*, **41**(February):pp.245–272.

Powers, T.C., Copeland, L.E., Hayes, J.C. and Mann, H.M., 1954. Permeability of portland cement paste. *Journal of American Concrete Institute*, **51**:pp.285–298.

Sansalone, M., 1997. Impact-Echo: the complete story. *ACI Structural Journal*, **94**(6):pp.777–786.

Shah, S.P., Popovics, J.S., Subramaniam, K. V. and Aldea, C., 2000. New directions in concrete health monitoring technology. *ASCE Journal of Engineering Mechanics*, **126**(7):pp.754–760.

Shihata, S.A. and Baghdadi, Z.A., 2001. Simplified method to assess freeze-thaw durability of soil cement. *ASCE Journal of Materials in Civil Engineering*, **13**(4):pp.243–247.

Stegemann, J.A. and Côté, P.L., 1996. A proposed protocol for evaluation of solidified wastes. *Science of the Total Environment*, **178**(1996):pp.103–110. doi:10.1016/0048-9697(95)04802-2.

Swamy, N. and Rigby, G., 1971. Dynamic properties of hardened paste , mortar and concrete. *Matériaux et Construction*, **1**(4):pp.13–40.

Yang, Y., Lepech, M.D., Yang, E.-H. and Li, V.C., 2009. Autogenous healing of engineered cementitious composites under wet–dry cycles. *Cement and Concrete Research*, **39**(5):pp.382–390. doi:10.1016/j.cemconres.2009.01.013.

CHAPTER 6: FREEZE/THAW EFFECT ON PERFORMANCE AND MICROSTRUCTURE OF CEMENT-TREATED SOILS

6.1. Introduction

Treatment of soil via Portland cement is performed in many applications (e.g. base layer for pavements, slope protection, and water retention systems), usually to improve an economically available soil in order to meet performance specifications (e.g. strength, hydraulic conductivity, etc.) (ACI (1990)). Portland cement is also used in cement-based solidification/stabilization (s/s), a source-control remediation technique, where it is mixed with contaminated materials to mitigate the release of contaminants to surrounding environments (ITRC (2010)). Given the diversity of soil-cement applications and the variety of the initial materials being treated, mix designs utilized for the treatment of soils using this technique may vary over a wide range. With respect to water content, for instance, while in most cement-treatment applications the values are controlled to provide optimum density of the final product due to compaction (i.e. compacted soil-cement prepared near proctor test optimum water content), there are situations where soil-cement is prepared at noticeably higher water content conditions creating mixtures with consistencies similar to plastering mortar at the time of the placement process (i.e. plastic soil-cement) (BRAB (1969)). The urge to prepare mix designs at high water contents may arise from construction requirements (i.e. self-consolidation, as opposed to compaction) or may be imposed by the initial high water content of the native materials (e.g. remediation of contaminated sludge in cement-based s/s projects).

Engineered designs of cement-treated systems are expected to maintain their structural integrity for decades (PASSiFy (2010)). However, it is suggested that under environmental exposure, similar factors that influence the long term performance of concrete (e.g. chemical attack, wet/dry (w/d) cycles, and freeze/thaw (f/t) exposure) may initiate these same degradation processes in soil-cement (Klich et al. (1999)). During the design stage of cement-treated materials, w/d and f/t exposure tests have been routinely used to examine their durability (ASTM-D559 (1996) (withdrawn in 2012); ASTM-D560 (2003)).

However, comparing the results of the laboratory investigations for cement-treated materials exposed to standard w/d and f/t cycles in the literature (e.g. Felt (1955); Al-Tabbaa & Evans (1998); Shihata & Baghdadi (2001a)) suggest that f/t exposure may generally be a dominant factor in the durability of soil-cement materials.

Influence of the f/t exposure on integrity and mechanical properties of compacted and plastic soil-cement has been widely studied in the literature (e.g. Felt (1955); Dempsey & Thompson (1973); Kettle (1986); Pamukcu et al. (1994); Shihata & Baghdadi (2001a)). In chapters three and four extensive laboratory investigations focusing on changes in the hydraulic performance of cement-treated soils after f/t exposure was conducted. Increases of up to three orders of magnitude as well as minor decreases in the hydraulic conductivity values were observed after 12 cycles of f/t. Both reductions and increases in UCS values were also reported in these studies, however UCS changes did not correspond to the variations of hydraulic conductivity values obtained within each mix design. Chapter five suggested that the impact resonance (IR) method may be a reliable non-destructive tool in predicting hydraulic conductivity changes in cement-treated soils subjected to cycles of f/t.

The majority of laboratory studies (e.g. ASTM-D560 (2003)) evaluating f/t resistance of soil-cement use a three-dimensional freezing exposure, as opposed to a more realistic one-dimensional exposure scenario expected in the field. The influence of one-dimensional freezing on mechanical properties of soil-cement has been previously investigated (e.g. Dempsey & Thompson (1973)), however possible correlation of the results between one- and three-dimensional exposure scenarios do not appear to exist. Also, variations in the hydraulic performance of soil-cement under one-dimensional freezing conditions have not been addressed in the literature. In addition, a systematic examination of the micro/macro-structural changes in soil-cement materials undergoing freeze-thaw is lacking in the literature.

The current chapter examines the influence of three cycles of f/t exposure on two mix designs of a cement-treated silty sand, representing compacted and plastic soil-cement conditions. Three-dimensional f/t exposure was performed under immature curing (16 days) and mature curing (over 110 days) conditions. Mature specimens from each mix

design were also exposed to a one-dimensional freezing process. Hydraulic conductivity, unconfined compressive strength, and longitudinal resonant frequency (RF) measurements were performed on control and f/t exposed specimens under each of the exposure scenarios described above. Transmitted light microscopy was also conducted on petrographic thin section samples obtained from specimens under these various exposure and freezing scenarios in order to examine potential mechanisms of damage development.

6.2. Materials and Methods

6.2.1. Soil Materials Used in Soil-Cement Mixes

Different size fractions from two base soils (i.e. soil A and soil B) were blended, as shown in Table 6.1, to create the soil used in this study. Soil A was a glacially derived silty sand (ASTM-D2487 (2011)) and Soil B was a waste by-product of quarry operations, both acquired from Nova Scotia. Mineral oxides analysis performed on soil A and B indicate silica, aluminum, potassium, sodium, and iron as the major oxides present in their composition (Table 6.2). Quartz and feldspars were also identified as the main crystalline phases in both soils based on X-ray diffraction analysis shown in Figure 6.1. Standard proctor tests (ASTM-D558 (2011)) performed on the blended soil (i.e. soil A and soil B) mixed with 10% (i.e. based on dry mass of soil) Portland-limestone blended cement (CSA type GUL) showed an optimum water content (OWC) of approximately 11 percent and a maximum dry density of approximately 1975 kg/m^3.

Table 6.1: Summary of the mix designs utilized for SIII(1.2) and SIII(2.1).

Mix designation	W/c ratio	Cement content, percent (dry weight of soil)	Mixing method*	Composition by dry weight, percent					ASTM classification of the blended soil
				Soil A				Soil B <0.08 mm	
				9.50-4.75 mm	4.75-1.20 mm	1.20-0.30 mm	0.30-0.08 mm		
SIII(1.2)	1.2	10	C	9	30	21	10	30	Silty sand
SIII(2.1)	2.1	10	S						

*C: compaction, S: self-consolidation.

6.2.2. Soil-Cement Specimen Preparation

The two mix designs used in the study were chosen to represent compacted soil-cement prepared at near OWC conditions (i.e. SIII(1.2) specimens in Table 6.1) and plastic soil-cement prepared at slightly over eight percent wet of OWC conditions (i.e. SIII(2.1) specimens in Table 6.1). To prepare the specimens from each mix design, the soil, cement and water were mixed using a drill-mounted paddle at the proportions presented in Table 6.1. SIII(1.2) specimens were compacted in standard proctor molds in three layers in accordance with ASTM-D558 (2011). SIII(2.1) specimens were placed into cylindrical plastic molds (101 mm in diameter and 118 mm in height) in three layers, each layer being tamped with 20 blows of a standard concrete slump testing rod to provide the required consolidation. After placement, the molds were placed in sealed plastic bags for five days, when specimens were extruded and kept in a 100% humidity moist room for further curing.

Table 6.2: Mineralogical composition of soil A and soil B (chapter 4).

	SiO_2	Al_2O_3	K_2O	Na_2O	Fe_2O_3	LOI (1000°C)*	Other
Soil A	71.82	14.57	3.27	3.03	2.66	2.41	2.24
Soil B	65.65	15.31	4.02	3.08	5.66	1.17	5.11

*LOI: Loss on ignition

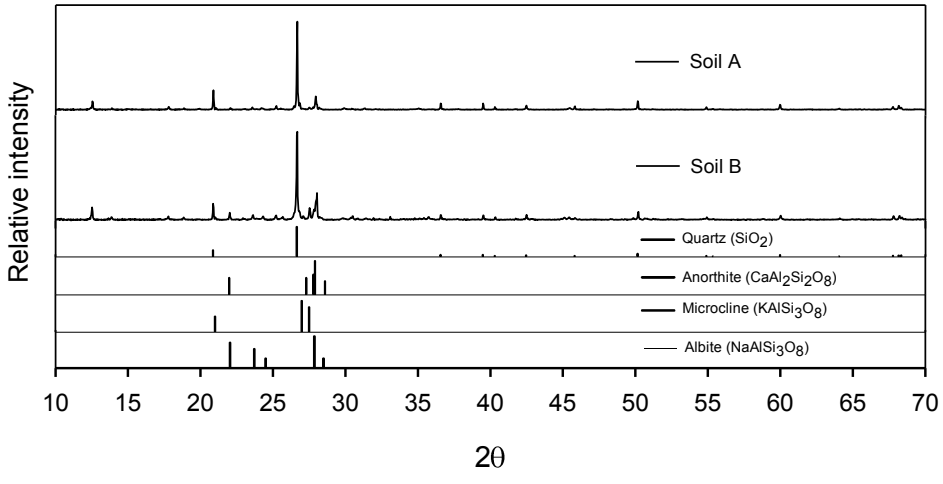

Figure 6.1: X-ray diffraction test results performed on powder samples from Soil A and B.

6.2.3. F/T Conditioning of Specimens

6.2.3.1. Immature- vs. Mature-Exposure

In previous chapters it was shown that mature specimens exposed to 12 f/t cycles exhibit higher amounts of damage compared to immature conditions. Non-destructive tests performed in chapter five also showed that a significant portion of the degradation during f/t exposure occurred at the initial f/t cycles. Given this, in the current study specimens from each mix design were exposed to three f/t cycles under immature and mature curing conditions. For immature-exposed specimens, initial f/t exposure started at a curing age of 16 days, while for mature-exposed specimens, f/t exposure started after over 110 days from specimen preparation. Each f/t cycle consisted of 24 hours of freezing the specimens in a freezer (i.e. three-dimensional freezing) set at -10±1^{o}C followed by thawing them in a 100% humidity room at a temperature of 22±1^{o}C. All specimens were saturated in a set-up presented in method A of ASTM-D5084 (2010) under a minimum back-pressure of 524 kPa and a confining pressure of over 558 kPa for a duration of at least seven days before f/t exposure.

6.2.3.2. One- vs. Three-Dimensional Specimen Freezing

Ground freezing occurs due to boundary conditions created by sub-zero air temperatures. Heat flux occurs one-dimensionally resulting in soil freezing progressively into underlying layers. A review of the interrelationships of soil, water, and temperature for a soil undergoing freezing has been presented by Nixon (1991). In durability studies of cement-based materials, however, it is common to apply three-dimensional freezing exposure conditions as a more convenient method. In the current study, mature specimens from both mix designs were exposed to three cycles of one-dimensional freezing followed by thawing in the moist room. The changes in the performance of these specimens were then compared to similar specimens exposed to three-dimensional f/t, with exposure conditions described in the previous section.

A test set-up shown in Figure 6.2 was used to one-dimensionally freeze duplicate specimens from each mix design. Specimens were placed in a plexiglass tube with a wall

thickness of 1.5 cm covered with approximately 1.2 cm of fibreglass insulation. One-dimensional flow of heat during the freezing process in a similar set-up was confirmed by Mcknight-Whitford (2013). To provide a tight contact between specimens and the plexiglass tube walls (i.e. the interior surface of plexiglass tubes), layers of plastic wrap was placed around each specimen and the final surface was coated with vacuum grease prior to the placement in the tubes. A dummy sample, having a similar mix design to specimens being tested, with a height of approximately 5 cm was placed underneath each specimen to facilitate achieving sub-zero temperatures at the bottom of the specimens during the freezing process. A mixture of ice and water was used to maintain the temperature at the base of the dummy sample at 0ºC. A compact refrigerated circulator (i.e. HAAKE DC30 liquid chiller with a K10 bath) was used to circulate a mix of water and antifreeze at a temperature of -10±1ºC through two stainless steel caps placed on top of each specimen. The whole set-up was placed in a room with an ambient temperature of 3±1ºC to provide the required working conditions for the compact refrigerated circulator. Thermocouples were placed between the specimens and the dummy samples to monitor the temperature changes at the base of the specimens and to ensure complete freezing of the specimens in order to provide proper comparison to the three-dimensional freezing conditions. Each freezing phase last for three days, after which specimens were extruded and placed in a moist room for approximately 24 hours for complete thawing. This process was repeated for a total of three f/t cycles.

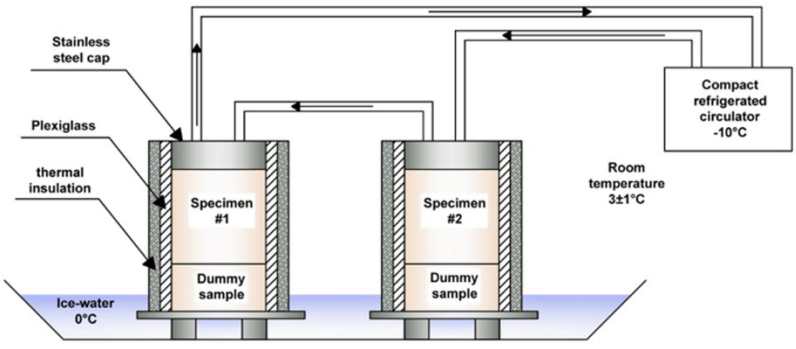

Figure 6.2: The set-up utilized for one-dimensional freezing of the cement-treated soils.

6.2.4. Specimen Testing

Hydraulic conductivity, unconfined compressive strength (UCS), and longitudinal resonance frequency (RF) measurements were performed on control and exposed specimens to monitor the changes in the performance of each mix design under different exposure scenarios and freezing conditions. Transmitted light microscopy was also performed on petrographic thin sections obtained from control and f/t exposed specimens in order to provide information regarding the microstructural changes and damage propagation mechanisms under various exposure conditions. A summary of the testing procedures used in the study follows.

6.2.4.1. Hydraulic Conductivity

Duplicate specimens were tested for hydraulic conductivity values before (i.e. control) and subsequently after three cycles of f/t exposure. General guidelines suggested in method A of ASTM-D5084 (2010) (i.e. constant head flexible-wall method) were followed during each test. Test duration ranged from 3 days to 2 weeks depending on the hydraulic conductivity of the specimens. Permeation was performed under a hydraulic gradient ranging from 29 to 60 until a steady hydraulic conductivity value was achieved as described in the standard.

6.2.4.2. Impact Resonance (IR)

Vibration-based non-destructive techniques have been used for structural health monitoring purposes in various applications (e.g. Nagy (1997); Sansalone (1997); Shah et al. (2000); Jin & Li (2001); Gheorghiu et al. (2005)). Since resonant frequency (RF) of a material measured using these techniques is related to its physical properties including density, shape, and the dynamic modulus of elasticity (Malhotra (2011)), it can be used as a reliable indicator for monitoring the changes in the material due to external stresses. In chapter five it was shown that the IR method, as an example of vibration-based non-destructive techniques, can be used for early detection of damage in cement-treated soils during exposure to cycles of f/t.

In the current study, longitudinal resonance frequency (RF) of specimens was measured using the IR method, before f/t exposure and subsequently at the end of the thawing phases of cycles 1, 2, and 3. The tests followed the general procedures presented in ASTM-C215 (2008). Impact load was generated using a steel ball with a diameter of 9.5 mm attached to a plastic band. An accelerometer (PCB model 352C68) and a Freedom Data PC Platform (Olson Instruments Inc.) were used for the data acquisition and signal processing. A bandwidth filter of [500-15000] Hz, sampling rate of 500 KHz, and record size of 8192 samples were used during the test. Each test consisted of five trials on the specimen with the average values being reported as the RF.

6.2.4.3. Unconfined Compressive Strength (UCS)

Unconfined compressive strength (UCS) measurements were performed on duplicate specimens for control and f/t exposed conditions. Sulfur-capped specimens were subjected to a vertical deformation rate of 0.5 mm/min during the loading process.

6.2.4.4. Transmitted Light Optical Microscopy

Study of the microstructural changes in the exposed specimens using petrographic methods can provide an insight on the mechanisms of damage formation during f/t exposure. Petrographic thin section samples were prepared by a specialized laboratory at the Geology and Earth Sciences department of Dalhousie University. Thin sections were taken from horizontal and vertical planes of resin impregnated samples from control and exposed specimens. Examination of the thin sections were performed using a Nikon Optiphot-Pol polarized light microscope equipped with a 12 megapixel digital scanning camera (Kontron ProgRes 3012).

6.3. Results and Discussion

A summary of the hydraulic conductivity, UCS, and resonant frequency results obtained from the study is presented in Table 6.3. Below is a discussion of these results as well as microstructural changes observed from the thin section samples using transmitted light microscopy.

6.3.1. Hydraulic Conductivity

Figure 6.3 shows the influence of water content in the mix design on hydraulic conductivity of the treated soil under both immature and mature curing conditions (i.e. without f/t exposure). Results from measurements performed in chapter four on a similar soil at different water contents are also presented in Figure 6.3 to better demonstrate the variations with respect to OWC conditions. Results show that the lowest hydraulic conductivity can be achieved by preparing mix designs slightly wet of OWC conditions. Hammad (2013) previously showed that for specimens cured for 28 days, the lowest hydraulic conductivity occurs at a water content ranging from 2 to 6 percent above the standard proctor OWC conditions. Figure 6.3 shows that hydraulic conductivity values increase at a slow rate as water content is increased from OWC up to a value of about 8 percent wet of OWC, after which the hydraulic conductivity seems to be very sensitive to even small additions of water in the mixture. This is possibly due to the excessive bleeding of the water during preparation of mixtures at high water contents creating high porosity areas within the final structure. Based on the results in Figure 6.3, hydraulic conductivity values also seem to be sensitive to water content changes towards dry of OWC conditions, as shown by about three to four orders of magnitude increase in the values as the w/c ratio in the mix design is decreased from a value of 1.2 (near OWC conditions) to 1 (dry of OWC conditions). Figure 6.3 also shows a decrease of as high as roughly two orders of magnitudes in the hydraulic conductivity values between immature and mature measurements as a result of the progression of the hydration process in the specimens.

Table 6.3: Summary of performance test results under control and exposed conditions.

Test		Hydraulic conductivity, m/s (Relative standard deviation, %)				UCS, MPa (Relative standard deviation, %)				Longitudinal resonance frequency, kHz (Relative standard deviation, %)							
		3D		1D		3D		1D		3D				1D			
Exposure condition		Control	Exposed	Control	Exposed	Control	Exposed	Control	Exposed	Control	Cycle 1	Cycle 2	Cycle 3	Control	Cycle 1	Cycle 2	Cycle 3
SIII(1.2)	Immature	3.8×10^{-11} (38.7)	3.5×10^{-11} (36.2)	-	-	10.6 (4.0)	10.8 (0.5)	-	-	12.4 (1.5)	12.3 (1.2)	12.2 (1.2)	12.4 (2.1)	-	-	-	-
	Mature	5.9×10^{-12} (10.2)	5.7×10^{-11} (68.4)	2.0×10^{-12} (18.0)	1.1×10^{-11} (5.3)	11.2 (0.7)	11.7 (7.6)	-	11.9 (9.1)	13.4 (1.4)	12.0 (4.9)	12.2 (4.8)	10.8 (6.3)	12.8 (0.5)	12.6 (1.0)	12.7 (0.4)	12.6 (0.6)
SIII(2.1)	Immature	3.4×10^{-9} (11.8)	4.0×10^{-8} (19.0)	-	-	3.0 (3.3)	2.5 (4.0)	-	-	8.4 (2.2)	4.8 (7.6)	3.3 (1.9)	2.5 (2.4)	-	-	-	-
	Mature	2.1×10^{-10} (2.4)	6.8×10^{-8} (48.2)	2.9×10^{-10} (1.8)	2.4×10^{-7} (60.3)	3.7 (10.5)	3.6 (6.7)	-	3.0 (22.6)	9.6 (1.6)	4.6 (3.3)	3.0 (1.0)	2.0 (1.5)	9.9 (0.3)	6.1 (1.0)	3.6 (11.1)	2.6 (52.3)

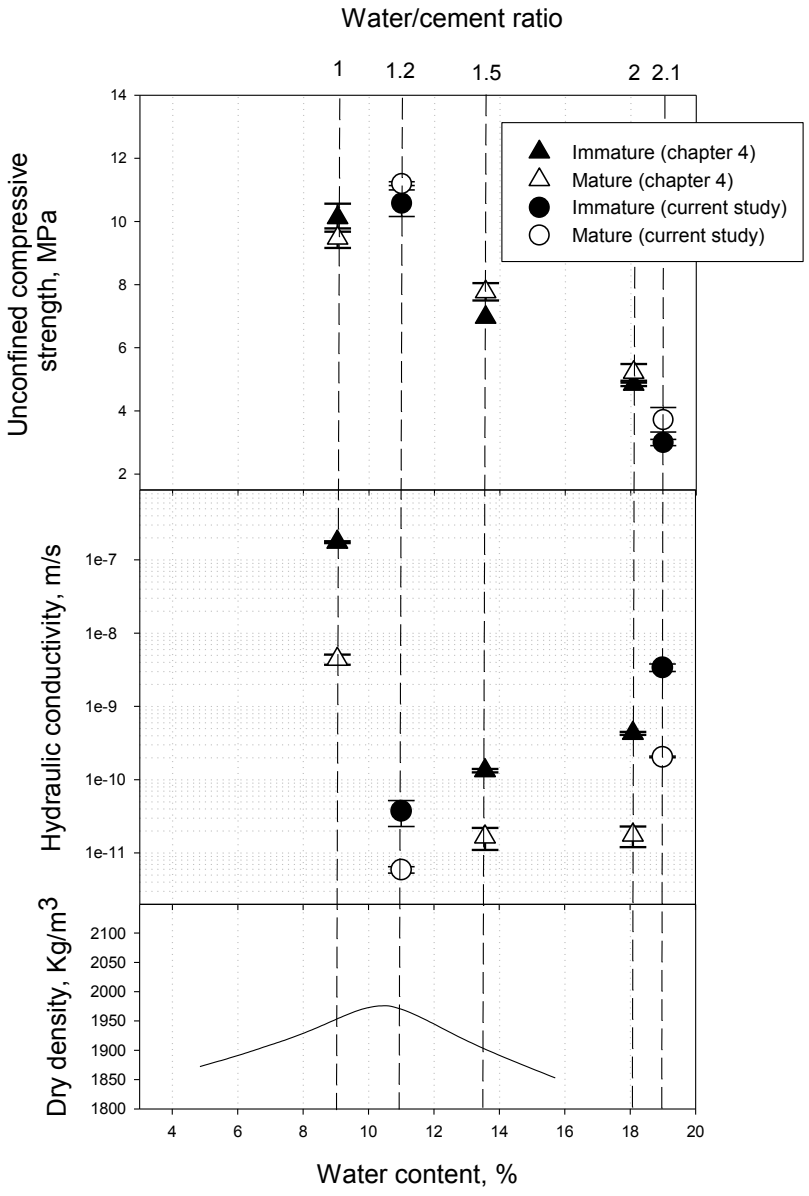

Figure 6.3: Variations of the hydraulic conductivity and UCS with respect to the changes in the water content in the mix design (control samples).

Changes in the hydraulic conductivity values for SIII(1.2) and SIII(2.1) specimens obtained under various f/t exposure conditions are presented in Figure 6.4. After three cycles of three-dimensional f/t exposure, a wide range of changes in hydraulic conductivity values was observed which appears to be dependent on the curing conditions and mix design. For the SIII(1.2) mix design, on average, immature specimens showed a slight reduction in hydraulic conductivity values, while mature specimens exhibited an increase of about one order of magnitude. Also of note is that the hydraulic conductivity values after f/t exposure,

even though they have undergone an increase, remain low (less than 10^{-10} m/s). Under similar conditions immature and mature specimens from SIII(2.1) showed increases of about 12 and 320 fold in the hydraulic conductivity values, respectively. Increase in hydraulic conductivity values after f/t exposure is likely a result of crack initiation and subsequent structural degradation due to expansion of pore water in soil-cement during the freezing process. The theory of damage development in cement-based materials during f/t exposure is discussed in previous research studies (e.g. Powers (1945); Setzer (2001)). Conversely, the decrease in hydraulic conductivity values after f/t exposure in SIII(1.2)-immature is likely due to the interaction of the continuing hydration of cement, as well as various healing mechanisms (e.g. mineral precipitation) acting in parallel with the deteriorating effect of freezing process. Hydraulic conductivity recovery of damaged soil-cement specimens after post-exposure curing was also reported in previous chapters.

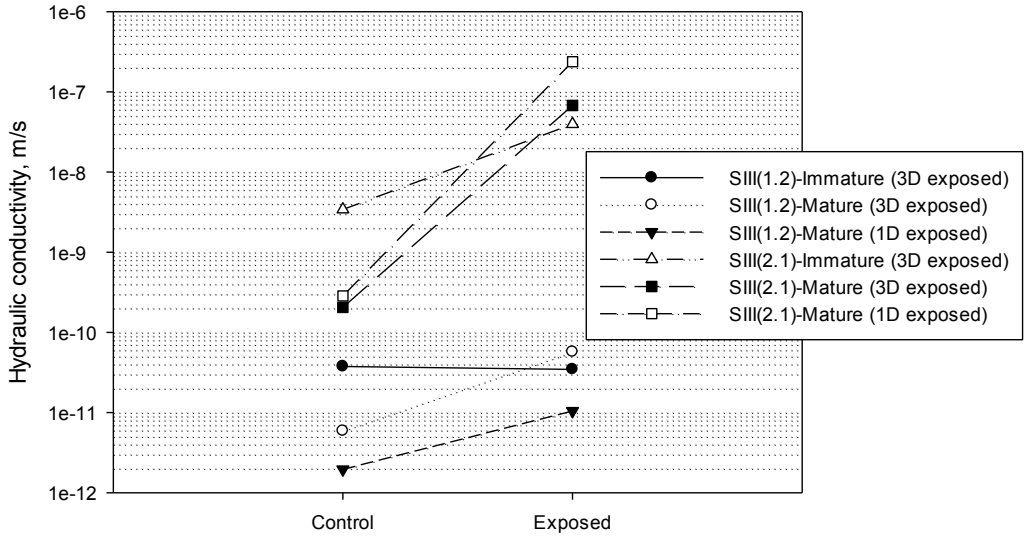

Figure 6.4: Changes in the hydraulic conductivity of specimens after three cycles of f/t exposure.

Examination of one-dimensional freezing conditions compared to three-dimensional freezing conditions has been conducted in the literature by Othman & Benson (1993) for compacted clay soils. Othman & Benson (1993) showed that f/t dimensionality has negligible influence on the changes in the hydraulic performance and the crack formation

pattern in compacted clay specimens. Comparing the hydraulic conductivity changes in mature specimens exposed to one- and three-dimensional freezing conditions in the current study (Figure 6.4) also shows changes in the hydraulic conductivity values are within the same order of magnitude for both freezing scenarios.

6.3.2. Longitudinal Resonant Frequency (RF)

Figure 6.5 presents the RF values measured on specimens at control conditions (i.e. cycle 0) and subsequently after 1st, 2nd, and 3rd f/t cycles. Values obtained for control specimens show mature specimens exhibit higher RF values compared to immature specimens, which is a result of increased structural integrity due to the curing process. Also, specimens from SIII(1.2) mix design show higher RF values compared to SIII(2.1) mix design for both immature and mature conditions. Higher RF values suggests a higher stiffness of these specimens, and is in agreement with lower hydraulic conductivity measurements presented in the previous section.

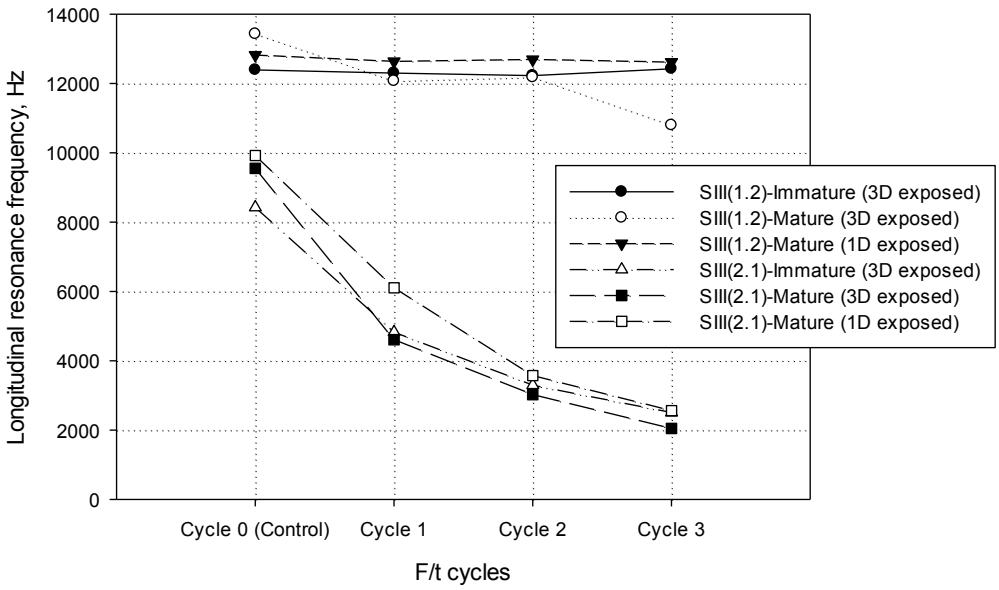

Figure 6.5: Variation of RF values at different f/t cycles.

For SIII(1.2)-immature specimens, RF values were relatively constant (slightly over 12000 Hz) through different f/t cycles, which suggests minor structural changes. This was in

agreement with the slight reductions in hydraulic conductivity values of these specimens after f/t exposure. For SIII(1.2) mature specimens exposed to three-dimensional f/t, RF values showed over 1000 Hz reduction after the initial cycle and reached a value of about 10800 Hz (i.e. a total decrease of approximately 2600 Hz) at the end of the third cycle. Reductions in the RF values were in agreement with the increases observed in the hydraulic conductivities of these specimens. For SIII(1.2) mature specimens exposed to one-dimensional freezing conditions, RF values showed only minor variations over three f/t cycles, which is in contrast to approximately five times increase observed in their hydraulic conductivity values. However, as noted previously, the final hydraulic conductivity values are still lower than 10^{-10} m/s, suggesting that the specimens are still relatively intact.

For SIII(2.1)-immature and SIII(2.1)-mature specimens, average RF values dropped from [8300-9600] Hz to values close to 2000 Hz after three cycles of f/t. This extensive drop in RF values is consistent with several orders of magnitude change in hydraulic conductivity for this mix, both observations suggesting a significant change in structure within the soil-cement specimens.

For the mature specimens tested from SIII(2.1) mix design, variations of results for one- and three-dimensional freezing conditions were insignificant. Also, irrespective of exposure scenario, the initial cycle had a significant effect in the degradation of the specimens, resulting in over 38 percent reduction in the RF values.

6.3.3. Unconfined Compressive Strength (UCS)

Trends in the UCS values for the treated soil at w/c ratios ranging from 1 (dry of OWC) to 2.1 is shown in Figure 6.3. Data presented in Figure 6.3 include both measurements performed in this study and UCS measurements conducted in chapter four on a similar soil treated at different w/c ratios. Maximum UCS values appear to correspond with the OWC, with values decreasing at a higher rate on the wet side of the compaction curve. Observations by Felt (1955) previously showed that for non-plastic soils the maximum UCS occurs slightly dry of OWC obtained from the standard proctor test.

Figure 6.6 presents the results of UCS testing for SIII(1.2) and SIII(2.1) specimens after three cycles of f/t exposure. On average, SIII(1.2) specimens showed a general increasing trend (with a maximum increase of about six percent) in UCS values for both immature and mature exposure conditions. SIII(2.1)-immature showed an average reduction of 17 percent after f/t exposure while SIII(2.1)-mature remained relatively unchanged after three-dimensional f/t exposure. A 19 percent reduction was observed for similar specimens exposed to one-dimensional freezing. Comparing the UCS measurements to the observations on hydraulic conductivity changes for similar mix designs, it is apparent that UCS is not a sensitive indicator to the changes in the hydraulic performance of cement-treated soils. This can be a result of different nature of these tests. For instance, it is possible that micro-crack formations during the freezing process can lead to increases in the hydraulic conductivity values, while under similar conditions the compressive forces applied during the UCS test can cause the micro-cracks to contribute to the strength of the specimen as a result of friction development on the crack walls.

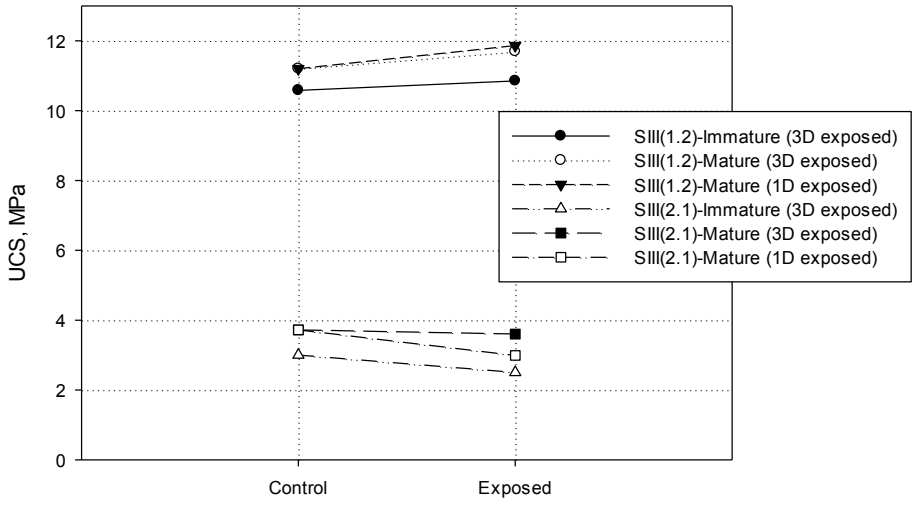

Figure 6.6: Comparison of UCS values for control (i.e. unexposed) and exposed conditions.

6.3.4. Optical Microscopy

An examination of the microstructure of the cement-treated soil using transmitted light optical microscopy was performed to examine how the soil-cement matrix was disrupted after exposure to f/t cycling. Comparison of the micrographs between the horizontal and vertical planes obtained from control and f/t exposed specimens did not suggest any noticeable spatial variation in the soil-cement structure and the damage formation mechanisms. Typical micrographs obtained from specimens under control and three-dimensional f/t exposed conditions are presented in Figure 6.7.

The blue color in the micrographs presented in Figure 6.7 represents the pore structures that were filled with the resin used during the impregnation of the samples prior to thin section preparation.

The soils used in the study appear to be "young", in the respect that they contain minerals associated with the disintegration/degradation of igneous and metamorphic rocks. These minerals, which are relatively thermodynamically unstable, form angular, coarser clasts. Minerals identified in the coarser fraction include microcline, plagioclase, ferromagnesian minerals, and micas. Some of the clasts present in the soil exhibit signs of degradation, including micro-cracking, suggesting that prior to use in the study, they were subject to mechanical or environmental loading (see images A, B, and G in Figure 6.7).

Discrete incidents of high porosity areas were observed in control samples from both SIII(1.2) and SIII(2.1) mix designs (see patches of blue color in images C and G in Figure 6.7). These features were likely induced during the placement of the specimens as a result of poor compaction and/or localized high water content areas in the matrix. It should be noted that the images presented in Figure 6.7 are in scales of millimeters and hence there were hundreds of potential images. Those presented in Figure 6.7 are considered typical of the visual observations of the samples.

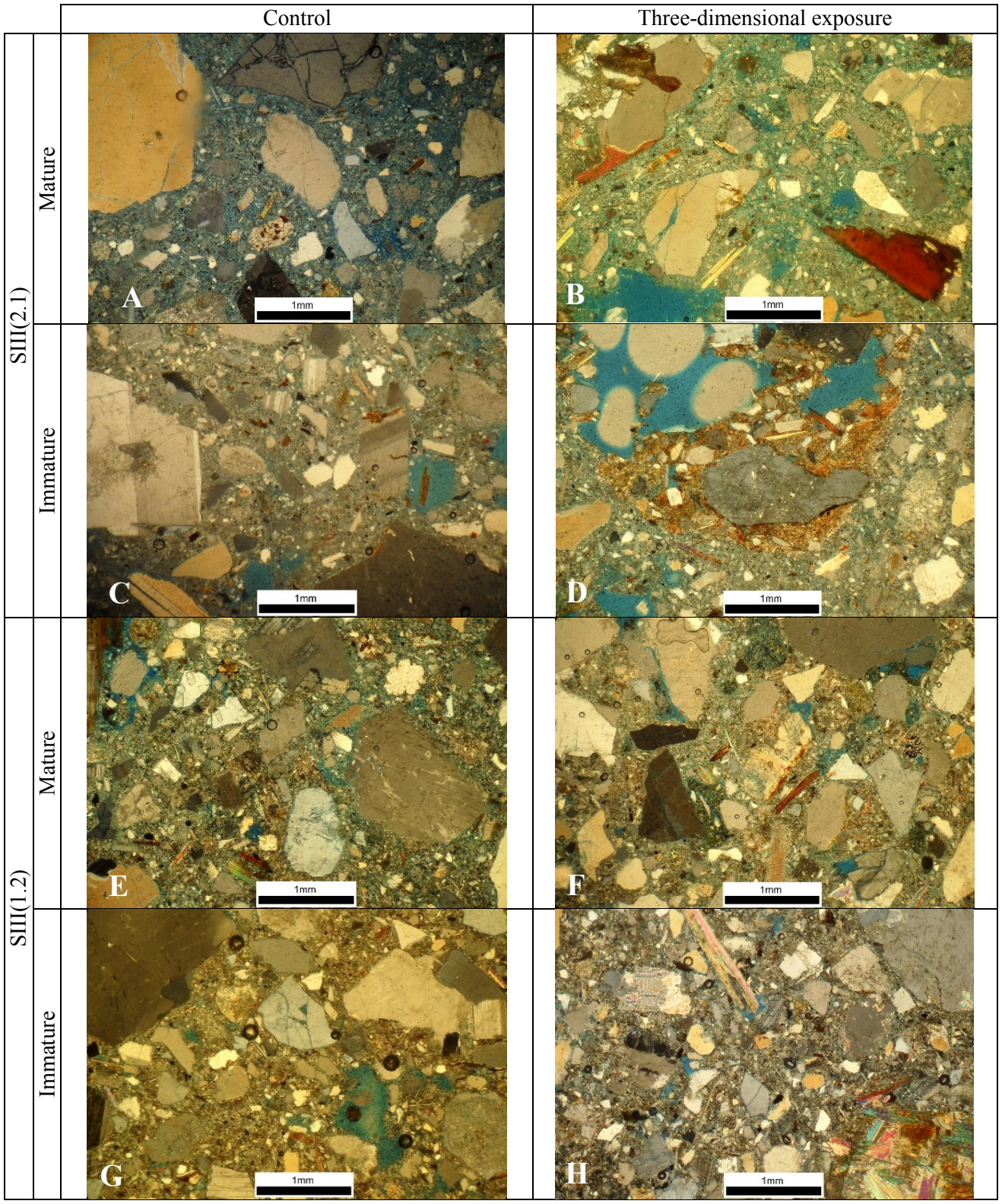

Figure 6.7: Typical micrographs from vertical planes of specimens under various curing and exposure scenarios.

Considering the control conditions in Figure 6.7, the microstructure in samples from SIII(2.1) with higher w/c ratio, appears less dense (see images A and C in Figure 6.7), especially at the matrix/aggregate interface. SIII(1.2) samples prepared at lower w/c ratio on the other hand have a denser packing and a less intense blue color (see images E and G in Figure 6.7).

Under the exposed conditions, in the thin sections from SIII(2.1)-immature specimens ($K_{exposed}/K_0 \approx 12$), minor matrix disruptions in scattered areas throughout the paste were noticeable as is shown in micrographs presented in Figure 6.8. For the same mix design under mature three-dimensional f/t exposure (i.e. SIII(2.1)-mature with a $K_{exposed}/K_0 \approx 320$), more evidence of matrix disruption as well as some micro-cracking along the paste-aggregate interface were observed (Figure 6.8). Damage in the thin sections from SIII(2.1)-mature was also evident by comparing the thin sections even at a larger scale as is shown in Figure 6.9 (note the increased intensity of blue color in exposed sample as compared to control sample). It can also be seen in Figure 6.9 that damage formation in soil-cement, at least at the high cement content used in this study, doesn't follow the mechanisms suggested for compacted clay (i.e. parallel ice lens formation), which is likely a result of higher tensile strength of these materials due to the binding capacity of cement hydration products.

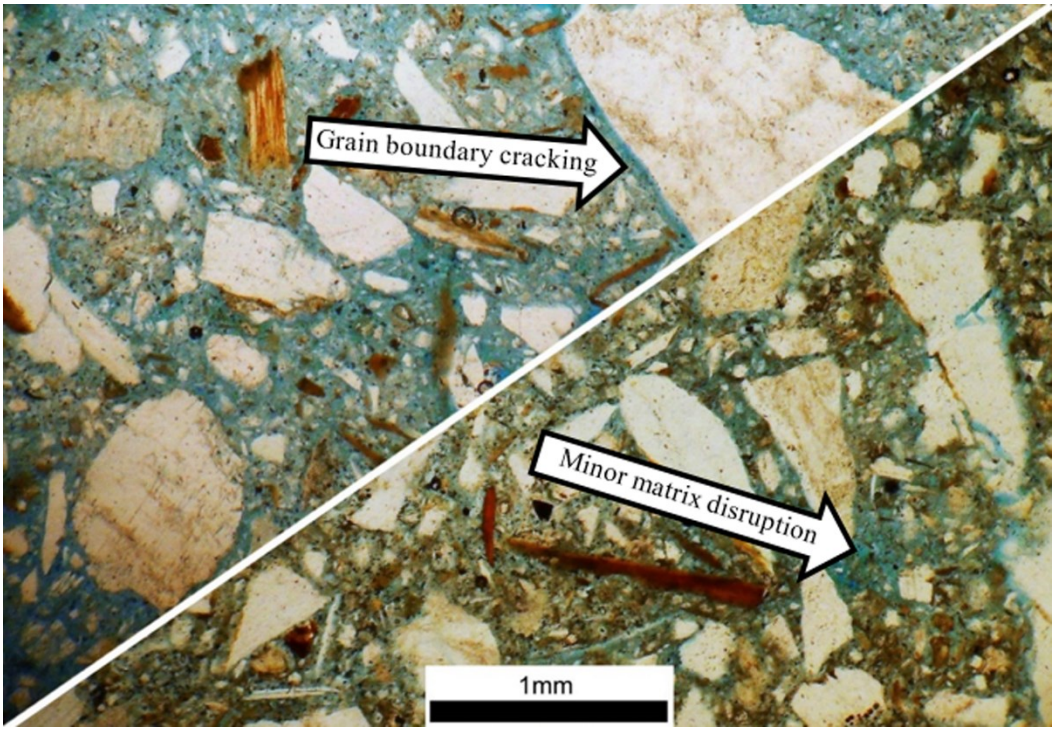

Figure 6.8: Micrographs taken from SIII(2.1)-immature ($K_{exposed}/K_0 \approx 12$) specimens (bottom corner) and SIII(2.1)-mature ($K_{exposed}/K_0 \approx 320$) specimens (top corner) under three-dimensional f/t exposed conditions.

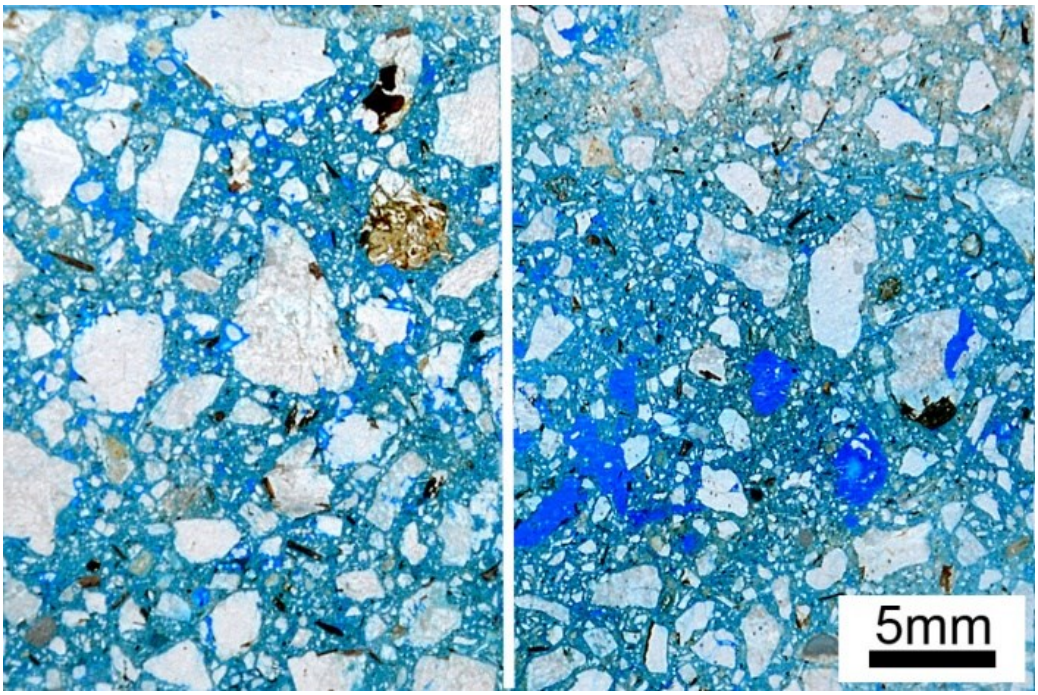

Figure 6.9: Damage formation in SIII(2.1)-mature at macro scale. Left: control; right: three-dimensional exposed conditions.

Considering SIII(1.2)-immature samples, the damage was less evident, although some disruption of the matrix was observed (Figure 6.10). This was despite the reduction of the hydraulic conductivity values in this mix design after f/t exposure. This reduction is likely a result of the decreased hydraulic conductivity of the paste due to the hydration process and the isolation of the disrupted areas by unaffected materials. In SIII(1.2)-mature, although approximately ten times increase in the hydraulic conductivity values were observed after three-dimensional f/t exposure, only minor scattered degradation of the matrix were observed during the analysis (Figure 6.10). It should be again noted that although increases in hydraulic conductivity were observed, the final hydraulic conductivity value of the SIII(1.2) mixtures was less than 10^{-10} m/s and hence tend to agree with the microscope observations.

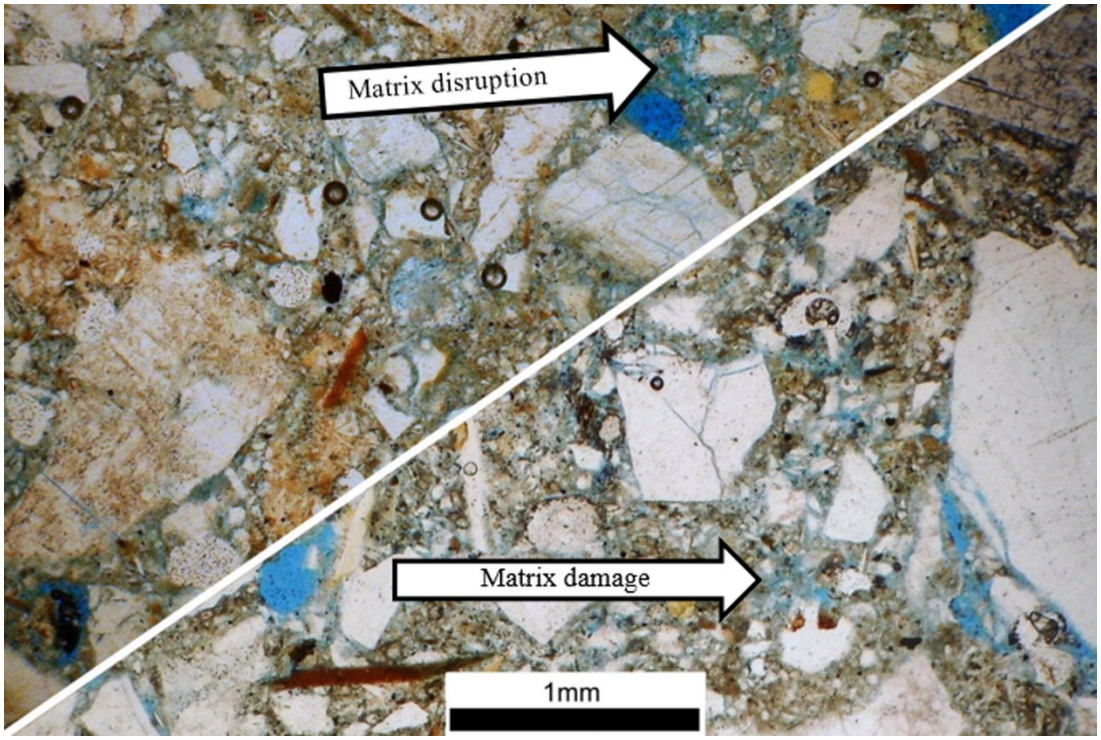

Figure 6.10: Micrographs taken from SIII(1.2)-immature specimens (bottom right) and SIII(1.2)-mature specimens (top left) under three-dimensional f/t exposed conditions.

Microstructural analysis of one-dimensionally exposed specimens didn't reveal any obvious differences in the mechanisms of f/t damage compared to three-dimensional exposure conditions. As was expected, more damage (in terms of matrix-aggregate interface cracking and matrix disruption) was observed in the micrographs obtained from

SIII(2.1) specimens (i.e. under one-dimensional f/t exposed conditions) with higher hydraulic conductivity changes as compared to minor structural changes in the SIII(1.2) specimens with slight increases in the hydraulic conductivity values (Figure 6.11).

Results of the microstructural analysis performed show that there are obvious limitations on sample observation using transmitted light microscopy. The degree of microstructural disturbance between samples and within individual samples is not as obvious as anticipated, even though other test methods showed a reduction in microstructural integrity for most of the scenarios investigated. Thus, the use of transmitted light microscopy may not be able to resolve the early stages of (sub-microscopic) matrix disruption, whereas the other indirect analytical methods employed have this capability. However, it was established that microstructural damage was mainly in the form of matrix disruption, cracking within the matrix, and cracking at aggregate boundaries. Other techniques to examine the microstructure, such as mercury intrusion porosimetry (MIP) and scanning electron microscopy (SEM), may provide further insight into the phenomena observed in this thesis.

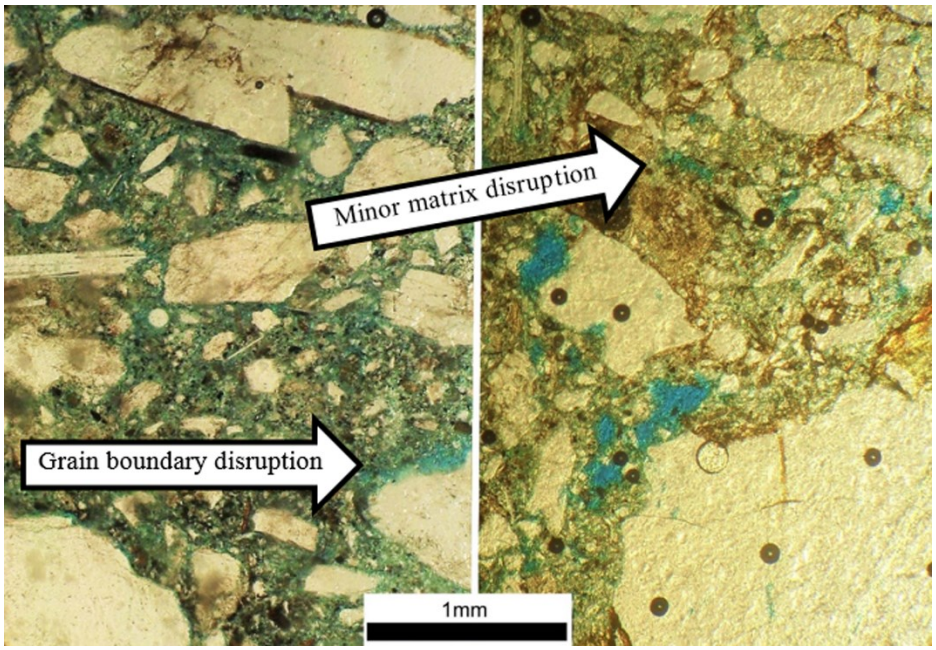

Figure 6.11: Micrographs taken from SIII(2.1)-mature specimens (left) and SIII(1.2)-mature specimens (right) under one-dimensional f/t exposed conditions.

6.4. Conclusions

Cement-treated silty sand specimens prepared at two w/c ratios representing compacted and plastic soil-cement mix designs were exposed to three cycles of f/t under various curing (i.e. immature vs. mature) and f/t dimensionality (i.e. one-dimensional vs. three dimensional) scenarios. Changes in performance of the specimens were monitored using hydraulic conductivity, UCS, and longitudinal RF measurements. Also, microstructural degradation of the specimens were evaluated by studying petrographic thin section samples obtained from the specimens, using transmitted light optical microscopy technique. The following conclusions can be drawn from the results.

1. Performance measurements on soil-cement specimens prepared over a wide range of water contents (i.e. without f/t exposure) showed that minimum hydraulic conductivity likely occurs at water contents slightly wet of optimum water content, while maximum UCS possibly occurs at water contents near or slightly dry of optimum water contents. Hydraulic conductivity values seem to be more sensitive to changes in the water contents towards dryer mix designs, while UCS values are more sensitive to changes in the water contents towards wetter mix designs, with respect to optimum water content conditions.
2. Specimens exposed to three f/t cycles exhibited a wide range of performance changes including minor enhancement of the performance (possibly due to the interaction of f/t degradation mechanisms with the hydration/healing processes) as well as increases in the hydraulic conductivity values and decreases in the UCS and RF values (i.e. performance degradation). Specimens prepared at higher water content (i.e. SIII(2.1)) exhibited more damage after f/t exposure as compared to the dryer mix design (i.e. SIII(1.2)). Also, it was found that mature specimens are more susceptible to f/t exposure compared to immature specimens, an observation discussed in detail in chapter four.
3. Under the testing conditions applied in the study, generally, changes in the performance of the specimens exposed to one-dimensional and three-dimensional f/t exposure didn't show any significant variation. This may suggest while one-dimensional f/t studies better mimic the exposure mechanisms

expected in the field, laboratory investigation of soil-cement using three-dimensional f/t exposure scenarios can still provide a reliable estimation of the performance degradation.

4. Microstructural analysis of petrographic thin section samples from control and f/t exposed specimens showed that optical microscopy is not able to identify structural degradation at early stages of damage development, suggesting presence of possible sub-microstructural disruption mechanisms. For highly damaged specimens (i.e. in terms of hydraulic conductivity changes), however, signs of matrix disintegration as well as matrix-aggregate interface cracking were identified.

6.5. References

ACI, 1990. *Report on soil cement*, Farmington Hills, MI: American Concrete Institute (ACI) Committee 230, ACI230.1R-90.

Al-Tabbaa, A. & Evans, C.W., 1998. Pilot in situ auger mixing treatment of a contaminated site. part 1: treatability study. *Proceedings of the Institution of Civil Engineers: Geotechnical Engineering*, **131**(1):pp.52–59.

ASTM-C215, 2008. Standard test method for fundamental transverse, longitudinal, and torsional resonant frequencies of concrete specimens. In *Annual Book of ASTM Standards*. West Conshohocken, PA: ASTM International.

ASTM-D2487, 2011. Standard practice for classification of soils for engineering purposes (unified soil classification system). In *Annual Book of ASTM Standards*. West Conshohocken, PA: ASTM International.

ASTM-D5084, 2010. Standard test methods for measurement of hydraulic conductivity of saturated porous materials using a flexible wall permeameter. In *Annual Book of ASTM Standards*. West Conshohocken, PA: ASTM International.

ASTM-D558, 2011. Standard test methods for moisture-density (unit weight) relations of soil-cement. In *Annual Book of ASTM Standards*. West Conshohocken, PA: ASTM International.

ASTM-D559, 1996. Standard test methods for wetting and drying compacted soil-cement mixtures. In *Annual Book of ASTM Standards*. West Conshohocken, PA.: ASTM International.

ASTM-D560, 2003. Standard test methods for freezing and thawing compacted soil-cement mixtures. In *Annual Book of ASTM Standards*. West Conshohocken, PA: ASTM International.

BRAB, 1969. *Chemical soil stabilization*, Washington, DC: Building Research Advisory Board, US National Academy of Sciences.

Dempsey, B.J. & Thompson, M.R., 1973. Vacuum saturation method for predicting freeze-thaw durability of stabilized materials. In *Highway Research Record 442*. Highway Research Board, US National Research Council, pp. 44–57.

Gheorghiu, C., Rhazi, J.E. & Labossière, P., 2005. Impact resonance method for fatigue damage detection in reinforced concrete beams with carbon fibre reinforced polymer. *Canadian Journal of Civil Engineering*, **32**(6):pp.1093–1102.

Hammad, A., 2013. *Evaluation of soil-cement properties with electrical resistivity*. M.A.Sc. Thesis, Civil and Resource Engineering Department, Dalhousie Univesity, Halifax, NS.

ITRC, 2010. *Development of performance specifications for solidification/stabilization (technical/regulatory guidance)*, Washington, DC: The Interstate Technology & Regulatory Council, Solidification/Stabilization Team.

Jin, X. & Li, Z., 2001. Dynamic property determination for early-age concrete. *ACI Materials Journal*, **98**(5):pp.365–370.

Kettle, R.J., 1986. The assessment of freeze-thaw damage in cement stabilized soils. In O. B. Andersland & F. H. Sayles, eds. *Proceedings of Research on Transportation Facilities in Cold Regions (ASCE)*. Boston, MA, pp. 16–31.

Klich, I., Batchelor, B., Wilding, L.P. & Drees, L.R., 1999. Mineralogical alterations that affect the durability and metals containment of aged solidified and stabilized wastes. *Cement and Concrete Research*, **29**:pp.1433–1440.

Malhotra, V.M., 2011. Nondestructive tests. In J. F. Lamond & J. H. Pielert, eds. *Significance of Tests and Properties of Concrete and Concrete-Making Materials (STP 169D)*. West Conshohocken, PA: ASTM International, pp. 314–334.

Mcknight-Whitford, H., 2013. *Development of an experimental device for monitoring frost heave in soils*. M.A.Sc. Thesis, Civil and Resource Engineering Department, Dalhousie Univesity, Halifax, NS.

Nagy, A., 1997. Determintaion of E-modulus of young concrete with nondestructive method. *ASCE Journal of Materials in Civil Engineering*, **9**(1):pp.15–20.

Nixon, J.F., 1991. Discrete ice lens theory for frost heave in soils. *Canadian Geotechnical Journal*, **28**(6):pp.843–859.

Othman, M.A. & Benson, C.H., 1993. Effect of freeze-thaw on the hydraulic conductivity and morphology of compacted clay. *Canadian Geothechnical Journal*, **30**:pp.236–246.

Pamukcu, S., Topcu, I.B. & Guven, C., 1994. Hydraulic conductivity of solidified residue mixtures used as a hydraulic barrier. In D. E. Daniel & S. J. Trautwein, eds. *Hydraulic Conductivity and Waste Contaminant Transport in Soil (STP 1142)*. Philadelphia, PA: ASTM International, pp. 505–520.

PASSiFy, 2010. *Performance assessment of solidified/stabilised waste-forms, an examination of the long-term stability of cement-treated soil and waste*, A Joint Research Consortium.

Powers, T.C., 1945. A working hypothesis for further studies of frost resistance of concrete. *Bulletin no. 5, Portland Cement Association. Research and Development Laboratories.*, **41**(February):pp.245–272.

Sansalone, M., 1997. Impact-Echo: the complete story. *ACI Structural Journal*, **94**(6):pp.777–786.

Setzer, M.J., 2001. Micro-ice-lens formation in porous solid. *Journal of Colloid and Interface Science*, **243**(1):pp.193–201.

Shah, S.P., Popovics, J.S., Subramaniam, K. V. & Aldea, C., 2000. New directions in concrete health monitoring technology. *ASCE Journal of Engineering Mechanics*, **126**(7):pp.754–760.

Shihata, S.A. & Baghdadi, Z.A., 2001. Long-term strength and durability of soil cement. *ASCE Journal of Materials in Civil Engineering*, **13**(3):pp.161–165.

CHAPTER 7: SUMMARY, CONCLUSIONS, AND RECOMMENDATIONS

7.1. Summary

An extensive laboratory investigation was performed in this dissertation to supplement the available literature on evaluation of changes in hydraulic and mechanical performance of cement-treated soils in cold regions, in particular under freeze/thaw (f/t) cycles exposure. Previous studies (e.g. Othman and Benson (1992); Othman and Benson (1993)) demonstrated the influence of f/t cycles on changes in hydraulic conductivity of compacted clay under various exposure and testing conditions. The current study has provided a new insight into the hydraulic performance of cement-treated soils subjected to cycles of f/t which was not presented in any level of detail in the literature. In summary, this work has:

1. Studied the influence of various testing conditions in the laboratory examination of cement-treated soils exposed to f/t cycles (chapter three). To perform this work, the number of f/t cycles, freezing temperature, and curing age at the time of initial f/t exposure were selected as the variable testing conditions in a "three factor"-"two level" factorial analysis. Hydraulic conductivity, unconfined compressive strength (UCS), and longitudinal resonant frequency (RF) were evaluated as the performance and structural degradation indicators under each factorial test scenario.
2. Examined the influence of mix design in resistance of cement-treated soils to f/t exposure (chapter four). As part of this study, the performance (i.e. hydraulic conductivity and UCS) of nine different mix designs representing compacted and plastic soil-cement materials, prepared at various water/cement (w/c) ratios and fines contents were evaluated under unexposed and f/t exposed scenarios. The reliability of using mass loss as an indicator for hydraulic performance degradation of soil-cement materials was evaluated by comparing the results of the brushing tests to hydraulic conductivity changes performed on specimens

from similar mix designs. The recovery of hydraulic conductivity of f/t exposed cement-treated materials were evaluated after a post-exposure healing period.

3. Investigated the potential for application of longitudinal RF measurements in monitoring structural changes in cement-treated soils (chapter five). In this study, the impact resonance (IR) test method was used to monitor curing progress, structural degradation due to f/t exposure, and the healing process in specimens from various mix designs. A screening scheme was proposed based on the IR test results for rapid laboratory evaluation of changes in the hydraulic conductivity of cement-treated soils subject to f/t cycles.
4. Compared the results of laboratory examination of cement-treated soils under three and one-dimensional f/t exposure scenarios (chapter six). In this study, transmitted light optical microscopy was also used to evaluate the mechanisms of f/t exposure damage in compacted and plastic soil-cement under various exposure scenarios.

7.2. Conclusions of Research Findings

An overview of the main conclusions of the thesis and their practical implications are provided in the following paragraphs. An attempt is made to provide an overall view of the results obtained from the work performed in the various chapters.

7.2.1. Influence of Various Testing Conditions in Laboratory Evaluation of F/T Exposure

An important stage in the design process of soil-cement materials evaluated for exposure to f/t cycles is the selection of realistic testing conditions during the experimental program. It was therefore necessary to examine the importance of various testing conditions on possible changes in the performance of treated materials under f/t cycles. Based on the results of the "three factor"-"two level" factorial experiments performed in chapter three, it was concluded that number of f/t cycles (examined at 4 and 12 cycles), freezing temperature (examined at -2^{o}C and -10^{o}C), and curing age prior to initial f/t cycle (examined at 16 and over 35 days) can influence the changes observed in the hydraulic

conductivity and UCS of the cement-treated silty sand. Maximum damage, for most cases, were observed when specimens cured for over 35 days (i.e. longer curing age) were exposed to 12 cycles with a freezing temperature of -10^{o}C. A set of complementary tests were presented in chapter three to examine the influence of further reduction in the freezing temperature to -20^{o}C, however the results were inconclusive.

Findings from chapter three signify the importance of adjusting testing conditions to those expected in the field. For instance, if freezing conditions are expected at early curing ages of soil-cement prior to placement of a cover system (e.g. implementation of a cement-based solidified/stabilized project in late fall), experimental evaluation of the material under f/t exposure using immature specimens exposed to freezing temperatures closer to 0^{o}C, depending on the environment where the project is implemented, can be adequate. However, when the long term performance of the material under environmental exposure is considered, it is necessary to test specimens at lower freezing temperatures and longer curing ages to account for worst case scenarios.

In chapter six, influence of f/t dimensionality (i.e. three-dimensional vs. one-dimensional exposure) on changes in the hydraulic conductivity and UCS of compacted and plastic soil-cement was examined on specimens cured for over 110 days. Comparison of the results didn't suggest any significant variation between the two scenarios, suggesting laboratory evaluation of cement-treated soils under three-dimensional f/t exposure can adequately simulate the level of damage experienced by one-dimensional freezing conditions expected in the field.

7.2.2. Influence of the Mix Design on Performance of Soil-Cement (Without F/T Exposure)

Results of the literature review presented in chapter two showed that previous studies on the performance of soil-cement were primarily focused on mechanical properties of these materials, with mix designs mainly prepared near proctor test optimum water content conditions (OWC). As part of the f/t studies on different mix designs presented in chapters four to six, specimens were made using three soils (varying in fines contents, i.e., 0, 15,

and 30 percent) at water contents ranging from dry of OWC to over 8 percent wet of OWC conditions (i.e. both compacted and plastic soil-cement). Results of hydraulic conductivity and UCS measurements on control specimens from these mix designs tested at two curing levels were presented in the respective chapters.

It was found that the minimum hydraulic conductivity occurs at a water content slightly wet of OWC conditions, with hydraulic conductivity values being sensitive to changes towards dryer mix designs (i.e. significant increase in hydraulic conductivity values at water contents dry of OWC conditions). For UCS values, a decreasing trend was observed for values in mixtures prepared at water contents wet of OWC conditions. Experiments performed on SIII soil (i.e. with 30 percent fines content) in chapter six showed that minimum UCS values may occur at a water content slightly dry of OWC conditions.

7.2.3. Influence of Mix Design on the Resistance of Soil-Cement to F/T Cycles

In chapter four, changes in the performance of specimens from nine different mix designs, each tested at two curing levels, were monitored after exposure to twelve cycles of freezing at -10±1^{o}C and thawing at room temperatures. Mix designs were selected to cover a range of water contents (i.e. w/c ratios of 1, 1.5, and 2) and fines contents in soil prior to stabilization (i.e. 0, 15, and 30 percent).

Changes in the hydraulic conductivity values after f/t exposure ranged from minor reductions, suggesting improvements in the structure, to increases of up to three orders of magnitude in the values as a result of material degradation. It was found that mature specimens (which were exposed to f/t after over 110 days of curing) were more susceptible to f/t exposure compared to immature specimens, something that was not previously accounted for in the literature. Increases in the water content generally resulted in more damage (i.e. in terms of hydraulic conductivity changes) in mature specimens, however, no clear trend was observed for immature specimens, possibly due to the interference of hydration processes with the damage development processes during f/t exposure. Variations in the fines content of the initial soil didn't result in any obvious trend in the

changes in the hydraulic conductivity values at each specific w/c ratio, although fines content clearly has a role in defining the position of the OWC for a particular mix design.

Changes in the UCS values after f/t exposure didn't show any clear trends with regards to variations in the water content, fines content in the soil, and curing level prior to f/t exposure. However, immature specimens prepared at, or slightly dry of, OWC were shown to be very sensitive to f/t exposure resulting in substantial decreases in the UCS values. Comparing the results of UCS and hydraulic conductivity changes within each mix design didn't suggest any correlation between the values.

Comparing the results of f/t exposed and unexposed UCS tests in chapter four showed a linear relation between the measurements. This finding suggests if the required relations between UCS values prior to and after f/t exposure are developed in a specific project, f/t exposed UCS values may be predicted without conducting the required 12 f/t cycles under conditions examined in this study.

7.2.4. Reliability of Mass Loss as an Indicator for Hydraulic Conductivity Changes Due to F/T Exposure

In chapter four, brushing tests were performed on f/t exposed specimens and the mass loss values were calculated and compared to the hydraulic conductivity changes for specimens with similar mix designs. Despite the significant range of changes in the hydraulic conductivity values after f/t exposure (as discussed earlier), mass loss values were mostly less than 7 percent and did not follow the trends observed in hydraulic conductivity changes. Observations suggested mass loss, an indicator commonly used in the industry to measure resistance of soil-cement under f/t exposure, is not necessarily reliable in predicting changes in the hydraulic conductivity of specimens exposed to f/t cycles.

7.2.5. Hydraulic Conductivity Recovery After Post-Exposure Curing

In the experiments presented in chapter four, it was shown that f/t damaged specimens recovered some of their increased hydraulic conductivity values after a period of post-

exposure curing. Under the limited number of experiments performed, hydraulic conductivity values never reached the values measured at control (i.e. pre-exposure) conditions. However, for most cases of slightly damaged immature specimens, values decreased to within an order of magnitude of the measurements prior to f/t exposure. For highly damaged mature specimens, although some reduction in hydraulic conductivity values were observed after the post-exposure healing period, results were still over two orders of magnitude higher than the measurements performed prior to f/t exposure.

7.2.6. Application of the IR Method in Monitoring Damage in Cement-Treated Soils

Monitoring changes in the longitudinal RF values measured on specimens exposed to various exposure scenarios in chapter three showed that the IR method has the potential to be used as an easy non-destructive technique for evaluation of f/t exposed cement-treated materials. An extensive examination of this observation was presented in chapter five. The IR method was used to monitor structural changes in the specimens due to curing process, f/t damage, and post-exposure healing. Results generally showed that longitudinal RF measurements using the IR method could reasonably predict improvements (due to curing or post-exposure healing) or degradations (due to f/t exposure) in the specimens, although magnitude of the changes in RF values were not necessarily proportional to changes measured on the performance of the specimens.

A screening scheme was suggested by comparing RF changes at the end of the initial f/t cycle to changes in the hydraulic conductivity of the same specimens after exposure to 12 cycles of f/t. Based on a total of 36 data points, it was found that specimens exhibiting less than 10 percent reduction in the RF values after one f/t cycle would likely show minor changes in the hydraulic conductivity values after 12 cycles of f/t. On the other hand, specimens with more than 30 percent reduction in the RF values after the initial f/t exposure would likely show substantial increases (i.e. over one order of magnitude) in the hydraulic conductivity values after 12 f/t cycles. RF reductions between 10 and 30 percent of the initial values were inconclusive in predicting changes in the hydraulic conductivity values after the 12^{th} f/t cycles. Although further testing and statistical analysis is required to

evaluate the reliability of the proposed scheme, it seems promising in reducing the total expected testing time for evaluation of hydraulic performance of cement-treated soils under cycles of f/t.

7.2.7. Evaluation of F/T Damage Mechanisms Using Transmitted Light Optical Microscopy

In chapter six, petrographic thin sections from control and f/t exposed specimens representing both compacted and plastic soil-cement mix designs were examined using transmitted light optical microscopy. While some damage in the form of matrix disruption and interface transition zone (ITZ) cracking was observed in highly affected specimens (i.e. specimens exhibiting substantial increase in the hydraulic conductivity values), this technique was found unsuitable for evaluating mechanisms of f/t damage at early stages of soil-cement matrix disruption.

7.3. Recommendations for Future Research

Based on the findings presented in this thesis, the following are recommendations for future studies in this field:

- Only one mix design was used in the study of the influence of testing conditions in the evaluation of soil-cement exposed to f/t cycles in chapter three. Future work could examine the influence of testing conditions on different types of soils and mix designs.

- In the study of the influence of mix design on the changes in the performance of cement-treated soils after f/t exposure, only three water contents (i.e. w/c ratios of 1, 1.5, and 2) were tested for each soil. Future work could repeat the experiments for a specific soil type at more water contents creating additional data points along the compaction curve (i.e. both dry and wet of OWC conditions).

- Hydraulic conductivity measurements on some specimens tested in the thesis showed minor changes as well as reductions after f/t exposure. It would be interesting to examine possible changes in the diffusion coefficient of such specimens after exposure to f/t cycles.

- All the experiments in this study were performed on uncontaminated soils. This is contrary to conditions expected in some soil-cement applications, specifically cement-based solidification/stabilization projects, where contaminated materials are treated using cement. Future work could investigate possible interaction of various contaminants in observed changes in the performance of treated materials after exposure to f/t cycles.

- The experiments presented in this study were performed on specimens treated at relatively high cement contents. Future work could examine the influence of f/t exposure on mixtures prepared at lower cement contents than those used in this study.

- The experiments presented in this thesis were performed on small specimens under controlled laboratory conditions. Future work could examine the reliability of such experimental works by comparing the results to large scale investigations in the field.

- Limited experiments performed on f/t exposed specimens after a post-exposure healing period showed some reduction in the hydraulic conductivity values. Future work could focus on evaluating the healing capacity of f/t exposed cement treated materials by creating a larger database of experimental results (i.e. different mix designs, curing conditions, etc.).

- In the study of the f/t damage mechanisms in chapter six, it was found that transmitted light optical microscopy provides a limited capacity in evaluation of disruptions in soil-cement matrix. Future work could examine the structural

changes in the f/t exposed soil-cement using other techniques (e.g. scanning electron microscopy (SEM)).

References

Ababneh, A.N. and Xi, Y., 2006. Evaluation of environmental degradation of concrete in cold regions. In *Proceedings of Cold Regions Engineering 2006: Current Practices in Cold Regions Engineering*. Edited by M. Davies & J. E. Zufelt. Orono, ME: American Society of Civil Engineers, pp. 1–10.

Abrams, D.A., 1919. *Design of concrete mixtures*, Chicago, IL: Bulletin No. 1, Published by Structural Materials Research Laboratory, Lewis Institute.

Abrams, D.A., 1913. *Test of bond between concrete and steel*, Urbana, IL: Bulletin No. 71, Published by the uinversity of Illinois.

ACI, 1999. *Controlled low-strength materials*, Farmington Hills, MI: Americal Concrete Institute (ACI) Committee 229, ACI229R-99.

ACI, 1990. *Report on soil cement*, Farmington Hills, MI: American Concrete Institute (ACI) Committee 230, ACI230.1R-90.

Aderibigbe, D.A., Akeju, T.A.I. and Orangun, C.O., 1985. Optimal water/cement ratios and strength characteristics of some local clay soils stabilized with cement. *Materials and Structures*, **18**(104):pp.103–108. doi:10.1007/bf02473376.

AECOM, 2013. Sydney Tar Ponds and Coke Ovens site remediation. *Accessed on April 8, 2014 at: http://www.aecom.com/vgn-ext-templating/v/index.jsp?vgnextoid=b5d743dfa94c5310VgnVCM100000089e1bacRCRD&cpsextcurrchannel=1*.

Al-Tabbaa, A. and Evans, C.W., 1998. Pilot in situ auger mixing treatment of a contaminated site. part 1: treatability study. *Proceedings of the Institution of Civil Engineers: Geotechnical Engineering*, **131**(1):pp.52–59. doi:10.1680/igeng.1998.30005.

Antemir, A., Hills, C.D., Carey, P.J., Gardner, K.H., Bates, E.R., Crumbie, A.K., 2010. Long-term performance of aged waste forms treated by stabilization/solidification. *Journal of hazardous materials*, **181**(1-3):pp.65-73.

ASTM-C1262, 2010. Standard test method for evaluating the freeze-thaw durability of dry-cast segmental retaining wall units and related concrete units. In *Annual Book of ASTM Standards*. West Conshohocken, PA: ASTM International. doi:10.1520/c1262-10.2.

ASTM-C215, 2008. Standard test method for fundamental transverse, longitudinal, and torsional resonant frequencies of concrete specimens. In *Annual Book of ASTM Standards*. West Conshohocken, PA: ASTM International. doi:10.1520/c0215-08.2.

ASTM-C305, 2013. Mechanical mixing of hydraulic cement pastes and mortars of plastic consistency. In *Annual Book of ASTM Standards*. West Conshohocken, PA: ASTM International. doi:10.1520/c0305-13.2.

ASTM-C666, 2008. Standard test method for resistance of concrete to rapid freezing and thawing. In *Annual Book of ASTM Standards*. West Conshohocken, PA: ASTM International. doi:10.1520/c0666.

ASTM-D2487, 2011. Standard practice for classification of soils for engineering purposes (unified soil classification system). In *Annual Book of ASTM Standards*. West Conshohocken, PA: ASTM International. doi:10.1520/d2487-11.

ASTM-D4842, 1996. Standard test method for determining the resistance of solid wastes to freezing and thawing. In *Annual Book of ASTM Standards*. West Conshohocken, PA: ASTM International.

ASTM-D5084, 2010. Standard test methods for measurement of hydraulic conductivity of saturated porous materials using a flexible wall permeameter. In *Annual Book of ASTM Standards*. West Conshohocken, PA: ASTM International. doi:10.1520/d5084-10.

ASTM-D558, 2011. Standard test methods for moisture-density (unit weight) relations of soil-cement. In *Annual Book of ASTM Standards*. West Conshohocken, PA: ASTM International. doi:10.1520/d0558-11.

ASTM-D559, 1996. Standard test methods for wetting and drying compacted soil-cement mixtures. In *Annual Book of ASTM Standards*. West Conshohocken, PA.: ASTM International.

ASTM-D560, 2003. Standard test methods for freezing and thawing compacted soil-cement mixtures. In *Annual Book of ASTM Standards*. West Conshohocken, PA: ASTM International. doi:10.1520/d0560-03.

ASTM-D6035, 2008. Standard test method for determining the effect of freeze-thaw on hydraulic conductivity of compacted or intact soil specimens using a flexible wall permeameter. In *Annual Book of ASTM Standards*. ASTM International. doi:10.1520/d6035-08.2.

ASTM-D6913, 2004. Standard test methods for particle-size distribution (gradation) of soils using sieve analysis. In *Annual Book of ASTM Standards*. West Conshohocken, PA: ASTM International. doi:10.1520/d6913-04r09.

Batchelor, B., 2006. Overview of waste stabilization with cement. *Waste Management*, **26**(7):pp.689–98. doi:10.1016/j.wasman.2006.01.020.

Bellezza, I. and Fratalocchi, E., 2006. Effectiveness of cement on hydraulic conductivity of compacted soil–cement mixtures. *Ground Improvement*, **10**(2):pp.77–90. doi:10.1680/grim.2006.10.2.77.

Benson, C.H. and Othman, M., 1993. Hydraulic conductivity of compacted clay frozen and thawed in situ. *Journal of Geotechnical Engineering*, **119**(2):pp.276–294.

Benson, C.H., Abichou, T.H., Olson, M.A. and Bosscher, P.J., 1995. Winter effect on hydraulic conductivity of compacted clay. *ASCE Journal of Geotechnical Engineering*, **121**(1):pp.69–79.

Benson, C.H., Daniel, D.E. and Boutwell, G.P., 1999. Field performance of compacted clay liners. *ASCE Journal of Geotechnical and Geoenvironmental Engineering*, **125**(5):pp.390–403.

Bone, B.D., Barnard, L.H., Boardman, D.I., Carey, P.J., Hills, C.D., Jones, H.M., MacLeod, C.L. and Tyrer, M., 2004. Review of scientific literature on the use of stabilisation/solidification for the treatment of contaminated soil, solid waste and sludges. *British Environmental Agency*, (SC980003/SR2).

Boynton, S.S. and Daniel, D.E., 1985. Hydraulic conductivity tests on compacted clay. *ASCE Journal of Geotechnical Engineering*, **111**(4):pp.465–478. doi:10.1061/(asce)0733-9410(1985)111:4(465).

BRAB, 1969. *Chemical soil stabilization*, Washington, DC: Building Research Advisory Board, US National Academy of Sciences.

Brown L.C., and Berthouex P.M., 2002. *Statistics for Environmental Engineers,* Second Edition. Lewis Publishers.

Chamberlain, E.J., Iskandar, I. and Hunsicker, S.E., 1990. Effect of freeze-thaw cycles on the permeability and macrostructure of soils. In *Proceedings of International Symposium on Frozen Soil Impacts on Agricultural, Range, and Forest Lands*. Spokane, WA, pp. 145–155.

Chatterji, S., 2003. Freezing of air-entrained cement-based materials and specific actions of air-entraining agents. *Cement and Concrete Composites*, **25**(7):pp.759–765. doi:10.1016/s0958-9465(02)00099-9.

Daniel, J.S. and Kim, Y.R., 2001. Laboratory evaluation of fatigue damage and healing of asphalt mixtures. *ASCE Journal of Materials in Civil Engineering*, **13**(6):pp.434–440.

Dempsey, B.J. and Thompson, M.R., 1973. Vacuum saturation method for predicting freeze-thaw durability of stabilized materials. In *Highway Research Record 442*. Highway Research Board, US National Research Council, pp. 44–57.

Edvardsen, C., 1999. Water permeability and autogenous healing of cracks in concrete. *ACI Materials Journal*, **96**(4):pp.448–54.

Eigenbrod, K.D., 2003. Self-healing in fractured fine-grained soils. *Canadian Geotechnical Journal*, **40**:pp.435–449. doi:10.1139/t02-110.

El-Korchi, T., Gress, D., Baldwin, K. and Bishop, P., 1989. Evaluating the freeze-thaw durability of Portland cement-stabilized-solidified heavy metal waste using acoustic measurements. In *Environmental Aspects of Stabilization and Solidification of Hazardous and Radioactive Wastes (STP 1033)*. Edited by P. Côté & M. Gilliam. Philadelphia, PA: ASTM International, pp. 184–191. doi:10.1520/stp22878s.

Felt, E.J., 1955. Factors influencing physical properties of soil-cement mixtures. *Highway Research Board Bulletin*, (108):pp.138–162.

Felt, E.J. and Abrams, M.S., 1957. Strength and elastic properties of compacted soil-cement mixtures. In *Second Pacific Area Meeting Papers (STP 206)*. Philadelphia, PA: American Society for Testing Materials, pp. 152–178.

Fitch, J. and Cheeseman, C.R., 2003. Characterisation of environmentally exposed cement-based stabilised/solidified industrial waste. *Journal of Hazardous Materials*, **101**(3):pp.239–255. doi:10.1016/s0304-3894(03)00174-2.

Fleri, M. A., and Whetstone, G. T., 2007. In situ stabilisation/solidification: project lifecycle. *Journal of Hazardous Materials*, **141**(2):pp.441–56. doi:10.1016/j.jhazmat.2006.05.096

Ganjian, E., Claisse, P.A., Tyrer, M. and Atkinson, A., 2004. Selection of cementitious mixes as a barrier for landfill leachate containment. *ASCE Journal of materials in civil engineering*, **16**(5):pp.477–486. doi:10.1061/(asce)0899-1561(2004)16:5(477).

Gheorghiu, C., Rhazi, J.E. and Labossière, P., 2005. Impact resonance method for fatigue damage detection in reinforced concrete beams with carbon fibre reinforced polymer. *Canadian Journal of Civil Engineering*, **32**(6):pp.1093–1102. doi:10.1139/l05-064.

Guney, Y., Aydilek, A.H. and Demirkan, M.M., 2006. Geoenvironmental behavior of foundry sand amended mixtures for highway subbases. *Waste Management*, **26**(9):pp.932–45. doi:10.1016/j.wasman.2005.06.007.

Hammad, A., 2013. *Evaluation of soil-cement properties with electrical resistivity*. M.A.Sc. Thesis, Civil and Resource Engineering Department, Dalhousie Univesity, Halifax, NS.

Haug, M.D. and Wong, L.C., 1992. Impact of molding water content on hydraulic conductivity of compacted sand-bentonite. *Canadian Geothechnical Journal*, **29**:pp.253–262. doi:10.1139/t92-029.

Hearn, N., Hooton, R.D., and Nokken, M.R, (2006). "Pore structure, permeability, and penetration resistance characteristics of concrete." *Significance of tests and properties of concrete and concrete making.* Edited by: Lamond J.F. and Pielert J.H., The American Society for Testing and Materials, Philadelphia, ASTM STP 169B.

Heide, N., 2005. *Crack healing in hydrating concrete*. M.Sc. thesis, Faculty of Civil Engineering and Geosciences, Delft University of Technology, The Netherlands.

Horpibulsuk, S., Rachan, R., Chinkulkijniwat, A., Raksachon, Y. and Suddeepong, A., 2010. Analysis of strength development in cement-stabilized silty clay from microstructural considerations. *Construction and Building Materials*, **24**(10):pp.2011–2021. doi:10.1016/j.conbuildmat.2010.03.011.

ITRC, 2010. *Development of performance specifications for solidification/stabilization (technical/regulatory guidance)*, Washington, DC: The Interstate Technology & Regulatory Council, Solidification/Stabilization Team.

Jacobsen, S. and Sellevold, E.J., 1996. Self healing of high strength concrete after deterioration by freeze/thaw. *Cement and Concrete Research*, **26**(I):pp.55–62.

Jin, X. and Li, Z., 2001. Dynamic property determination for early-age concrete. *ACI Materials Journal*, **98**(5):pp.365–370.

Joint Departments of the Army and Air Force, 1994. *Soil stabilization for pavements*, Washington, DC: Joint Departments of the Army and Air Force, TM 5-822-14.

Kettle, R.J., 1986. The assessment of freeze-thaw damage in cement stabilized soils. In *Proceedings of Research on Transportation Facilities in Cold Regions (ASCE)*. Edited by O. B. Andersland & F. H. Sayles. Boston, MA, pp. 16–31.

Kim, W. and Daniel, D.E., 1992. Effects of freezing on hydraulic conductivity of compacted clay. *Journal of Geotechnical Engineering*, **118**(7):pp.1083–1097. doi:10.1061/(asce)0733-9410(1992)118:7(1083).

Klich, I., Batchelor, B., Wilding, L.P. and Drees, L.R., 1999. Mineralogical alterations that affect the durability and metals containment of aged solidified and stabilized wastes. *Cement and Concrete Research*, **29**:pp.1433–1440.

Koskiahde, A., 2004. An experimential petrographic classification scheme for the condition assessment of concrete in façade panels and balconies. *Journal of Materials Characterization*, **53**(2-4):pp.327–334. doi:10.1016/j.matchar.2004.09.004.

Kosmatka, H., Kerkhoff, B. and Panarese, W.C., 2003. *Design and control of concrete mixtures* 14th editi., Skokie, IL: Portland Cement Assosiation.

Malhotra, V.M., 2011. Nondestructive tests. In *Significance of Tests and Properties of Concrete and Concrete-Making Materials (STP 169D)*. Edited by J. F. Lamond & J. H. Pielert. West Conshohocken, PA: ASTM International, pp. 314–334.

Mcknight-Whitford, H., 2013. *Development of an experimental device for monitoring frost heave in soils*. M.A.Sc. Thesis, Civil and Resource Engineering Department, Dalhousie Univesity, Halifax, NS.

Micah Hale, W., Freyne S., Russell B. 2009. Examining the frost resistance of high performance concrete. *Construction and Building Materials*. **23**(2):pp.878-888.

Mindess, S., Young, J.F. and Darwin, D., 2003. *Concrete;* Second Edi., Upper Saddle River, NJ: Pearson Education, Inc.

Mitchell, J.K., Hooper, D.R. and Campanella, R.G., 1965. Permeability of compacted clay. *Journal of Soil Mechanics & Foundations Division, Proceedings of the ASCE*, **91**(SM4):pp.41–65.

Nagy, A., 1997. Determintaion of E-modulus of young concrete with nondestructive method. *ASCE Journal of Materials in Civil Engineering*, **9**(1):pp.15–20. doi:10.1061/(asce)0899-1561(1997)9:1(15).

Nixon, J.F., 1991. Discrete ice lens theory for frost heave in soils. *Canadian Geotechnical Journal*, **28**(6):pp.843–859.

Nmai, C.K., 2006. Freezing and thawing. *Significance of tests and properties of concrete and concrete making.* Edited by: Lamond J.F. and Pielert J.H., The American Society for Testing and Materials, Philadelphia, ASTM STP 169B.

Othman, M.A. and Benson, C.H., 1993. Effect of freeze-thaw on the hydraulic conductivity and morphology of compacted clay. *Canadian Geothechnical Journal*, **30**:pp.236–246.

Othman, M.A. and Benson, C.H., 1992. Effect of freeze-thaw on the hydraulic conductivity of three compacted clay from Wisconsin. *Advances in Geotechnical Engineering, Transportation Research Record*, (1369):pp.118–125.

Othman, M.A., Benson, C.H., Chamberlain, E.J. and Zimmie, T.F., 1994. Laboratory testing to evaluate changes in hydraulic conductivity of compacted clays caused by freeze-thaw: state-of-the-art. In *Hydraulic Conductivity and Waste Contaminant Transport in Soil (STP 1142)*. Edited by D. E. Daniel & S. J. Trautwein. Philadelphia, PA: ASTM International, pp. 227–254. doi:10.1520/stp23890s.

Pamukcu, S., Topcu, I.B. and Guven, C., 1994. Hydraulic conductivity of solidified residue mixtures used as a hydraulic barrier. In *Hydraulic Conductivity and Waste Contaminant Transport in Soil (STP 1142)*. Edited by D. E. Daniel & S. J. Trautwein. Philadelphia, PA: ASTM International, pp. 505–520. doi:10.1520/stp23905s.

Paria, S. and Yuet, P., 2006. Solidification/stabilization of organic and inorganic contaminants using Portland cement: a literature review. *Journal of Environmental Reviews*, **14**:pp.217–255. doi:10.1139/a06-004.

PASSiFy, 2010. *Performance assessment of solidified/stabilised waste-forms, an examination of the long-term stability of cement-treated soil and waste*, A Joint Research Consortium.

PCA, 1992. *Soil-cement laboratory handbook*, Skokie, IL: Portland Cement Assosiation.

Penttala, V., 2006. Surface and internal deterioration of concrete due to saline and non-saline freeze–thaw loads. *Cement and Concrete Research.* 36:pp.921–928.

Popovics, S. and Ujhelyi, J., 2008. Contribution to the concrete strength versus water-cement ratio relationship. *ASCE Journal of Materials in Civil Engineering*, **20**(7):pp.459–464. doi:10.1061/(asce)0899-1561(2008)20:7(459).

Powers, T.C., 1945. A working hypothesis for further studies of frost resistance of concrete. *Bulletin no. 5, Portland Cement Association. Research and Development Laboratories.*, **41**(February):pp.245–272.

Powers, T.C., Copeland, L.E., Hayes, J.C. and Mann, H.M., 1954. Permeability of portland cement paste. *Journal of American Concrete Institute*, **51**:pp.285–298.

Powers, T.C., Copeland, L.E. and Mann, H.M., 1959. *Capillary continuity or discontinuity in cement paste*, Skokie, IL: Bulletin no. 10, Portland Cement Association Research and Development Laboratories.

Powers, T.C. and Helmuth, R.A., 1953. Theory of volume changes in hardened portland-cement paste during freezing. In *Proceedings of the Thirty-Second Annual Meeting of the Highway Research Board*. Edited by F. Burggra & W. J. Miller. Washington, D.C., pp. 285–297.

Powers, T.C. and Willis, T.F., 1949. The air requirement of frost-resistant concrete. In *Proceedings of the Twenty-Ninth Annual Meeting of the Highway Research Board*. Edited by R. W. Crum, F. Burggraf, & W. N. Carey. Washington, D.C., pp. 184–211.

Sansalone, M., 1997. Impact-Echo: the complete story. *ACI Structural Journal*, **94**(6):pp.777–786.

Setzer, M.J., 2001. Micro-ice-lens formation in porous solid. *Journal of Colloid and Interface Science*, **243**(1):pp.193–201. doi:10.1006/jcis.2001.7828.

Shah, S.P., Popovics, J.S., Subramaniam, K. V. and Aldea, C., 2000. New directions in concrete health monitoring technology. *ASCE Journal of Engineering Mechanics*, **126**(7):pp.754–760.

Shane, J.D., Mason, T.O., Jennings, H.M., Garboczi, E.J. and Bentz, D.P., 2000. Effect of the interfacial transition zone on the conductivity of Portland cement mortars. *Journal of the American Ceramic Society*, **83**(5):pp.1137–1144.

Shea, M.S., 2011. *Hydraulic conductivity of cement-treated soils and aggregates after freezing*. M.A.Sc. thesis, Department of Civil and Environmental Engineering, Brigham Young University, Provo, UT.

Shihata, S.A. and Baghdadi, Z.A., 2001a. Long-term strength and durability of soil cement. *ASCE Journal of Materials in Civil Engineering*, **13**(3):pp.161–165.

Shihata, S.A. and Baghdadi, Z.A., 2001b. Simplified method to assess freeze-thaw durability of soil cement. *ASCE Journal of Materials in Civil Engineering*, **13**(4):pp.243–247.

Stegemann, J.A. and Côté, P.L., 1996. A proposed protocol for evaluation of solidified wastes. *Science of the Total Environment*, **178**(1996):pp.103–110. doi:10.1016/0048-9697(95)04802-2.

Stegemann, J.A. and Côté, P.L., 1990. Summary of an investigation of test methods for solidified waste evaluation. *Waste Management*, **10**(1):pp.41–52. doi:10.1016/0956-053x(90)90068-v.

Swamy, N. and Rigby, G., 1971. Dynamic properties of hardened paste , mortar and concrete. *Matériaux et Construction*, **1**(4):pp.13–40.

USEPA, 2013. *Superfund remedy report, Forteenth Edition*, USEPA Solid Waste and Emergrncy Respose, EPA 542-R-13-016.

Verbeck, G. and Landgren, G., 1960. Influence of physical characteristics of aggregate on frost resistance of concrete. In *ASTM Proceedings (Vol. 60)*. Phyladelphia, PA, pp. 1063–1079.

Yang, Y., Lepech, M.D., Yang, E.-H. and Li, V.C., 2009. Autogenous healing of engineered cementitious composites under wet–dry cycles. *Cement and Concrete Research*, **39**(5):pp.382–390. doi:10.1016/j.cemconres.2009.01.013.